ANALYTICAL AND EXPERIMENTAL INVESTIGATION OF GAS-CHARGED HYDRAULIC ACCUMULATORS

J.P. Gilles Bouchard

A THESIS

in the

Faculty of Engineering

Presented in Partial Fulfillment of the Requirements

for the Degree of Master of Engineering

at Concordia University

Montréal, Québec, Canada

March, 1980

ABSTRACT

ANALYTICAL AND EXPERIMENTAL INVESTIGATION OF GAS-CHARGED HYDRAULIC ACCUMULATORS

J.P. Gilles Bouchard

Gas-charged hydraulic accumulators are investigated. A mathematical model is developed using the heat conduction distribution equations to describe the time related temperature process within the charge-gas.

This time relation is approximately an exponential decay curve and may be described by a time constant. The time constant is directly related to the geometry of accumulator but it is also a function of the pressure and temperature state of the charge-gas. Thus it is a variable which must be calculated continuously in the model. For a 28 litre piston type accumulator, the time"constant"is approximately 25 seconds.

The thermal phenomena are described in detail and equations derived from first principles. The model is then shown to be valid by comparing to experimental results with several piston-type hydraulic accumulators over a broad range of operating conditions.

The model greatly improves the accuracy of simulations of which accumulators are part. It permits proper sizing and tuning of systems. As a result, the use of accumulators is increased with subsequent energy saving.

ACKNOWLEDGEMENT

The author acknowledges the help of his thesis directors, Drs. S. Katz and J. Svoboda, for the development of heat conduction theory and help during the experimental phases.

TABLE OF CONTENTS

Page

LIST OF SYMBOLS

a	Beattie-Bridgeman constant.	$=933.7\times10^{-6}$	$m^2\ kg^{-1}$
A	Beattie-Bridgeman coefficient		$Pa\ m^6\ kg^{-2}$
A_0	Beattie-Bridgeman constant.	$=172.608$	$Pa\ m^6\ kg^{-2}$
A_s	Surface in contact with charge-gas		m^2
b	Beattie-Bridgeman constant.	$=-2.4736\times10^{-4}$	$m^2\ kg^{-1}$
B	Beattie-Bridgeman coefficient		$m^3\ kg^{-1}$
B_e	Exponential term	$=\Psi_m^2-\varepsilon_n^2/(L/D)^2$	
B_0	Beattie-Bridgeman constant.	$=1.8006\times10^{-3}$	$m^3\ kg^{-1}$
c	Beattie-Bridgeman Temperature coefficient.	$=15.017\times10^{-6}$	$m^3\ K^3\ kg^{-1}$
C_f	Capacitance of an accumulator.		$m^5\ N^{-1}$
C_{gas}	Capacitance of Charge-Gas		$m^5\ N^{-1}$
C_{oil}	Capacitance of Oil		$m^5\ N^{-1}$
C_p	Specific heat of gas at constant pressure.		$J\ kg^{-1}\ K^{-1}$
C_v	Specific heat of gas at constant volume.		$J\ kg^{-1}\ K^{-1}$
C_1	Constant for C_v	$=1.49\times10^{-4}$	$J\ kg^{-1}\ K^{-3}$
C_2	Constant for C_v	$=-3.17\times10^{-2}$	$J\ kg^{-1}\ K^{-2}$
C_3	Constant for C_v	$=740.6479$	$J\ kg^{-1}\ K^{-1}$
C_5	Factor to correct for proximity of P to P_l		
D	Accumulator inside diameter		m
D_p	Inlet pipe inside diameter		m
e	Base for natural logarithms	$=2.71828$	

e	Elemental error	$=1.0X10^{-11}$	
E	Total energy of a process		J
g	Constant of gravitation	=9.80665	$m\ s^{-2}$
h	Coefficient of convective heat transfer		$J\ m^{-2}k^{-1}s^{-1}$
i,j	Counters		
j	Upper limit of summation	$=t/\Delta t$	
J_0	Bessel function of the first kind, zero order.		
J_1	Bessel function of the first kind, first order.		
k	Thermal conductivity		$J\ m^{-1}s^{-1}K^{-1}$
K_1	Proportionality constant relative to L/D	=0.428	
K_3	Constant for convection in enclosed spaces.	=0.23	
K_5	Proportionality constant for pipe resistance.	=100.0	$Pa^{\frac{1}{2}}\ s\ m^{-2}$
K_{10}	Constant for N_{pr}.	$=-2.325X10^{-4}$	T^{-1}
K	Constant for N_{pr}.	=0.783	
L	Internal diameter of accumulator		m
L_p	Internal diameter of inlet pipe.		m
m	Mass of charge-gas in accumulator		kg
m	Summation index		

n	Exponent for calculation of α_e	$=0.23$	
n	Summation index.		
N_{gr}	Grashoff number		
N_{nu}	Nusselt number		
N_{pr}	Prandtl number		
P	Average pressure of charge at any instant of time.		Pa
P_a	Pressure after adiabatic expansion		Pa
P_{init}	Value of P from initial calculations		Pa
P_ℓ	Line pressure (in conduit outside of accumulator)		Pa
P_s	Pressure at standard conditions (absolute)		Pa
P_0	Precharge pressure		Pa
P_1	Initial compression pressure		Pa
P_2	Any pressure state other than P_1		Pa
P_3	Pressure after discharge	$=P_a$	Pa
Q	Net flow of oil into or out of accumulator		$m^3 s^{-1}$
Q_h	Heat into or out of a thermodynamic system		J
r	Radial dimension		m
r'	Normalized radius	$= r/R$	

R	Internal radius of accumulator		m
R_{es}	Resistance of inlet pipe		$Pa^{\frac{1}{2}} s\ m^{-3}$
R_u	Universal gas constant	= 296.797	$J\ kg^{-1}\ K^{-1}$
t	Time		s
t'	Normalized time	$= \alpha_e t/R^2$	s
T	Temperature as function of position and time		K
T_a	Temperature after adiabatic expansion		K
T_0	Precharge or ambient temperature		K
T_2	Temperature immediately after initial oil charge		K
T_3	Temperature immediately after discharge	$= T_a$	K
U	Internal energy of gas in a process		J
v	Specific volume as function of time		$m^3 kg^{-1}$
v_0	Specific volume of charge gas at precharge conditions		$m^3 kg^{-1}$
v_s	Specific volume of nitrogen at STP	= 0.87	$m^3 kg^{-1}$
v_1	Specific volume of charge gas immediately after initial oil charge		$m^3 kg^{-1}$
v_2	Specific volume of charge gas after initial oil charge at steady state		$m^3 kg^{-1}$

V	Volume of charge-gas at any instant of time		m^3
V_{init}	Volume of charge-gas after compression to P_{init}		m^3
V_{oil}	Volume of oil in accumulator at any instant of time		m^3
V_0	Original volume of gas at precharge		m^3
V_1	Compressed volume on gas side		m^3
W	Work done by a process		J
x	Axial dimension from midpoint of cylinder		m
x'	Normalized axial dimension	$= x/L$	
X	Transfer variable	$= R_u T/P_a$	$m^3 kg^{-1}$
α_e	Effective thermal diffusivity		$m^2 s^{-1}$
α_0	Thermal diffusivity at precharge conditions		$m^2 s^{-1}$
α_s	Thermal diffusivity at STP for charge gas (nitrogen)	$= 22X10^{-6}$	$m^2 s^{-1}$
β	Coefficient of thermal expansion		K^{-1}
γ	Ratio of specific heats		
δ	Characteristic dimension		m
ΔE	Difference in total energy in a process		J
ΔP_i	Pressure difference across inlet		P_a

Δt	Real time simulation step size		s
ΔT	Temperature difference between each iteration		K
ΔU	Difference in internal energy in a process		J
Δv	Specific volume difference between each iteration		$m^3 kg^{-1}$
ΔV_{oil}	Difference in oil volume for each iteration		m^3
ε	Transfer variable	$= (2n-1)\pi/2$	
ν_s	Kinematic viscosity of charge-gas (nitrogen) at STP	$= 15.6X10^{-6}$	$m^2 s^{-1}$
ν_0	Kinematic viscosity of charge-gas at precharge		$m^2 s^{-1}$
ν_1	Any kinematic viscosity different from ν_2		$m^2 s^{-1}$
ν_2	Any kinematic viscosity different from ν_1		$m^2 s^{-1}$
ξ	Emissivity of charge-gas		
ρ	Bulk fluid density		$kg\ m^{-3}$
ρ_0	Bulk fluid density in heated layer of gas		$kg\ m^{-3}$
τ	Thermal time factor (constant or variable)		s
Ψ_m	Zeroes of Bessel function $(J_0(\Psi_m) = 0)$		

Note: Bibliographic reference numbers are shown thus: |79|

LIST OF FIGURES AND TABLES.

LIST OF APPENDIXES

CHAPTER 1

INTRODUCTION

Recent developments in the world energy situation has prompted research into all areas of energy conservation and storage.

One of these, hydraulic power systems, is under close examination at Concordia University. Hydraulic power offers advantages in areas of energy conservation and storage such as regenerative braking and off-peak accumulation of energy along with the more obvious advantages of flexible short distance transmission and fast system response.

As the basic energy storage component of hydraulic power systems, the accumulator is an important subject of research. Also, with the advance of computers as a tool for analysis, mathematical modelling is becoming one of the most popular methods of research. An accurate mathematical model of the hydraulic accumulator would improve computer simulation of large hydraulic systems.

Hydraulic accumulators are energy storage devices used in hydraulic power systems. They consist primarily of a vessel into which hydraulic fluid is stored at system pressure, to be used when needed. The energy storage takes place by

compression of a spring, by compression of a gas, by lifting a weight, or by a combination of these.

Older accumulators consisted of a tank in which pressurized air and the hydraulic fluid were enclosed. Water, as the hydraulic fluid compressed the air. (Some of the air would dissolve into the water and the mixture became very corrosive).

Today, most hydraulic fluids are corrosion inhibited, fire retardant oils. The accumulators are charged with a stable gas such as nitrogen and isolated from the fluid to prevent loss of gas by dissolution.

The two most commonly used types are:

1) A cylindrical piston accumulator that uses nitrogen for the charge gas.
2) A spherical diaphragm accumulator that has a rubber membrane enclosing the charge-gas.

Although the diaphragm accumulator is more common (less precision is required in its construction), the thermal properties of the diaphragm and the different diaphragm configurations available make analysis of the thermal phenomena quite complex. The piston accumulator, on the other hand, has more homogeneneous configuration and is a logical first step in preparing mathematical models for accumulators.

The object of this thesis is, therefore, to present an accurate mathematical model for nitrogen charged hydraulic piston accumulators, and to confirm this model with experiments.

Original mathematical models considered the hydraulic accumulator as having the characteristics of an electrical capacitor for example, Shearer, Murphy, Richardson |1|. This led to rather large errors in some cases, as can be seen by examination of the typical charge - discharge cycle shown in figure 1.1.

a) Originally, the accumulator has been precharged with nitrogen to a pressure (P_0), giving a specific volume of (v_0), at an ambient wall temperature (T_0). (figure 1.1 a).

b) The accumulator is then charged with oil rapidly such that the compression is not isothermal (any velocity faster than the ability of the gas to transfer heat to the walls. Since a gas has slow heat transfer characteristics, almost any oil velocity is adequate). The charge gas now has instantaneous state (P_1, v_1, and T_1), different from (P_0, v_0, T_0), (since this is a compression, $T_1 > T_0$). (figure 1.1 b).

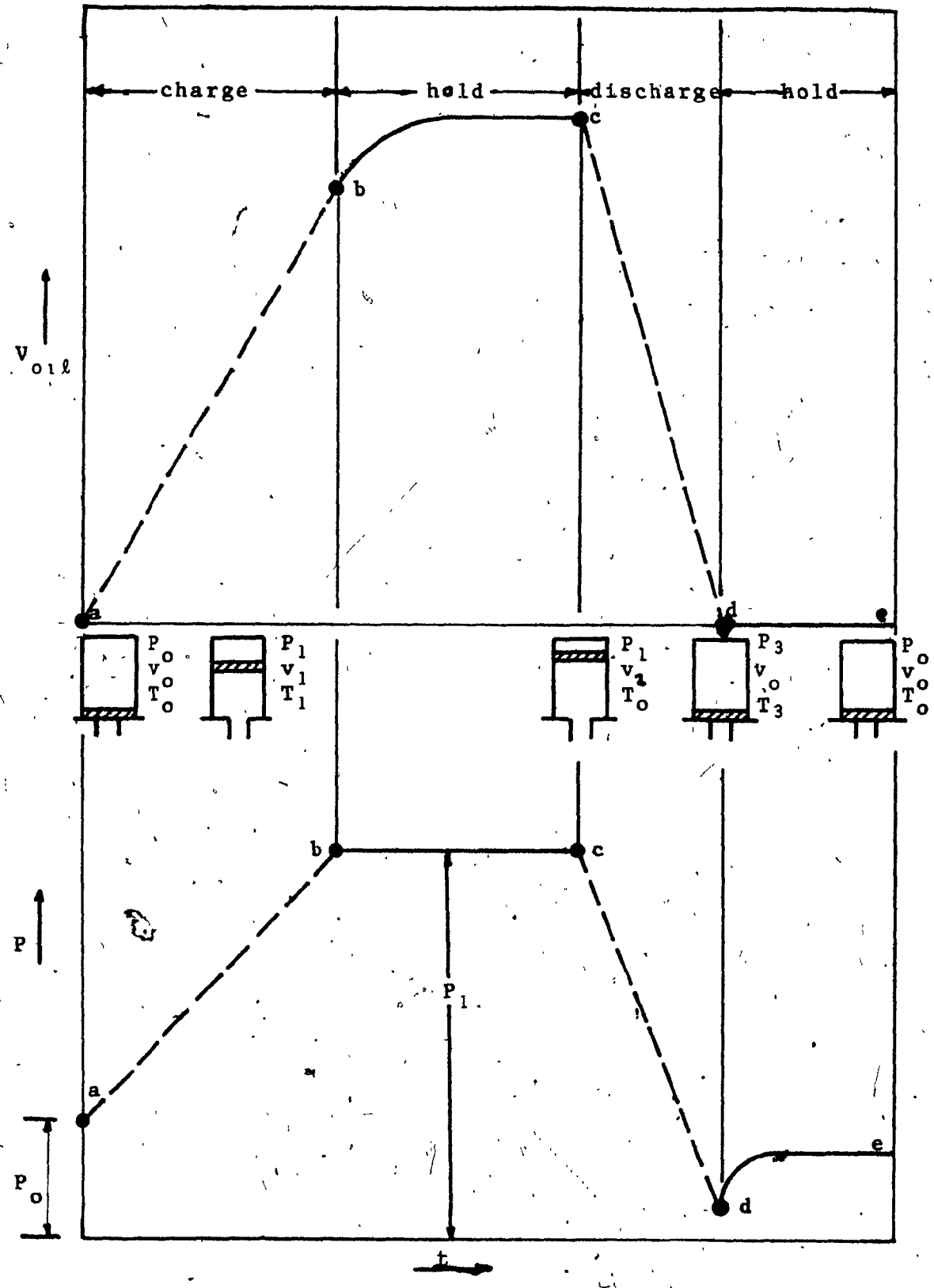

Fig. 1.1 Charge and Discharge Cycle for an Accumulator.

Pressure - and Oil Volume - Time Relations.

c) Oil pressure is maintained at P_1 until steady state is reached. Heat transfers slowly from the gas to the walls of the accumulator until, at steady state, $T_1 = T_0$. Therefore v_1 has decreased to v_2. This implies that more oil has flown into the accumulator. (figure 1.1 c).

d) The accumulator is then completely discharged "rapidly". The charge gas takes on the state (P_3, v_0, T_3) where $P_3 < P_0$ and $T_3 < T_0$ since this was not an isothermal discharge. (figure 1.1 d).

e) Heat is transfered slowly from the walls to the gas until steady state is reached at $P_3 = P_0$ and $T_3 = T_0$. (figure 1.1 a).

Let us now examine what has happened:

The ideal fluid capacitance constitutive relationship given by Shearer, Murphy, Richardson |1|is:

$$V_{oil} = C_f P_l \qquad (1.1)$$

where (P_l) is line pressure and (C_f) is the capacitance, a constant and (V_{oil}) is the volume of oil in the accumulator at any time.

From figure 1.1 we see that V_{oil} is time varying in the interval from (b) to (c), while P_l is invariant. Similarly, V_{oil} is invariant from (d) to (e), while P_l is varying.

Clearly, C_f in the above constitutive relationship cannot be a constant and the equation becomes highly inaccurate under these conditions.

Indeed, from Lindsay and Katz |2|:

$$C_f = \frac{V_{oil}}{P} \quad \text{isothermal process} \qquad (1.2\ a)$$

and,

$$C_f = \frac{V_{oil}}{\gamma P} \quad \text{adiabatic process} \qquad (1.2\ b)$$

Where (P) is the absolute pressure of the accumulator gas and (γ) is the ratio of specific heats of the gas.

It is seen that C_f is dependent upon the geometry of the accumulator, the instantaneous pressure and the speed of the process (which specifies the value of (γ) the polytropic exponent).

Although these models are adequate for coarse simulations, they are not accurate enough to design a modern, energy efficient power system. They could not, for example, be used to size an accumulator for attenuation of pulsations in a system nor could they be used to balance a system nor to size the power supply. Thus, an accurate model, capable of taking into account the time dependent thermal effects is needed.

If we consider using a model such as represented by equation 1.2b, a value for the polytropic exponent (γ) is needed, but Graze |3| |4| states that the use of a single polytropic exponent is "fundamentaly wrong in principle". The initial change is adiabatic while the overall steady state change is isothermal. He proposes a formulation for pressure changes that includes the effect of a rational convective heat transfer process.

The performance of gas-charged accumulators is similar to that of enclosures and is dependent on the thermodynamic process which takes place in the gas. Gagnath and White |5| also consider the process as either isothermal or adiabatic depending on the speed of the cycle. They derive an optimum pressure ratio as a function of the process and show that the gas behaviour deviates considerably from ideal.

Klein |6| finds the efficiency of various load cycles by using a polytropic exponent somewhere between the isothermal and adiabatic values.

Roper |7| in the same manner as proposed by Lindsay and Katz |2| makes use of the electrical analogy and represents the accumulators as a capacitor, the capacitance of which is a function of a polytropic exponent.

Green |8| on the other hand, connects the polytropic index to an empirical exponential cooling curve.

This exponential cooling curve concept is also used by Otis |9| |10| |11|, and Elder and Otis |12|. Accumulator performance is here described by an exponential thermal time constant which must be determined experimentally.

The mathematical model proposed in this thesis also uses an exponential cooling curve with thermal time constant to represent the accumulator characteristics but there are two basic differences from Green and from Otis. First, the time constant is shown to be calculatable, dependent on the particular thermal state of the charge gas and on the geometry of the accumulator. Secondly, that this time constant is not constant.

CHAPTER 2

THEORY

2.1 General

This chapter will analyze the thermal phenomena within the charge gas of the accumulator and will derive, based on the heat conduction distribution equations from Carslaw and Jaeger |13| further developed by Svoboda, Bouchard and Katz |14|, a set of thermal equations on which the mathematical model will be based.

Enclosed tanks have been modelled as capacitors. The capacitive effect has been well researched and has been used in widely divergent fluid systems from common domestic water systems through hydraulics, fluidics and hydraulic power systems. In general, they may be classified by levels of operating pressure and by frequency and speed of operation.

At low pressure levels, the thermal transient effects are mainly due to conduction whereas at high pressures convection effects take predominance. On the other hand, slow operating speeds or infrequent use imply an isothermal process and high speeds or high frequency of cycling imply an adiabatic process.

The hydraulic, gas-charged accumulators of this study are normally used in hydraulic systems operating at pressures from 3.5 to 35 MPa, where convection effects predominate. Also, the charge and discharge of these accumulators is very rarely slow enough for the process to be considered isothermal.

2.2 Thermal Analysis

2.2.1 Heat Conduction Distribution

The thermal analysis is performed by considering the accumulator as a cylindrical configuration as shown in figure 2.1. This represents a gas-charged hydraulic accumulator after adiabatic discharge of the oil. The cylinder of length (L) and diameter (D) consists of a non-moving gas in a solid container. The temperature throughout the gas, due to the sudden adiabatic expansion, has fallen to temperature (T_a), below ambient. All the contact surfaces of the gas are maintained at constant temperature (T_0) by the isothermal walls of the container.

At this point, the basic assumptions of this analysis must be stated:

1) The temperature distribution in the gas is similar to that in a solid (this is heat conduction distribution).
2) The walls of the accumulator remain at constant temperature (isothermal, infinite, heat sink).

Based on these assumptions, the temperature (T) in the gas at any point and at any time after the sudden expansion is given by Garslaw and Jaeger |13| as:

$$\frac{T - T_a}{T_o - T_a} = 1 - \frac{8}{\pi} \sum_{n=0}^{\infty} \sum_{m=1}^{\infty} \frac{(-1)^n \; J_0(r' \; \Psi_m)}{(2n-1) \; \Psi_m \; J_1(\Psi_m)} \cos \{2\varepsilon_n x'\} \; e^{(-B_e t')} \qquad (2.1)$$

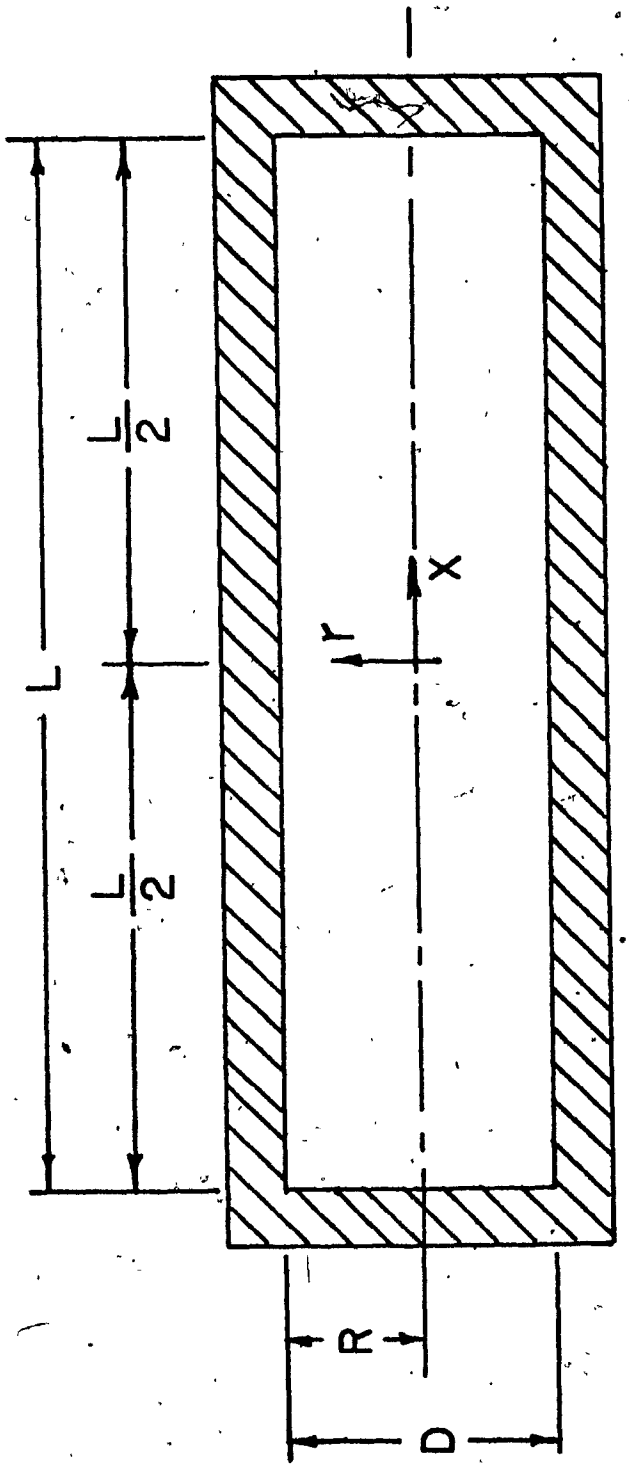

Fig. 2.1 Configuration of a Typical Accumulator for Thermal Analysis. From [14].

where:

$r' = r/R$; $x' = x/L$; $t' = \alpha_e\, t/R^2$;

$\epsilon_n = (2n - 1)\pi/2$; and Ψ_m are zeroes of $J_0(\Psi_m) = 0$;

J_0 and J_1 are Bessel functions of the first kind;

$B_e = \Psi_m^2 + \epsilon_n^2 /(L/D)^2$ and α_e is the effective thermal diffusivity (m^2/s).

The diffusivity of a gas is related to its conductivity, and we can say that:

$$\frac{\alpha_e}{\alpha_0} = \frac{k_e}{k_0} \qquad (2.2a)$$

Where (α_0) is the diffusivity at precharge pressure, k_e and k_0 are, respectively, the effective conductivity and the conductivity at precharge conditions.

This effective conductivity (k_e) is given by Holman |15|, by Jakob |16|, and by Welty, Wicks, Wilson |17|, as having the following relationship:

$$\frac{k_e}{k_0} = N_{nu} = K_3 \left[N_{gr\delta}\ N_{pr}\right]^n \qquad (2.2b)$$

Where (N_{nu}) is the Nusselt number;

(N_{gr}) is the Grashoff number for (δ)

(N_{pr}) is the Prandtl number

and (n) for laminar convection is generally given the value of 0.25 .

For the constant (K_3) in the particular case of a horizontal or vertical cylinder with free convection from a gas inside of the cylinder, no value is available from the authors cited. Examination of a range of values given for similar cases plus some empirical fitting has led to the use of $K_3 = 0.23$.

The average temperature ratio is defined by integration over the entire volume:

$$\left(\frac{T - T_a}{T_o - T_a}\right)_{average} = \int_0^1 \int_{-\frac{1}{2}}^{+\frac{1}{2}} r^2 \left(\frac{T - T_a}{T_o - T_a}\right) dx' \, dr' \qquad (2.3)$$

Equation (2.1) is substituted into equation (2.3), the integration is performed giving:

$$\left(\frac{T - T_a}{T_o - T_a}\right)_{average} = 1 - 8 \sum_{n=0}^{\infty} \sum_{m=1}^{\infty} \frac{e^{(-B_e t')}}{(\varepsilon_n^2 \Psi_m^2)} \qquad (2.4)$$

The average temperature ratio is plotted and shown as figure 2.2, where the abscissa is normalized time. Several curves are plotted to show the effect of different L/D ratios (A parameter of the variable (B_e) in equation (2.4)). After adiabatic expansion of the gas, where (T) at all points has

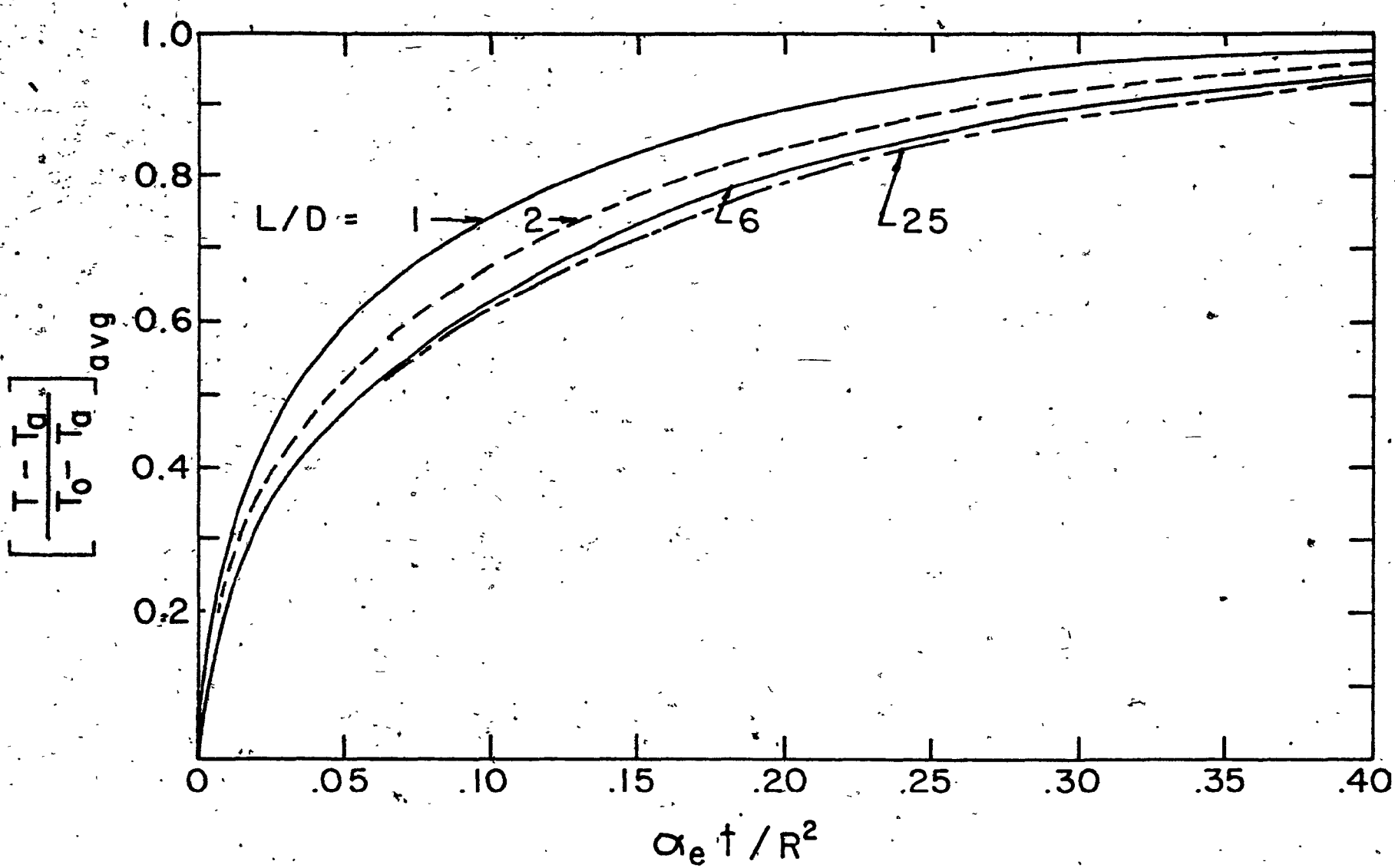

Fig. 2.2 Average Temperature vs Normalized Time. From |14|.

dropped well below (T_0) to a value such that the ATR (average temperature ratio) equals zero, heat transfer from the walls to the gas raise the temperature of the gas until, as time approaches infinity, ($T \rightarrow T_0$) (the ATR $\rightarrow$ 1).

Observe that the L/D ratio parameter affects the time required for this temperature change. Indeed, the time decreases as the L/D ratio decreases. The L/D to time relationship is non-linear as shown by the curves in figure 2.2.

Although the shape of the curves of figure 2.2 is not a pure exponential, the effect of L/D may be demonstrated by defining the time constant (τ) as the time at which the ATR reaches a value 0.632 (a standard definition of time constants). Thus for L/D = 1 at ATR = 0.632, we have $\alpha_e \cdot t/R^2 = 0.06 = \alpha_e \tau/R^2$. On figure 2.3, the solid curve is a plot of the $\alpha_e \tau/R^2$ values as a function of the L/D ratios. As L/D increases the time constant parameter increases less and less and approaches a constant value at large L/D values. This behaviour suggests the time constant parameter may be proportional to the volume / surface area ratio. To test this possibility in normalized form, the following relation is suggested:

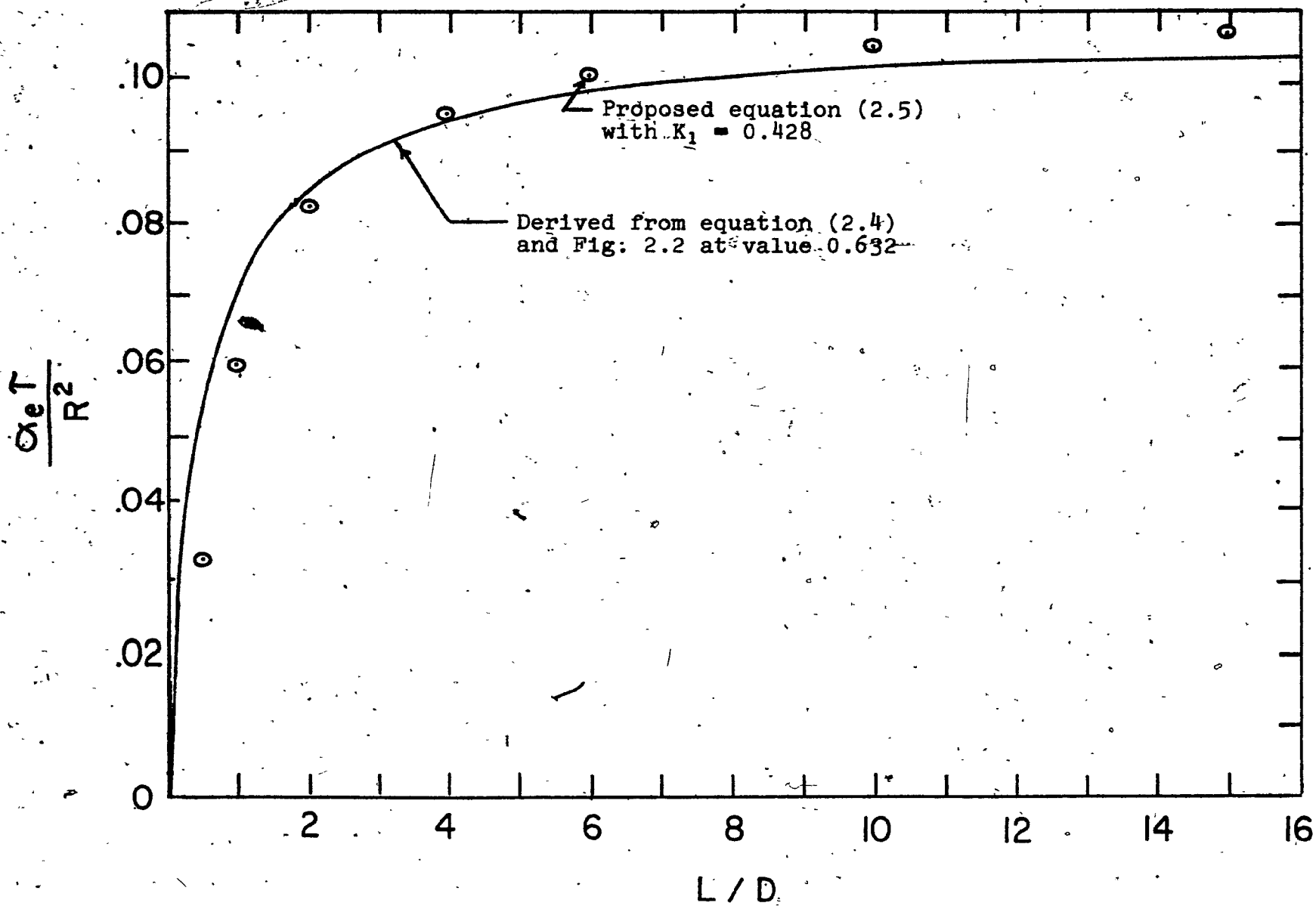

Fig. 2.3 Time Constant Parameter vs L/D. From |14|.

$$\frac{\alpha_e \tau}{R^2} = \frac{K_1 \quad (\text{volume})}{(\text{Dia})\ (\text{surface area})} = K_1 \left[\frac{\pi L D^2/4}{(D)\ ((2\pi D^2/4) + \pi D L)} \right]$$

$$= K_1 \left[\frac{L/D}{2 + 4L/D} \right] \omega \qquad (2.5)$$

Where (K_1) is a proportionality constant. This data is also plotted on figure 2.3, as discrete points, (with (K_1) selected as 0.428 to provide good agreement). The close correspondence of equation (2.4) shows that the volume to surface ratio is a useful concept in understanding the effect of L/D on the time constant.

2.2.2 Pressure - Time Relations

The performance of accumulators is measured in terms of pressure rather than temperature, thus relations between temperature and pressure must be found to convert our heat conduction distribution equations. Referring back to figure 1.1, we note that with no oil in the accumulator, but after precharge with nitrogen, the steady state values are (P_0 , v_0 , T_0). The accumulator is then charged with oil and after steady state is reached the values are (P_1 , v_1 , T_0). If all pressures are absolute, we may use Boyle's law and obtain:

$$\frac{P_1}{P_0} = \frac{v_0}{v_1} = \frac{V_0}{V_1} \qquad (2.6)$$

Where (V_0) is the original volume at precharge and (V_1) is the compressed volume of gas.

The accumulator oil is suddenly discharged. Gas pressure drops instantaneously and adiabatically to a pressure (P_a). Since the volume (V) after discharge is the same as before charge, we can say that the relation between (P_a) and (P_1) is:

$$\frac{P_1}{P_a} = \left(\frac{V_0}{V_1}\right)^{\gamma} \qquad (2.7)$$

where (γ) is the ratio of specific heats of the charge-gas.

Immediately after the oil is removed, the time period for calculations begin. In the transient heat transfer period which follows, the charge-gas pressure (P) is a function of time.

Since the gas specific volume is constant during this time, by the equation of state, we may relate (P) directly with temperature, therefore, we can say:

$$\frac{P - P_a}{P_0 - P_a} = \frac{T - T_a}{T_0 - T_a} \qquad (2.8)$$

where (T) is the average temperature.

Equations (2.4) (2.5) and (2.8) can be combined to obtain the heat conduction distribution model as:

$$\left[\frac{P - P_a}{P_0 - P_a}\right] HCD = 1-8 \sum_{n=0}^{\infty} \sum_{m=1}^{\infty} \frac{e^{\left(-K_2 B_e t/\tau\right)}}{\varepsilon_n^2 \cdot \Psi_m^2} \qquad (2.9)$$

where $K_2 = \frac{\alpha_e \tau}{R^2} = \frac{K_1 \quad (L/D)}{2 + 4 \ (L/D)}$ from equation (2.5).

2.2.3 Derivation of the Exponential Model

The exponential model derived by Otis |9| |10| |11| is used as a base for this model. It is derived in the following manner, starting with the second law of thermodynamics:

$$Q_h = \Delta E + W \qquad (2.10)$$

where (Q_h) is the net amount of heat transferred into or out of the charge-gas; (ΔE) is the total change in energy of the gas and (W) is the work done on or by the process. If we ignore potential energy, magnetic energy and all other minor energy sources, we can say:

$$Q_h = \Delta U + W \qquad (2.11)$$

where (ΔU) is the change in internal energy of the gas. Since this is a low friction process, we may assume it to be frictionless and:

$$W = \int P dV \qquad (2.12)$$

and,

$$\Delta U = mC_v (T_o - T) \qquad (2.13)$$

where (V) is the volume of the gas at any instant in time; (P) is the pressure at that instant; and (m) is the mass of charge gas, a constant.

Using (2.12) and (2.13) into (2.11), we have:

$$Q_h = mC_v (T_o - T) + \int PdV \qquad (2.14)$$

deriving with respect to time gives:

$$\frac{dQ_h}{dt} = -mC_v \frac{dT}{dt} + P \frac{dV}{dt} \qquad (2.15)$$

Now, the rate of heat transfer in the charge-gas, i.e. Newton's law of cooling for a (convection) process, is given by Welty Wicks Wilson |17| as:

$$\frac{dQ_h}{dt} = h A_s (T_o - T) \qquad (2.16)$$

where (h) is the coefficient of convective heat transfer and (A_s) is the surface area in contact. Replacing $\frac{dQ_h}{dt}$ in (2.15) by (2.16) gives:

$$h A_s (T_o - T) = -mC_v \frac{dT}{dt} + P \frac{dV}{dt} \qquad (2.17)$$

This equation will be used in the model, but for purposes of examining the transient after a discharge, it can be defined here that this is a constant volume process for which:

$\frac{dV}{dt} = 0$ and rearranging (2.17) we obtain:

$$\frac{-1}{T_o - T} dT = \frac{h A_s}{mC_v} dt \qquad (2.18)$$

Integrating both sides, we have:

$$T - T_o = e^{-\left(\frac{h A_s}{mC_v}\right)t} \qquad (2.19)$$

which implies, at the instant of adiabatic discharge, when $T = T_a$ and $t = 0$, that:

$$T_a - T_o = e^0 \qquad (2.20)$$

and:

$$\frac{(T - T_o) - (T_a - T_o)}{-(T_a - T_o)} = \frac{e^{-\left(\frac{h A_s}{m C_v}\right)t} - e^0}{-e^0} \qquad (2.21)$$

or:

$$\left(\frac{T - T_a}{T_o - T_a}\right)_{ave} = 1 - e^{-\left(\frac{h A_s}{m C_v}\right)t} \qquad (2.22)$$

Using equation (2.8):

$$\frac{P - P_a}{P_o - P_a} = 1 - e^{-\left(\frac{h A_s}{m C_v}\right)t} \qquad (2.23)$$

For Otis, $\tau = mC_v / (hA_s)$, and he suggests that this value be found experimentally for each case. This derivation shows the validity of using an exponential equation as a model for a hydraulic accumulator. However the time constant (τ), varies as a function of the surface (A_s) of contact. The area in turn varies as the accumulator is charged. In addition, (C_v) and (h) also vary. As a result, the use of a time constant based on fixed parameters will cause inaccuracies in the calculation of pressure.

2.2.4 Comparison of the Heat Conduction Distribution Model vs the Exponential Model.

Comparison of the results of the H C D (Heat Conduction Distribution) model of equation (2.9) and the exponential model of equation (2.23) is made in figure 2.4.

The H C D model is now relatively insensitive to the L/D ratio because of normalization by including the time constant parameter. The pressure ratio in the H C D model increases more rapidly initially than in the exponential model. However, the exponential approaches the final value in less time. By definition, both models have the values 0.632 at $t/\tau = 1$.

A logical conclusion of this comparison is to use the exponential model proposed by Otis with calculation of the time constant by the derived equation (2.5). This is the base used for preparation of the models developed in chapter 3.

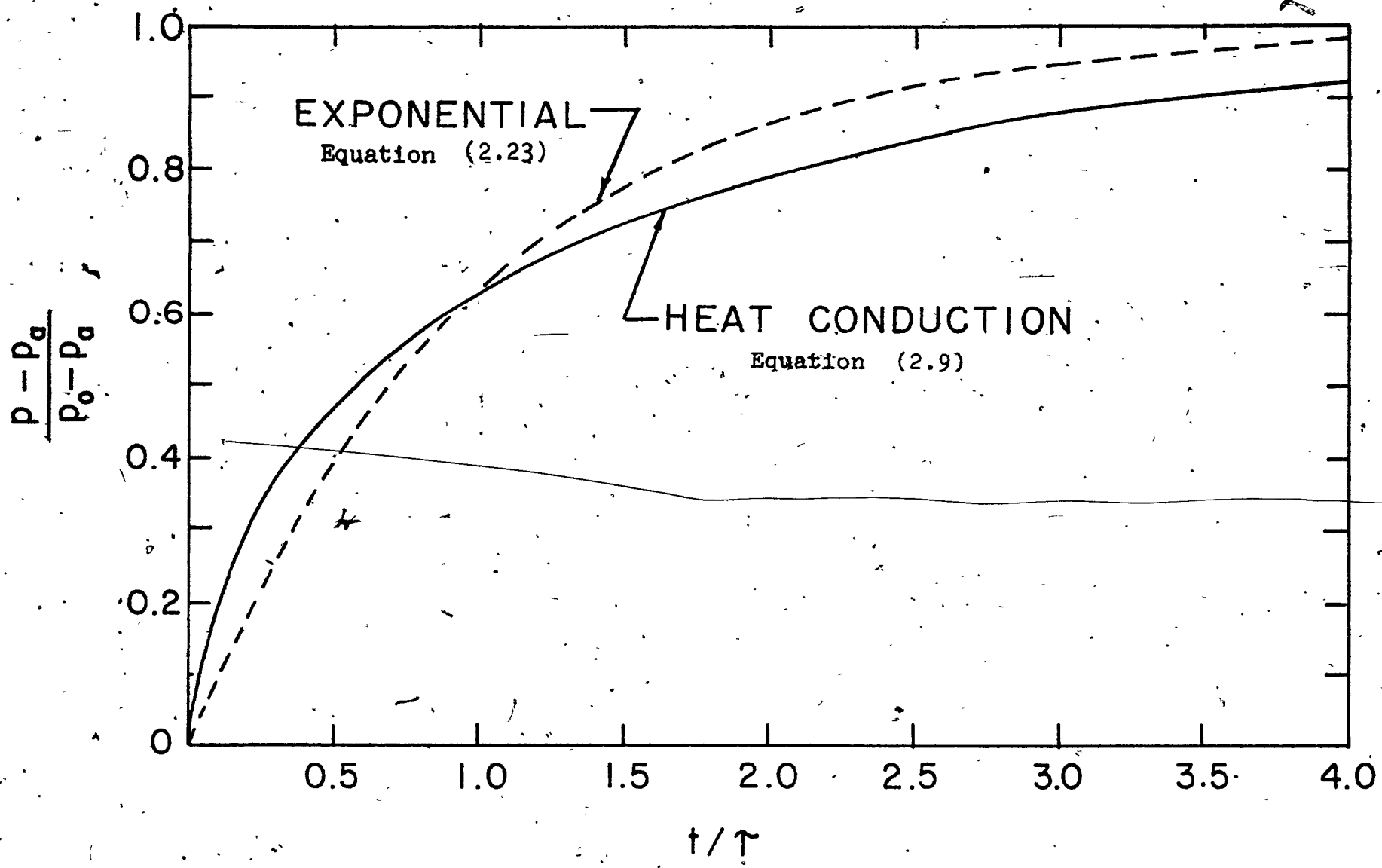

Fig. 2.4 Comparison of Proposed Thermal Models. From [14].

CHAPTER 3

MODELLING

3.1 General

As we have stated in the previous chapter, the models proposed are those developed by Otis |9| |10| |11| and Elder and Otis |12|, with the main modifications that:

1) The time constant is calculated using the equations developed by Svoboda, Bouchard and Katz |14| for the time constant which, in effect, is temperature dependent and must therefore be recalculated at every iteration: It is a variable.
2) Equations for a real gas are used.

Two models are proposed. The first model behaves as a fluid capacitance: the input variable is pressure at the inlet to the accumulator and the output is flow of fluid into or out of the accumulator (see figure 3.1a). This model is for use when pumps in the system act as combined pressure-flow sources such as a centrifugal pump.

After initial calculations the input signal (oil pressure outside the accumulator at the discharge point) is used to calculate the flow rate (Q). The flow rate is then

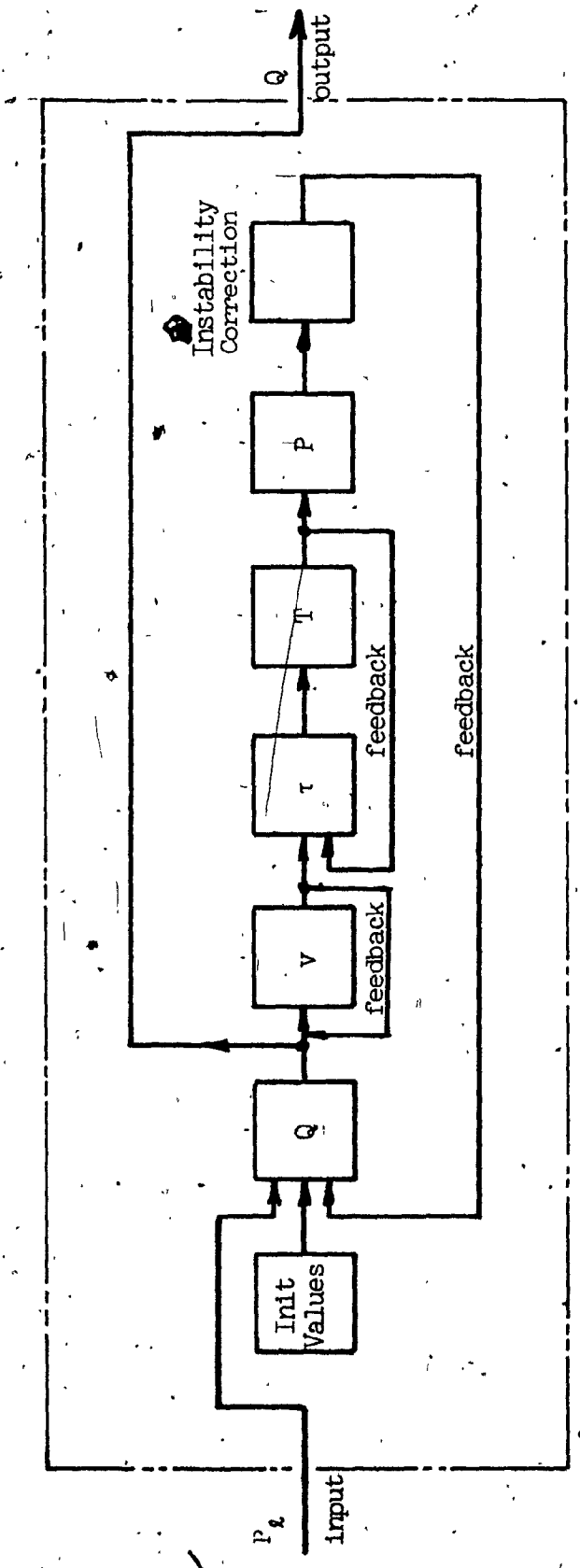

Fig. 3.1a Pressure Input Model Block Diagram.

used to calculate the specific volume (v) the time 'constant', (τ) the gas temperature (T), and finally the gas pressure (P). After a stability test, the previously calculated (Q) is sent out to the system simulation while (P, T and v) are fed back into the model for use in the next iteration.

The second model behaves in the inverse manner: the input variable is flow into or out of the accumulator whereas the output is pressure in the accumulator acting on the system (see figure 3.1b). This model is for use with systems using positive displacement pumps acting as flow sources only. This type of pump is more frequent in hydraulic power systems.

After initial calculations the input signal, the flow rate of oil out of the accumulator (Q) is tested to prevent discharging more oil than there is in the accumulator. If (Q) is valid, it is used to calculate (v, τ, T and P). (P) is sent out to the system simulation while (T) and (v) are fed back for the next iteration. If (Q) is invalid, a valid (Q) is calculated and an alarm message sent to the system simulation while the valid (Q) is used to continue the simulation.

As can be seen in figure 3.1, each model is made up of a series of algorithms each with one specific purpose or variable to calculate. The algorithms, where repeated, are exactly the same in both models and will be developed only once.

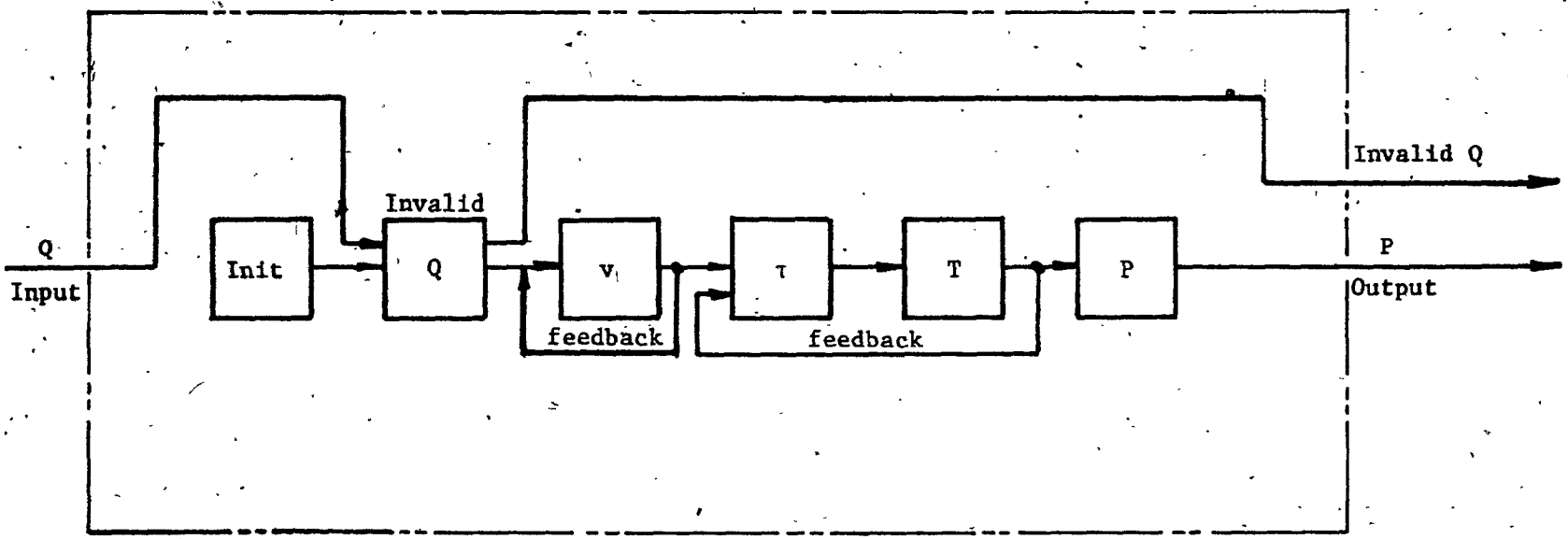

Fig. 3.1b Flow Input Model Block Diagram.

3.2 Algorithm for Pressure Within the Charge-Gas, P.

The equation used for calculation of pressure in the charge-gas at any instant in time is the Beattie-Bridgeman derivation from Jones and Hawkins |18|:

$$P = R_u T \frac{(v+B)}{v^2}(1-\xi) - \frac{A}{v^2} \qquad (3.1)$$

where:

(P) is the average pressure of the charge-gas at any time;

(R_u) is the universal gas constant;

(T) is the temperature at that instant of time;

(v) is the specific volume of the charge-gas at that instant;

(A, B) and (ξ) are Beattie-Bridgeman coefficients, functions of the specific volume and the temperature.

These are calculated from the Beattie-Bridgeman constants: (A_o, a, B_o, b and c), in the following equations:

$$A = A_o \left(1 - \frac{a}{v}\right) \qquad (3.2)$$

$$B = B_o \left(1 - \frac{b}{v}\right) \qquad (3.3)$$

$$\xi = \frac{c}{vT^3} \qquad (3.4)$$

Equations 3.2 and 3.3 will be used as part of the specific volume algorithm in article 3.3.

Calculations of the maximum value of (ξ) for the ranges under consideration, have shown it to be of the order of 3×10^{-10}. Its effect on the pressure results is negligible. The term, $(1 - \xi)$, can be dropped from the equation leaving the schema for the algorithm as per figure 3.2 where (P) is a function only of (T, v, A and B). The inputs to the algorithm are the values of (T, v, A and B) for the iteration. The output is (P).

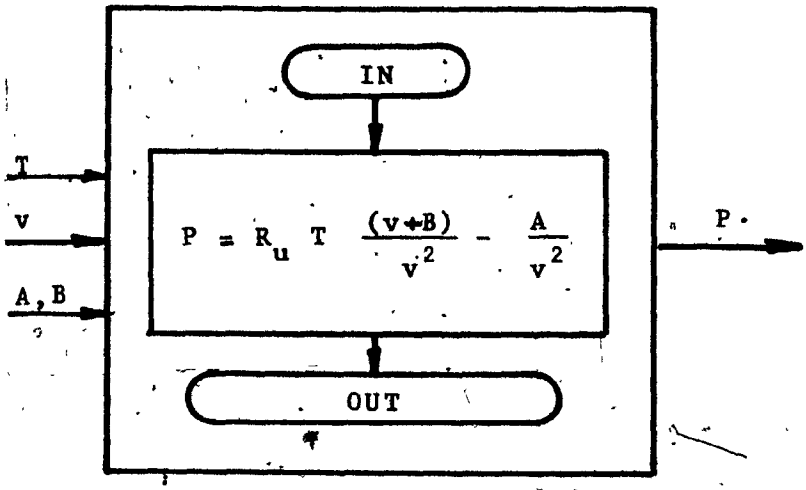

Fig. 3.2 Schema: Algorithm for (P).

3.3 Algorithm for Specific Volume, v.

Specific volume (v) is, by definition, a function of the volume of the gas (V) at any time and the mass of the gas, (m) (constant for any given system) or:

$$v = \frac{V}{m} \tag{3.5}$$

differentiating:

$$\frac{dv}{dt} = \frac{1}{m} \frac{dV}{dt}$$

Since $\frac{dV}{dt}$, the change in volume of the gas is directly proportional to (Q), the flow rate of oil out of the accumulator, we can say that:

$$dv = \frac{1}{m} Q\, dt \tag{3.6}$$

In finite difference form equation (3.6) becomes:

$$\Delta v = \frac{1}{m} Q \Delta t \tag{3.7}$$

and:

$$v = \int dv - \frac{1}{m} \int_{o}^{t} Q\, dt - v_o \tag{3.8}$$

where (v_o) is the value of (v) at precharge. This, in finite difference form becomes:

$$v = v_o + \sum_{m=1}^{j} \Delta v_m \tag{3.9}$$

where the upper limit, $j = t/\Delta t$ at any instant in time.

Having now an accurate value for (v) for the present iteration, it is appropriate to calculate accurate values of the Beattie-Bridgeman coefficients, (A) and (B) as part of this algorithm since they will be subsequently used. Equations (3.2) and (3.3) are added for this purpose. The schema for this algorithm is shown in fig. 3.3. The input is the flow rate (Q) and the time step parameter (Δt). From these, using equations 3.7, 3.9, 3.2, and 3.3, the values of (Δv, v, A and B) are calculated and stored for access by the other algorithms. The algorithm calculates the instantaneous value of the specific volume (v) by calculating (Δv), and adding to the previous value of (v). This is an "integrator".

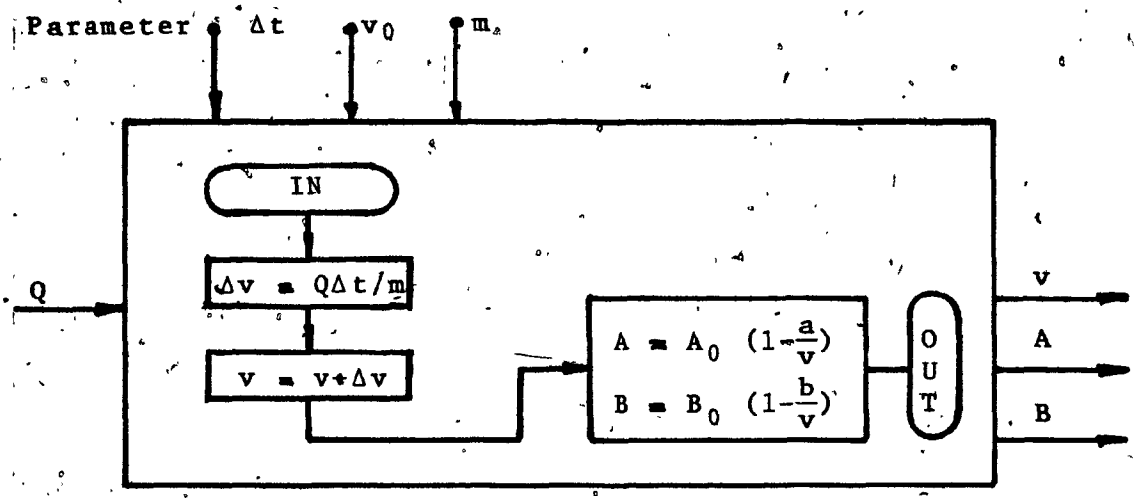

Fig. 3.3 Schema: Algorithm for (v).

3.4 Algorithm for the Time Constant, τ.

As we have shown in article 2.3 of chapter 2 of this thesis, the time 'constant' (τ) is dependent on the geometric properties of the accumulator and on the state of the gas at each instant of time. It is therefore a variable which must be recalculated at each iteration.

A method of calculation based on the heat conduction distribution equations developed by Svoboda, Bouchard and Katz |14| was partly derived in article 2.2 of chapter 2 and continues here. Using equation (2.5) and rearranging, we have:

$$\tau = \frac{R^2}{\alpha_e} \cdot K_1 \left[\frac{L/D}{2 + 4L/D}\right] \qquad (3.10)$$

where $K_1 = 0.428$ as per Svoboda, Bouchard and Katz.

(α_e) is the effective diffusivity for free convection in enclosures. This is given by equation (2.2) transposed:

$$\alpha_e = \alpha_o K_3 \left[N_{gr} N_{pr}\right]^{\frac{1}{4}} \qquad (3.11)$$

where (N_{gr}) is the Grashoff number; (N_{pr}) the Prandtl number; (K_3) is a constant = 0.23 and (α_o) is the diffusivity at the precharge pressure.

The Grashoff number is given by Welty Wicks Wilson - |17|, for heat transfer calculation as:

$$N_{gr} = \frac{\beta g}{\nu_0^2} \delta^3 \Delta T \qquad (3.12)$$

where (g) is the gravitational constant: (δ) is a characteristic dimension of the volume undergoing heat transfer; (ν) is the kinematic viscosity at precharge pressure and (β) is the coefficient of thermal expansion, (β) is then given to be:

$$\beta = \frac{\rho - \rho_o}{\rho_o \Delta T} \qquad (3.13)$$

where (ρ) is the bulk fluid density and (ρ_o) is the fluid density inside the heated layer of gas. Since $\rho \propto T$ for a gas at constant pressure we can write:

$$\beta = \left[\frac{T_o - T}{T_o}\right] \frac{1}{\Delta T} \qquad (3.14)$$

which, if inserted into (3.12) gives:

$$N_{gr} = \frac{g\delta^3}{\nu_o^2} \frac{T_o - T}{T_o} \qquad (3.15)$$

Since the temperature at precharge is stated to be the same as for gas standard conditions, properties such as diffusivity, (α_o) and kinematic viscosity (ν_o), at precharge are dependent on pressure only and may be related to standard conditions by:

$$\alpha_o = \alpha_s \frac{P_s}{P_o} \qquad (3.16)$$

$$\nu_o = \nu_s \frac{P_s}{P_o} \tag{3.17}$$

where (α_s, ν_s, P_s) are properties at standard conditions.

Using (3.17) and (3.14), equation (3.12) becomes:

$$N_{gr} = \left[\frac{g\,\delta^3}{\nu_s\left(\frac{P_s}{P_o}\right)}\right]^2 \left[\frac{T_o - T}{T_o}\right] \tag{3.18}$$

and (3.16) into (3.11) gives:

$$\alpha_e = \alpha_s \frac{P_s}{P_o} K_3 \left[N_{gr}\, N_{pr}\right]^{\frac{1}{4}} \tag{3.19}$$

(N_{pr}), the Prandtl number is, by definition:

$$N_{pr} = \frac{\nu\, C_p}{v\, k} \tag{3.20}$$

where (k) is the thermal conductivity, invariable with pressure according to Welty Wicks Wilson |17|; (C_p) is the specific heat at constant pressure (invariable over the pressure range of interest). (ν), is the kinematic viscosity and (v) the specific volume.

Both (ν) and (v) vary inversely with pressure. Therefore:

$$\nu_1 = \nu_2 \frac{P_2}{P_1} \quad \text{and} \quad v_1 = v_2 \frac{P_2}{P_1} \tag{3.21}$$

thus, $$\frac{\nu_1}{v_1} = \frac{\nu_2}{v_2}\,\frac{P_2/P_1}{P_2/P_1} = \frac{\nu_2}{v_2} \qquad (3.22)$$

The ratio $\frac{\nu}{v}$ is constant.

Thus (N_{pr}) is not variable with pressure over the range of interest. However, it is slightly variable with temperature (2.0% over the range) and the following relation may be used.

$$N_{pr} = K_{10}\,T + K_{11} \qquad (3.23)$$

where:

$$K_{10} = -2.325 \times 10^{-4}$$

$$K_{11} = 0.783$$

and (T) is the temperature at any instant of time. This curve was fitted from data in appendix I in Welty Wicks Wilson |17|.

Our algorithm must also provide for these cases where $\tau = \infty$. (Since (α_e) is the only term than can equal zero and this occurs when $N_{gr} = 0$. This in turn requires that $T = T_o$). Logic is incorporated in the algorithm to limit the value of (τ) under the condition where $T = T_o$.

The algorithm is shown in fig. 3.4. The input variable is the temperature (T) with parameters (P_o, δ, R, D and L) also available. Use of equations 3.17, 3.18, 3.23, 3.19 and 3.10 calculates the output variable (τ) the time constant.

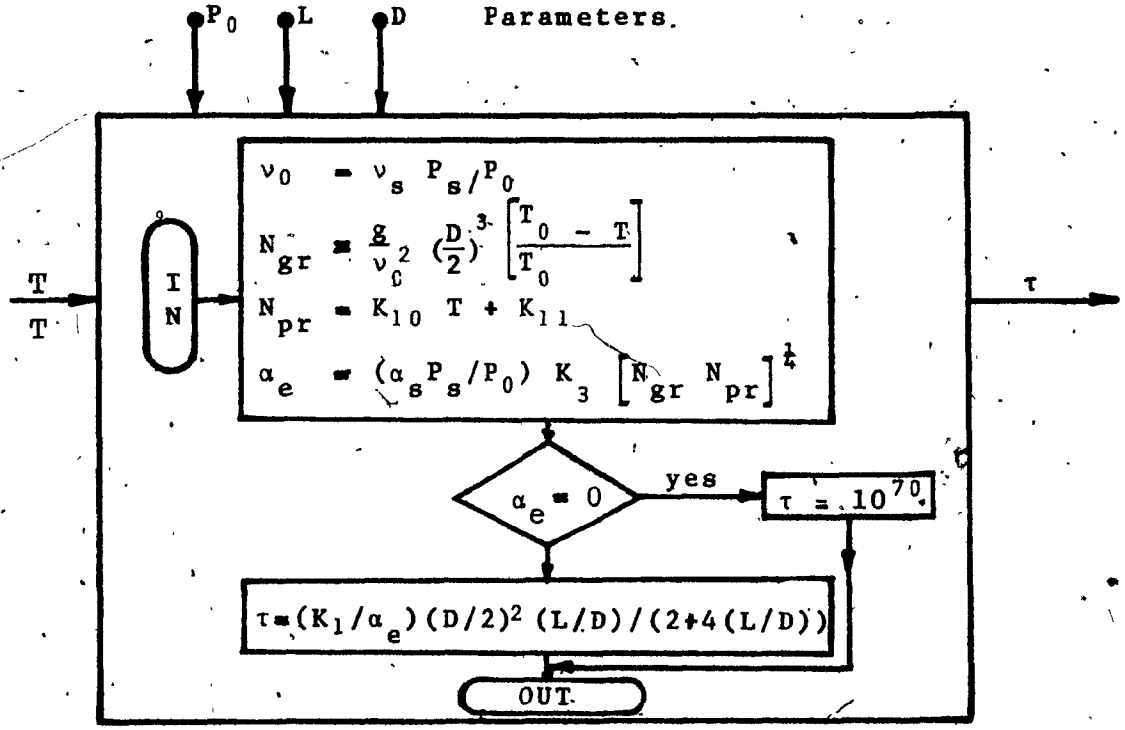

Fig. 3.4 Schema: Algorithm for (τ).

3.5 Algorithm for Temperature, T.

The charge gas temperature is instantly changing with time and must be derived from Otis' equations mentioned in chapter 2, article 2.3, equation (2.17).

$$hA_s\ (T_o - T) = mC_v\ \frac{dT}{dt} + P\ \frac{dV}{dt} \qquad (2.17)$$

dividing through by mC_v, replacing $\frac{dV}{dt}$ by Q, the flow rate of oil:

$$\frac{hA_s}{mC_v}\ (T_o - T) = \frac{dT}{dt} + \frac{P\ Q}{mC_v} \qquad (3.24)$$

We have already stated in article 2.3 of chapter 2 that we are assuming a model which behaves as an exponential system, and that $\tau = mC_v/hA_s$ therefore:

$$\frac{1}{\tau}\ (T_o - T) = \frac{dT}{dt} + \frac{P\ Q}{mC_v} \qquad (3.25)$$

or:
$$dT = \frac{1}{\tau}\ (T_o - T)\ dt - \frac{P\ Q}{mC_v}\ dt \qquad (3.26)$$

which, in finite difference form becomes:

$$\Delta T = \frac{1}{\tau}\ (T_o - T)\ \Delta t - \frac{P\ Q}{mC_v}\ \Delta t \qquad (3.27)$$

and:
$$T = \int dT + T_o \qquad (3.28)$$

in finite difference form:

$$T = T_o + \sum_{m-1}^{j} \Delta T_m \qquad (3.29)$$

where $j = t/\Delta t$.

The equation of pressure for a real gas must be used here to compensate for the effect which the iterative change in specific volume has had on the pressure. The same form of modified equation (3.1) is used in (3.28) to obtain:

$$\Delta T = \Delta t \left[\frac{1}{\tau} (T_o - T) - \frac{Q}{mC_v} \left(\frac{R_u T (v+B) - A}{v^2} \right) \right] \qquad (3.30)$$

Since (C_v), the specific heat at constant volume, is used in this equation and since it is a function of temperature, a relation was found by curve fitting the data from table 4.2 in Jones and Hawkins |18|:

$$C_v = C_1 T^2 + C_2 T + C_3 \qquad (3.31)$$

where:

$$C_1 = 1.49 \times 10^{-4}$$

$$C_2 = -3.17 \times 10^{-2}$$

$$C_3 = 740.6479$$

This curve is valid to within 0.05 J/kg K over the range from 213 K to 422 K.

Using equations (3.31), (3.30), and (3.29), the algorithm was prepared and is shown in fig. 3.5. Thus temperature is calculated from the input variables (τ, Q, v, A and B) and the parameters (Δt) and (m). Since this algorithm is an "integrator", the value of (T) from the previous iteration is required as an input.

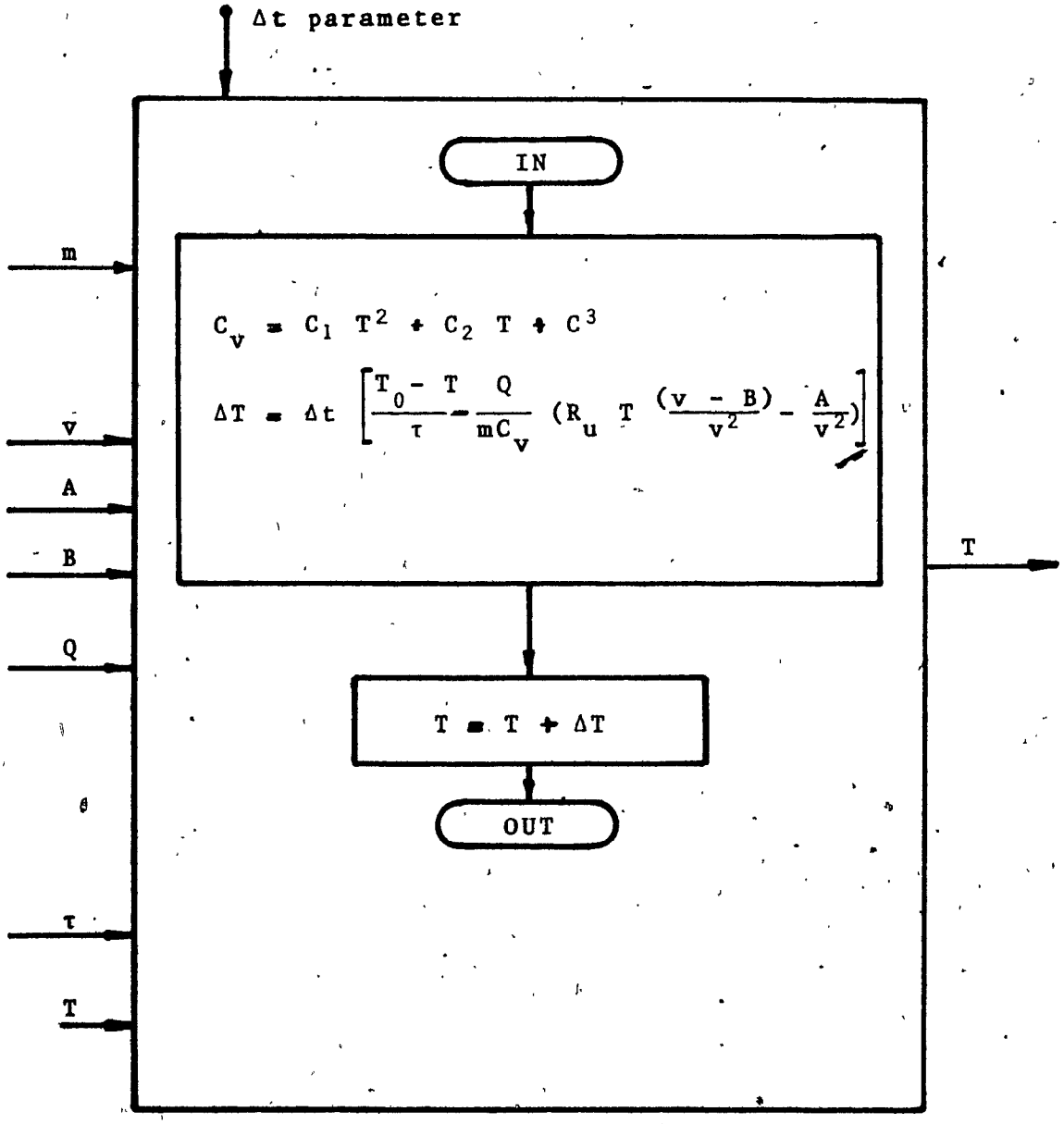

Fig. 3.5 Schema: Algorithm for (T).

3.6 Algorithms for Calculation of Initial Conditions.

In any model, variations of parameters make it mandatory that some calculations be made for initial conditions. Here the following are required:

1) Exact specific volume at the ambient temperature given and at the pressure given.

2) The operating volume of oil in the accumulator at the pressure given.

3) The mass of charge gas from the precharge pressure and the geometry of the accumulator.

4) Time must be set to zero; temperature must be set to ambient; accumulator pressure must be set equal with line pressure.

3.6.1 Initial Conditions: Specific Volume.

For the stability of the model, all equations have to be reversible. Therefore it was necessary to reverse equation (3.1) to find (v), the specific volume giving:

$$v = \frac{1}{2}\left(X + \sqrt{X^2 - \frac{4A}{P} + 4\,X\,B}\right) \qquad (3.32\ a)$$

and:

$$X = \frac{R_u T}{P} \qquad (3.32\ b)$$

where (X) is a dummy variable and equation (3.32) is a solution of quadratic equation (3.1) modified.

But here the values of (A) and (B) are dependent upon, (v), and a Gauss-Siedel iteration technique is utilized to find the exact value of (v).

The algorithm is shown as part of figure 3.6. The value of (v) is first calculated using the given initial conditions of (T) and (P) along with some arbitrary values for (A) and (B). (A) and (B) are then calculated with the new (v). The calculated value of (v) is compared to the previously calculated value. (If this is the first pass, (v) is compared to an arbitrary value of (v) which corresponds to the arbitrary (A) and (B) originally chosen). If the difference is within a predefined elemental error, the calculation is stopped, the value of (v) calculated is the value desired. If the difference is not within the bounds of the elemental error, the iteration restarts and recycles until the error is within the prescribed value.

3.6.2 Initial Conditions: Operating Volume of Oil.

The volume of oil in the accumulator at any time is very important since it sets limitations on the amount of and the rate of discharge of oil. If the initial accumulator pressure is larger than the precharge pressure then there will be some oil in the accumulator which must be accounted for.

Under steady state and ambient temperature condi-

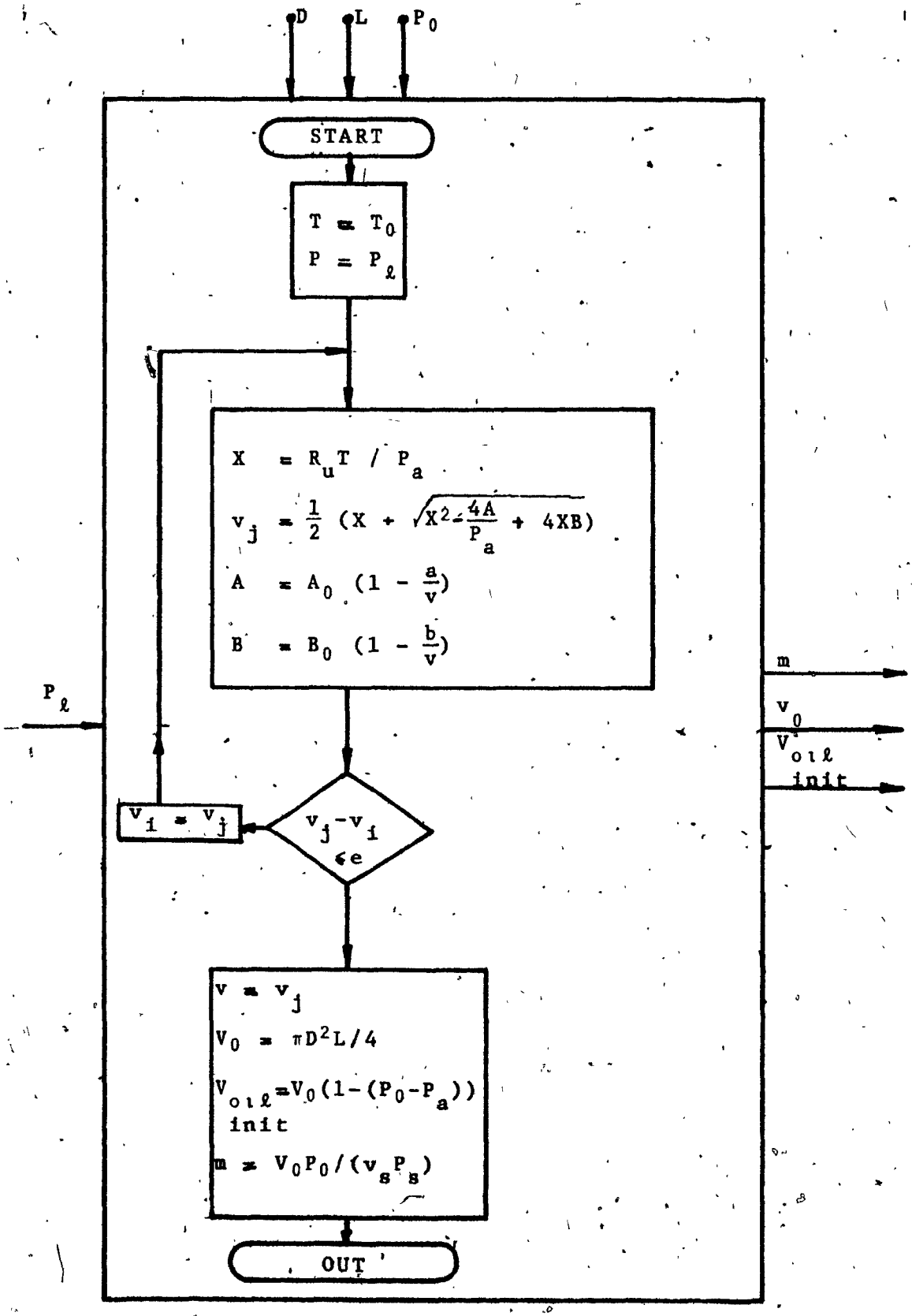

Fig. 3.6 Schema: Algorithm for Initial Values

tions, the initial volume of oil in the accumulator is proportional to the change of volume of the charge-gas from volume at precharge pressure to volume at initial pressure. That is:

$$V_{oil} = V_o - V_{init} \qquad (3.33)$$

Where, $V_o = \pi D^2 L/4$, is the charge-gas volume at the precharge pressure (P_o). (V_{init}) is the charge gas volume after initial compression to pressure (P_{init}).

From Boyle's Law, at the same temperature,

$$P_{init}\ V_{init} = P_o\ V_o \qquad (3.34)$$

Therefore, using (3.33) and (3.34):

$$V_{oil} = V_o \left(1 - \frac{P_o}{P_{init}}\right) \qquad (3.35)$$

This equation is part of the algorithm shown in figure 3.6. (V_o) is first calculated from parameters (D) and (L). Then, (V_{oil}) is calculated using parameters (P_o) and (P_{init}). (P_{init}) is the line pressure at an assumed steady state condition which must exist prior to the start of operation of the cycle under simulation).

3.6.3 Initial Conditions: Mass of Charge-Gas.

The mass of charge-gas is related to the known specific volume of the charge-gas and to the precharge pressure

along with the volume of the charge-gas at precharge, (V_o) in the following manner:

$$\dot{m} = \frac{V_o}{v_s \ (P_s/P_o)} \qquad (3.36)$$

This equation is part of figure 3.6.

3.7 Algorithm for Oil Flow Rate, Q.

The flow rate of oil (Q) through the inlet pipe is a function of the geometry of this pipe. It is a very important part of the model since it governs the speed of operation of the system. Many complex inlet configurations are available. Here we have assumed the inlet pipe to be a restriction. A value of resistance (R_{es}) is set based on the configuration (inlet pipe internal diameter and length) with the following relationship:

$$R_{es} = \frac{K_5 \, L_p}{D_p^2} \qquad (3.37)$$

where (K_5) is a constant arbitrarily set to give a predetermined rate of flow for a given differential pressure. (L_p) and (D_p) are the length and diameter of the inlet pipe, respectively.

The flow rate (Q) is a function of the pressure differential, ($P - P_\ell$), across the inlet pipe. We assume here that a positive differential where $P > P_\ell$ means a positive flow rate (flow out of the accumulator is positive)

$$Q = \sqrt{\frac{P - P_\ell}{R_{es}}} \qquad (3.38)$$

Control of the volume of usable oil is necessary to limit the quantity of oil drawn. This is done by the following set of equations:

$$V_{oil} = V_{oil_{init}} + \sum_{m=1}^{j} \Delta V_{oil_m} \qquad (3.39)$$

where: $\Delta V_{oil} = -Q\ \Delta t \quad \{\text{for } Q \leq 0\}$ (3.40a)

$$\Delta V_{oil} = -V_{oil} \quad \{\text{for } Q > 0 \text{ and } V_{oil} - Q\ \Delta t < 0\} \qquad (3.40b)$$

and: $j = t / \Delta t$

Also, since $Q > 0$ and $V_{oil} - Q\ \Delta t < 0$ imply that, because of the iteration step size, the accumulator would discharge oil which it does not contain (an impossibility), flow rate is then set at whatever is left in the accumulator. That is:

$$Q = \frac{V_{oil}}{\Delta t} \qquad (3.41)$$

The algorithm is shown in figure 3.7. Inlet, pipe resistance factor (R_{es}) is first calculated using the input parameters (D_p and L_p). Using (R_{es}) and the input (P_ℓ), a tentative value of flow rate (Q) is calculated. If this value is positive (flow out of accumulator), then (V_{oil}) is checked to see if there is enough oil in the accumulator.

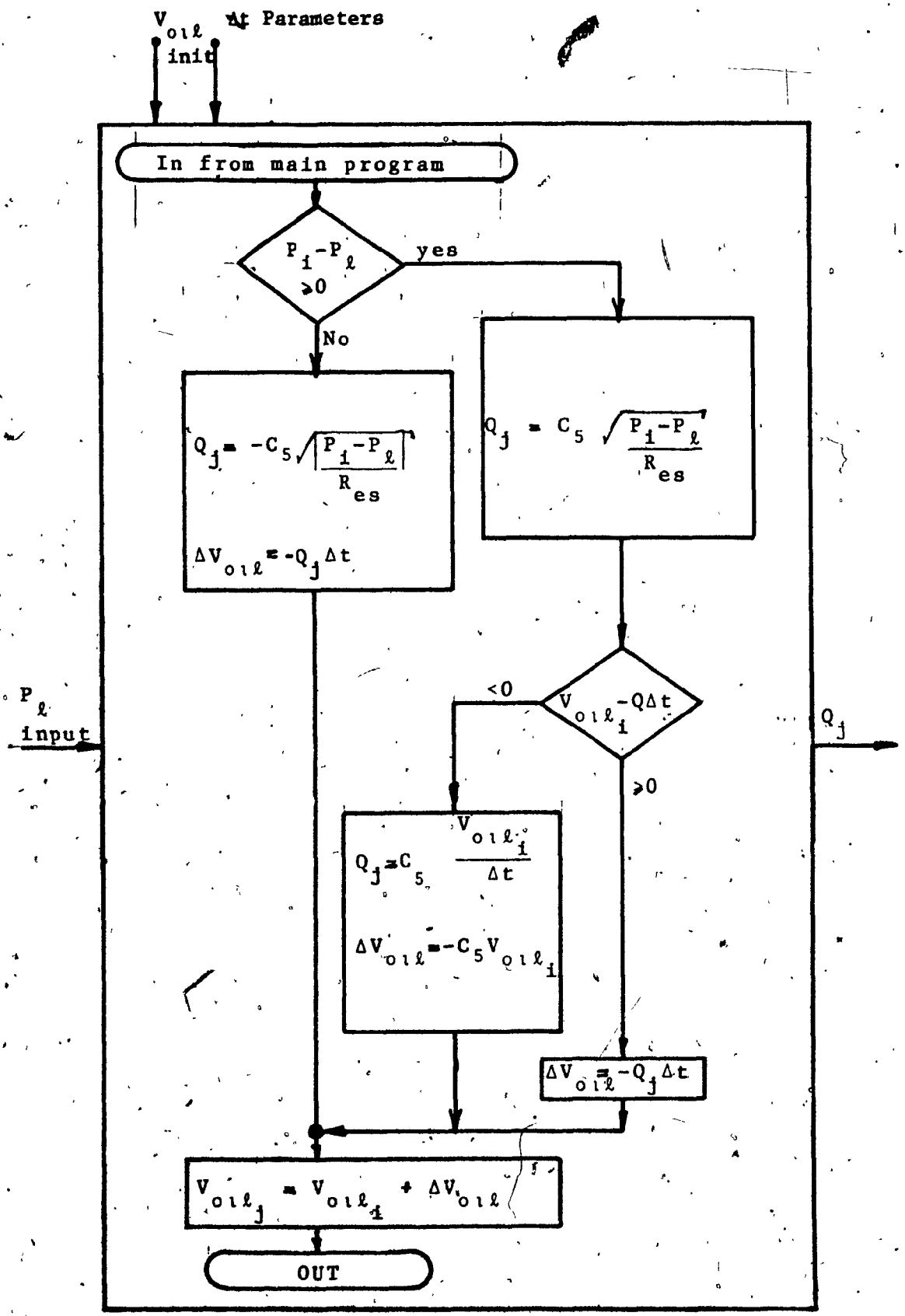

Fig. 3.7 Schema: Algorithm for (Q).

If there is enough oil, the value of (Q) is confirmed as the output, the value of (V_{oil}) is reduced by an amount corresponding to the discharge ($Q \Delta t$).

If there is not enough oil, then the flow rate (Q) is recalculated as per equation (3.41) and (V_{oil}) is reduced to zero.

3.8 Algorithm for Invalid Input Flow Rate.

In the flow input model, if there is little or no usable oil volume in the accumulator, an input request for a fixed flow rate may result in incorrect negative oil volumes. To prevent this, the flow rate is checked upon entering the algorithm. If the flow request is incorrect, the flow rate (Q) is set to ($V_{oil}/\Delta t$) and an error message is printed out.

Control of the volume of oil is the same as in article 3.7. This algorithm, as described, is shown in figure 3.8.

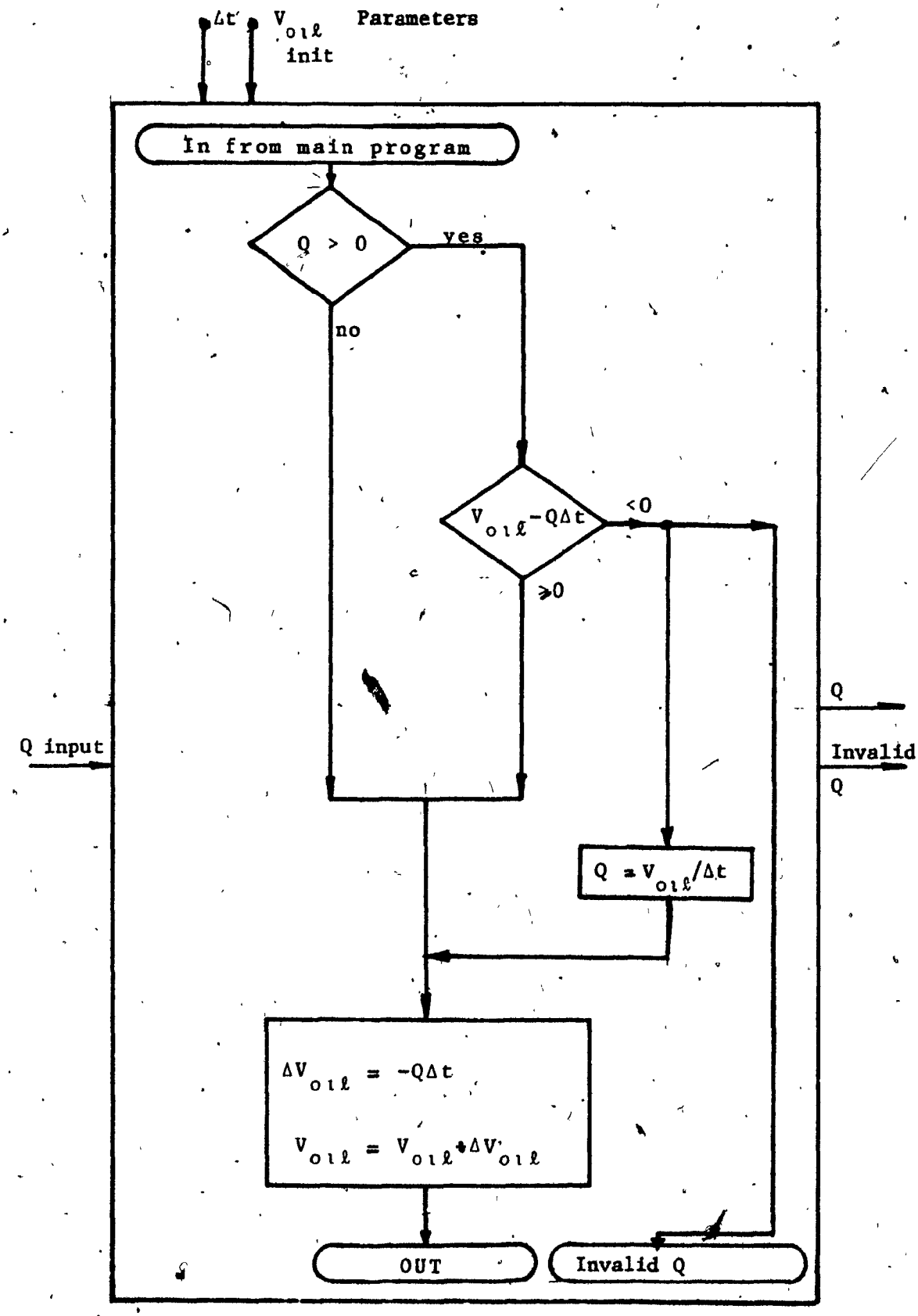

Fig. 3.8 Schema: Algorithm for Invalid (Q) Input.

3.9 Algorithm for Correction of Instability.

The Euler method of numerical simulation is used for the development of both models. This is one of the simple methods and gives quite accurate results if the iteration steps are small enough.

This method, on the other hand, will permit overshoot and oscillation, (see Hornbeck |19|). These oscillations are acceptable if they are small but since their growth is sometimes exponential, it can lead to instability.

In order to prevent instability, all the relations between variables in the model must be reversible. This is not always possible, as is the case in our pressure input model, where the relation between flow rate (Q) and pressure difference ($P - P_\ell$) is given first by equation (3.38) as a direct exponential relationship. From the calculated (Q), ($P - P_\ell$) is recalculated with thermodynamic and heat conduction distribution relations taken into account, along with the past history of the temperature. This causes an inherent instability in the model which can be corrected either by using a more complex numerical method such as a Runge-Kutta formula or it can be corrected by an artificial method.

Since a Runge-Kutta formula would have been difficult to apply because of the large number of system equations

involved and because of the limited available program space of our method of development, an artificial means of stabilizing the model was chosen.

Some of the instability was found to be due to the nature of the relation between the flow rate (Q), the differential pressure ($\Delta P_i = P - P_\ell$), and the iteration variable step size (Δt). This relation is shown in figure 3.9. (This graph assumes a condition where (ΔP_i) approaches zero in a linear manner). The (Δt) steps are arbitrarily chosen as that the ($\Delta P_i = 0$) point happens in the middle of the step. The (Q) curve shows the exponential relation with the (ΔP_i) curve. (There is no vertical scale).

The real amount of oil flow is the integral, or the area under the (Q) curve. Use of the Euler method calculates (Q) to be proportional to the (ΔP_i) at the start of each iteration and assumes this value to be valid over the whole (Δt). Thus the calculated amount of oil flow for each iteration is the integral, or the area of the rectangle with height equal to the flow rate at the beginning of the step. The truncation error is shown at the top of each step.

This error increases as (ΔP_i) approaches zero. At ($\Delta P_i = 0$), the error is, at best 40% and at worst infinity. It is therefore easily understood, from figure 3.9, that the model is unstable about ($\Delta P_i = 0$). It can also be seen that

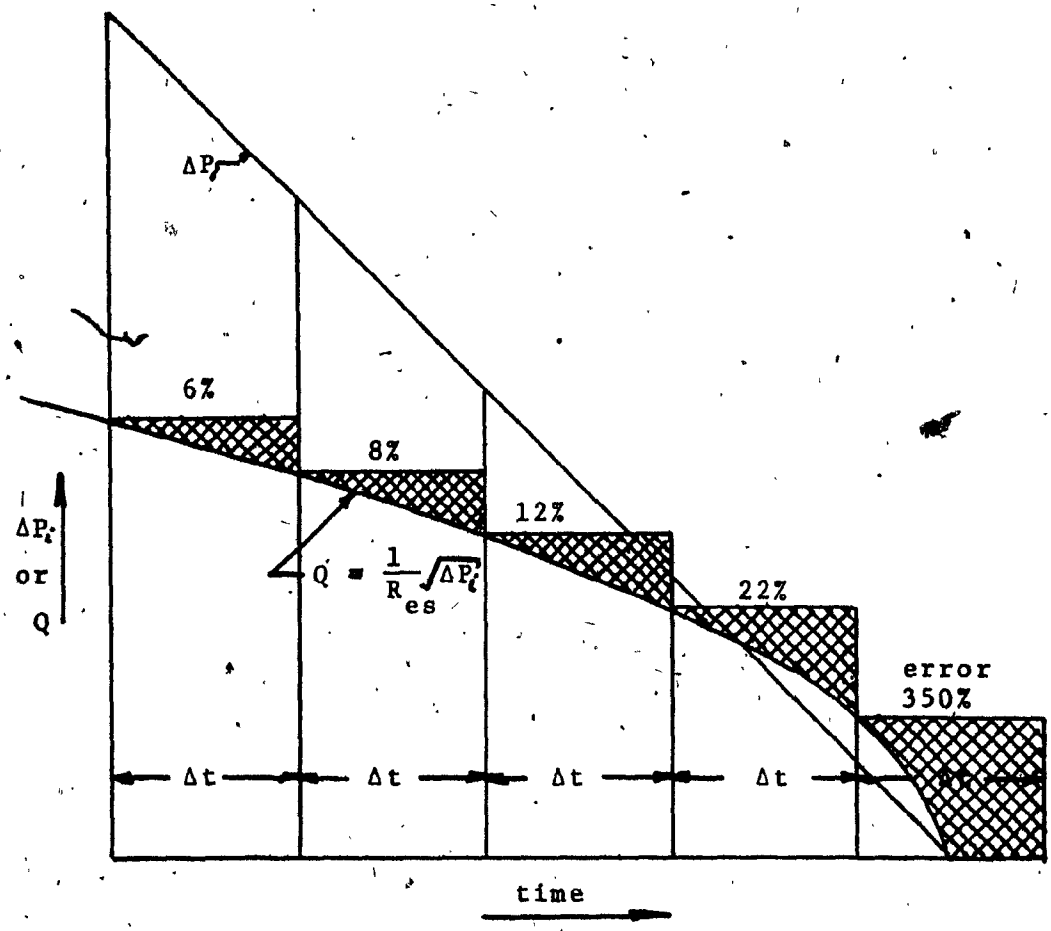

Fig. 3.9 Reason for Instability in Pressure Input Model.

the error rapidly decreases with increasing (ΔP_i). (At maximum reasonable operating conditions, with line discharge velocity of 10 m/s and $\Delta t = 0.02$ s the error is 1%). Since the accumulator is a cyclic machine, negative errors will cancel positive errors over a cycle and small errors can be ignored. The only problem to be resolved remains the instability about the point ($\Delta P_i = 0$).

The proposed artificial means of stabilization consists of a correction of the flow rate (Q) on detection of either a pressure overshoot or (ΔP_i) within a specified limit. The correction is by a slide-wire factor (C_5), which modifies flow rate equation 3.39 to:

$$Q = \frac{C_5}{R_{es}} \sqrt{|\Delta P_i|} \qquad (3.42)$$

Where the slide-wire factor (C_5) can have either of two values:

1) If a "forward" calculation shows either an overshoot or $\Delta P_i < 100$ P_a then:

$$C_5 = .3 \times 10^{-4} \sqrt{|\Delta P_i|} \qquad (3.43a)$$

2) Otherwise:

$$C_5 = 1.0 \qquad (3.43b)$$

Figure 3.10 shows the schema for the correction of instability algorithm. Three conditions are detected by the logic:

a) Either an overshoot or very small pressure difference. If this is the first time this particular overshoot or small pressure difference is detected.

   a-1) A flag[1] is set to indicate detection.

   a-2) The factor (C_5) takes values as per equation (3.43a).

   a-3) All calculated values for the iteration just completed are discarded.

   a-4) The complete iteration is repeated with the new value of (C_5).

[1] Flag: used in a similar sense to a flag in automobile racing to advise the drivers of a particular situation on the race track (oil slick, accident, etc.). It is a device which allows the computer to recognize the existence of a particular situation in the program. Here the existence of an overshoot on the iteration just completed.

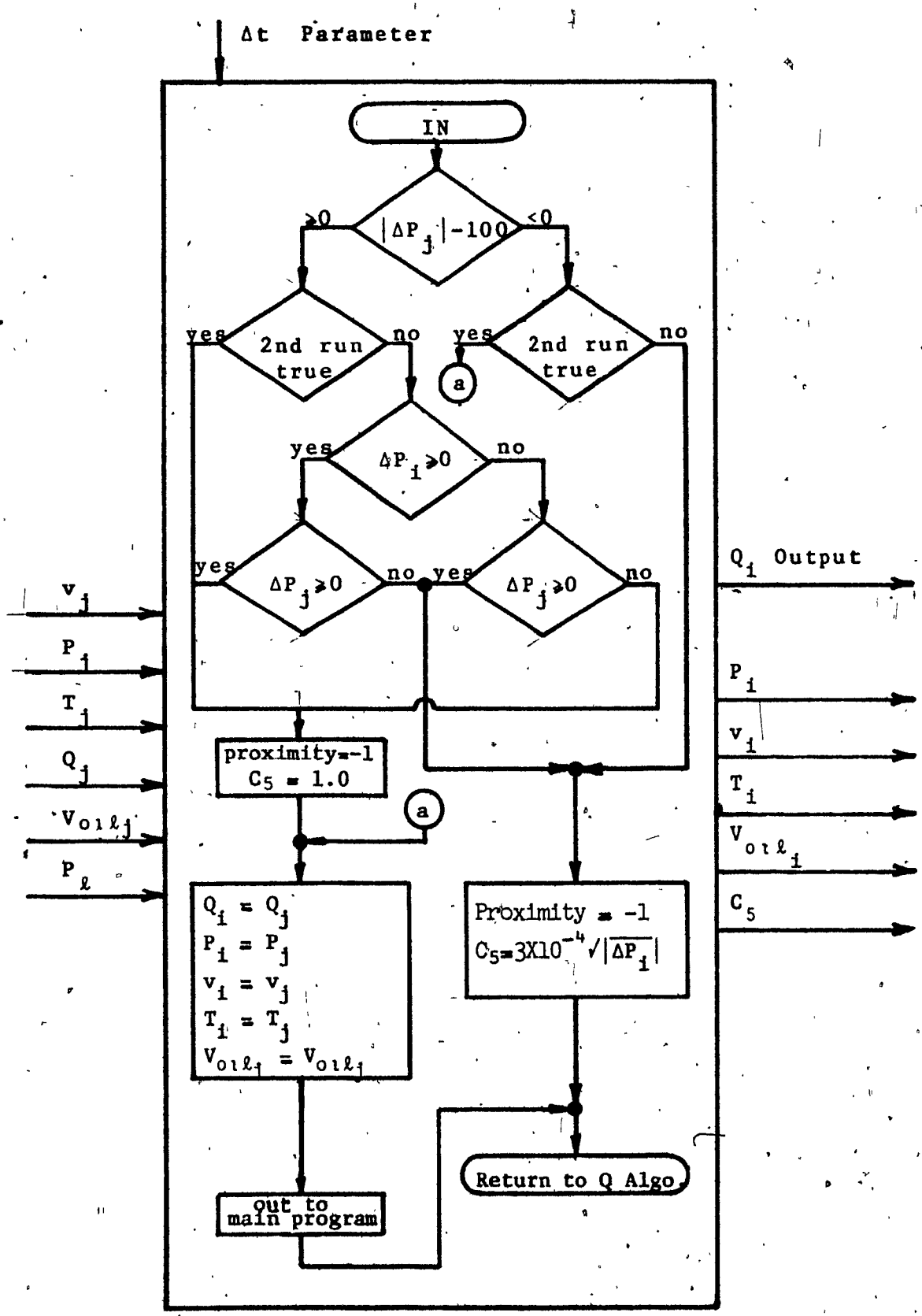

Fig. 3.10 Schema: Algorithm for Correction of Instability.

b) Very small pressure difference ($|P-P_{\ell}|<100$ Pa) after at least one iterative cycle through a) above.

b-1) The factor (C_5) is calculated as per equation (3.43a).

b-2) Calculated values for (Q, P, v, T and V_{oil}), for the iteration just completed are accepted.

b-3) Control returns to Main System Simulation for new input.

c) Pressure difference greater than 100 Pa and no overshoot or overshoot exists but this is second iteration.

c-1) The detection flag is reset.

c-2) Factor $C_5 = 1.0$ as per equation (3.43b).

c-3) Calculated values for (Q, P, v, T and V_{oil}), for the iteration just completed, are accepted.

c-4) Control returns to Main System Simulation for new input.

3.10 The Models

3.10.1 Pressure Input Model

The pressure input model of fig. 3.1a is made up of the algorithms described successively under articles 3.6, 3.7, 3.3, 3.4, 3.5, 3.2, and 3.9. The complete mathematical model is given in Appendix A.

This model behaves, as stated previously, as a fluid capacitance. Its input variable (signal coming from the Main System Simulation) is the oil pressure in the system at the point of discharge of the accumulator. Its output variable (signal going back to the Main System Simulation), is the net flow rate of hydraulic fluid into the main system from the accumulator.

Figure 3.11 shows pressure to flow characteristics of typical pumps. Curve A, (the solid line) is for a centrifugal pump driven by an induction motor. Curve B, (the dashed line) is for a positive displacement pump driven by a synchronous motor. Other arrangements are possible, such as a positive displacement pump driven by an induction motor. The characteristic curves would be somewhere in between the two given in this figure.

The pressure input model is meant to be used in system simulations where the power source has the combined.

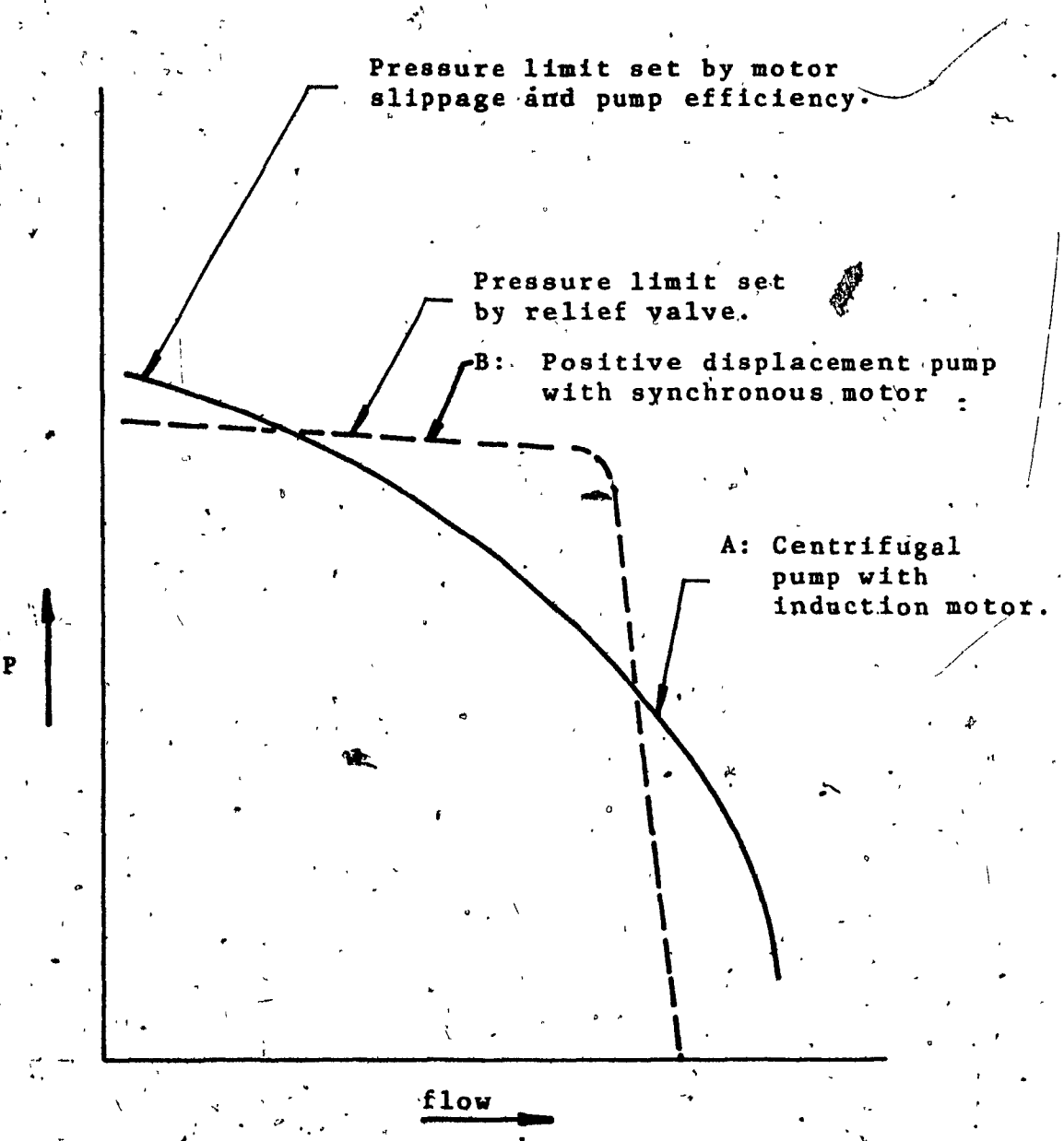

Fig. 3.11 Typical Pump Curves

flow-pressure characteristics shown in figure 3.11, curve "A".

Figure 3.12 is an analog circuit representation of a system using this accumulator model. The system has an energy source and a load. The accumulator is connected in parallel with the load. The pressure input model includes modelling of the accumulator components within the phantom line. It includes the gas capacitance, the oil capacitance and the inlet resistance. Since the inlet resistance is modelled, the signal input to the accumulator model needs only be (P_ℓ), the pressure in the pipe at the discharge of the accumulator. The model output is then the flow rate of oil into or out of the accumulator (Q).

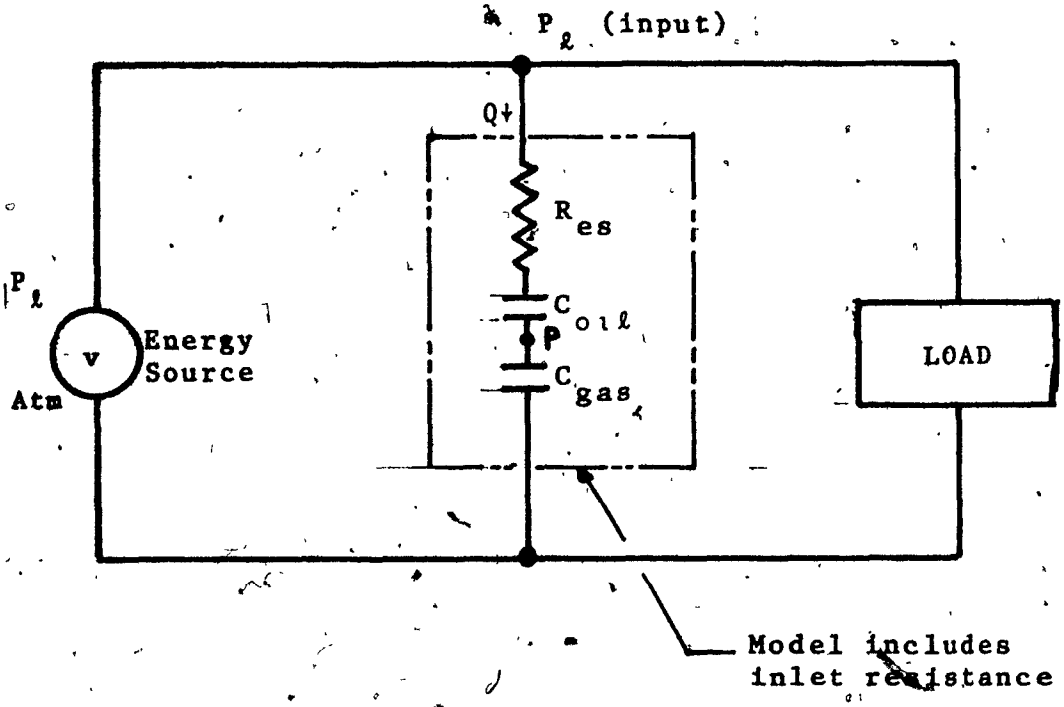

Fig. 3.12 Pressure Input Model Analog Circuit

3.10.2 Flow Input Model

The flow input model of figure 3.1b is made up of the algorithms described successively under articles 3.6, 3.8, 3.3, 3.4, 3.5, and 3.2. The complete mathematical model is given in Appendix B.

This model has as input variable the oil flow rate out of the accumulator. The output variable is the pressure of the charge-gas acting on the main system.

The model is to be used in system simulations where the power source has the characteristics of a pure flow source. The pump curve for a source of this type is shown as curve "B" of figure 3.11. The pressure developed by the pump is independent of the flow rate. (This pressure is limited by a relief valve in order to protect the system).

The model has one major limitation. Although its input variable is flow rate, it cannot accept a signal requesting a flow out of an empty accumulator. It must revert to acting on the input signal to change the requested flow to zero.

Figure 3.13 is an analog circuit representation of a system using the flow input accumulator model. The system has a flow energy source driving a load. The accumulator is connected in parallel with the load. The flow input model

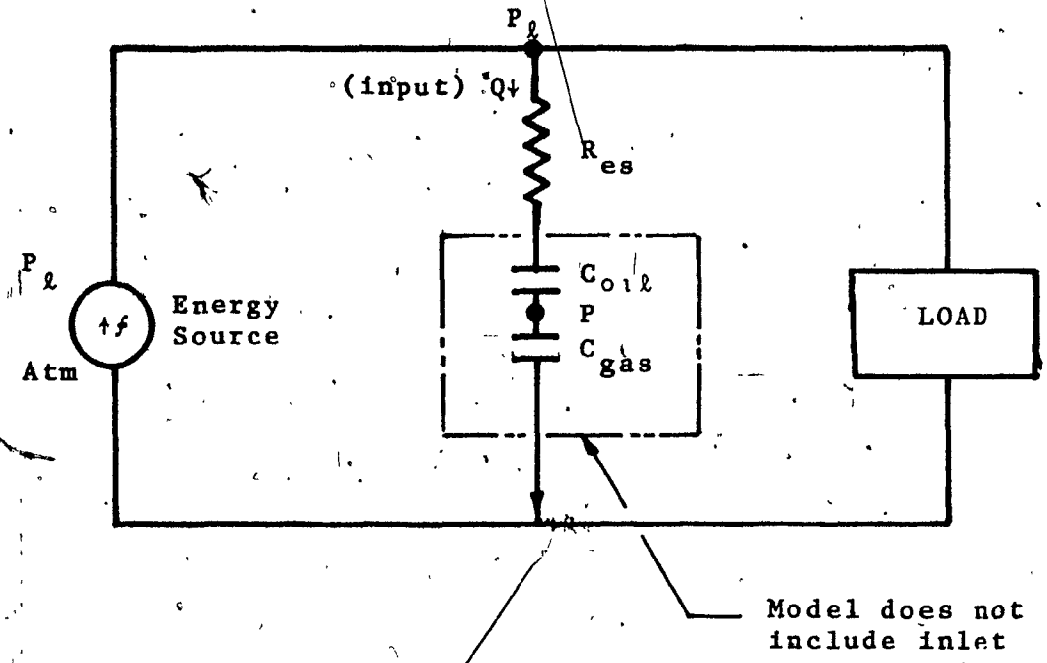

Fig. 3.13 Flow Input Model Analog Circuit.

includes modelling of the accumulator components within the phantom line. This model does not include the resistance of the inlet. The input signal must therefore be the flow rate of oil (Q) into or out of the accumulator. The output signal is then (P), the pressure of the charge-gas acting on the oil. All subsequent pipe pressure drops must be accounted for by the Main System Simulation. Thus (P_ℓ) the pressure in the oil line at the discharge of the accumulator, must be calculated, based on the output of the model (P), the pressure of the charge-gas, by the Main System Simulation.

3.11 Model Considerations

3.11.1 Iteration Step Size

The models are designed for use with main system simulations using time as the iterative step variable. The size of this step variable will be the same as that of the main program. The models are more accurate at steps less than 0.1 seconds.

3.11.2 Units

The models are designed to operate in the S.I. system of units:

- Pressure is given in Pascals. All pressures are absolute. (1.0 lb/in^2 = 689 475.7 Pa)
- Temperature is given in Kelvin (1.0° R = 0.5556 K)
- Linear measure in meters (1.0 in. = 0.0254 m)
- Mass is given in kilograms (1.0 lbm = 0.4535924 kg)
- Force is given in Newtons (1.0 lbf = 4.448222 N)
- Energy is given in Joules (1.0 Btu = 1055.056 J)
- Time is given in seconds.

3.11.3 Model Development

Both models were developed using a Texas Instrument TI-59 programmable calculator with printer. Once the models were properly operating, a FORTRAN program was prepared and tested. The TI-59 and the FORTRAN programs are included in appendix, along with sample outputs from each model.

These models are designed to be included as part of a larger system simulation program. To permit testing and operation without such a system, a control and printout algorithm has been included as shown in the block diagram, figure 3.14.

The lower box represents the Main System Simulation. In it are the printout function, the input signal generator and the time control system. Note also that the Initial Value Calculation Algorithm is part of the Main System Simulation.

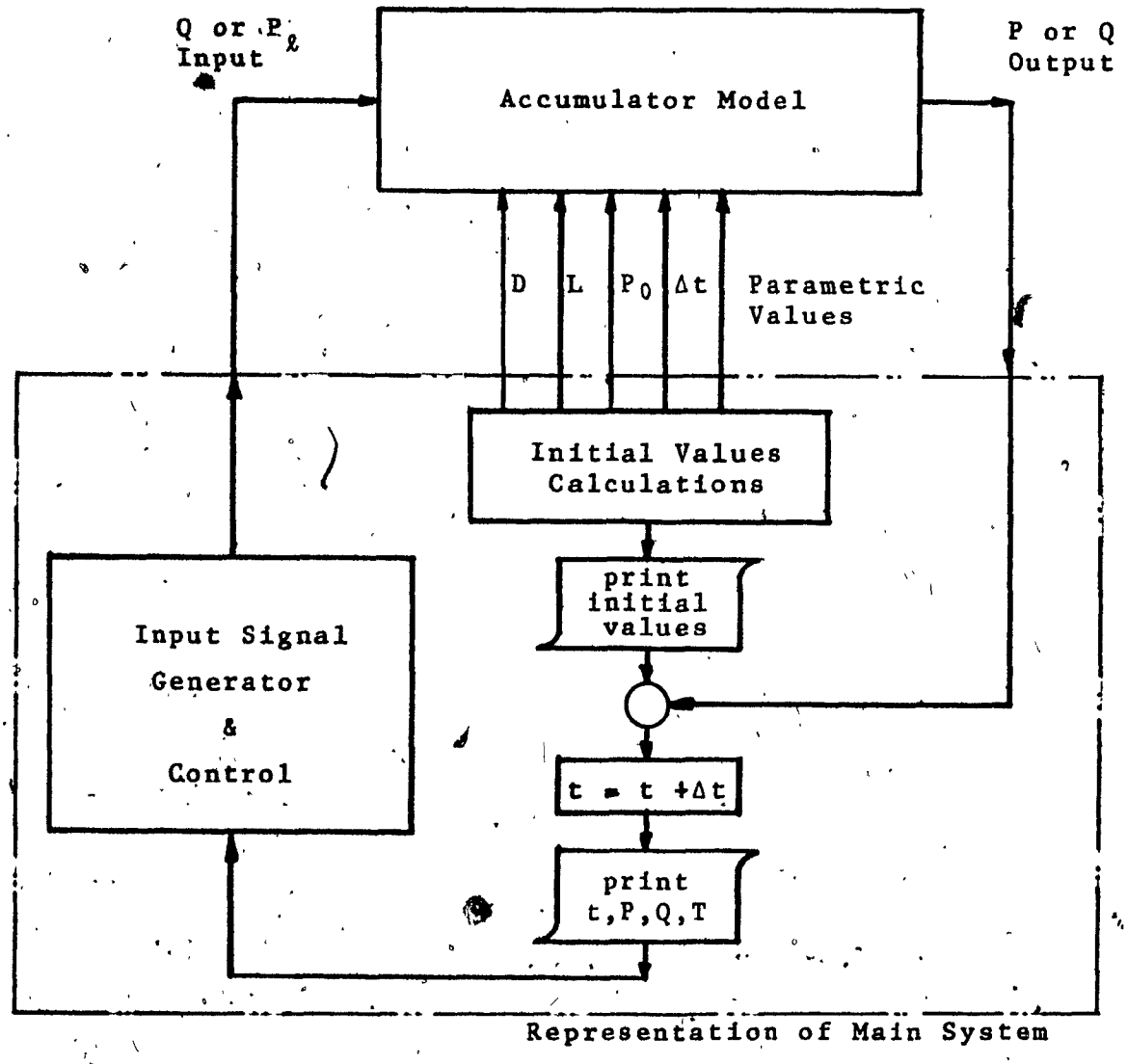

Fig. 3.14 Block Diagram of a Typical Model

CHAPTER 4

EXPERIMENTS

4.1 Description of the Experimental Program

4.1.1 General

The experimental program consisted of tests on 3 nitrogen charged piston accumulators: A 4 litre accumulator with an L/D ratio of 1.8; a 28 litre unit with L/D ratio of 5.4 and a 38 litre unit with L/D ratio of 13.6. The purpose of the tests was to verify the apparent exponential characteristics of the accumulator by comparing experimental data to the time constant calculated using the heat conduction distribution equations, and to compare the developed models to actual operation of accumulators.

Each accumulator was operated at three precharge values (3.55, 6.996, and 10.44 MPa), and at three initial pressure to precharge pressure ratios (1.1, 1.5, and 3.0).

The tests consisted of:

1) Putting initial oil charge into an accumulator which is precharged with nitrogen gas to a set pressure.
2) Discharging the accumulator oil to atmosphere,

and recording the pressure-time relations of the transient in the charge-gas after discharge.

This test includes high and low process velocities. It includes pressures over the full range of normal operation. Finally, it includes the maximum thermodynamic transient possible in an operating cycle. Therefore, it is a logical experimental cycle with which to test the accuracy of a mathematical model.

4.1.2 Test Procedure

The set-up was as shown in figure 4.1. The oil side of the accumulator was connected to a high pressure hydraulic power supply unit through a filter, check valve and manual isolation valve. Discharge took place through a pilot-operated check valve driven by a three way solenoid valve. A trimming valve was connected to the accumulator oil discharge to permit fine adjustment of starting conditions.

The gas side of the accumulator was connected, through a pressure regulator and shut-off valve to a nitrogen bottle. A pressure gauge was installed on the accumulator gas inlet to permit rough setting of the precharge pressure. The charge-gas inlet was also connected to a precision pressure transducer whose signal, after conditioning, was sent to a digital voltmeter and an x-y plotter. (For the first few experiments, an oscilloscope was added to permit examination

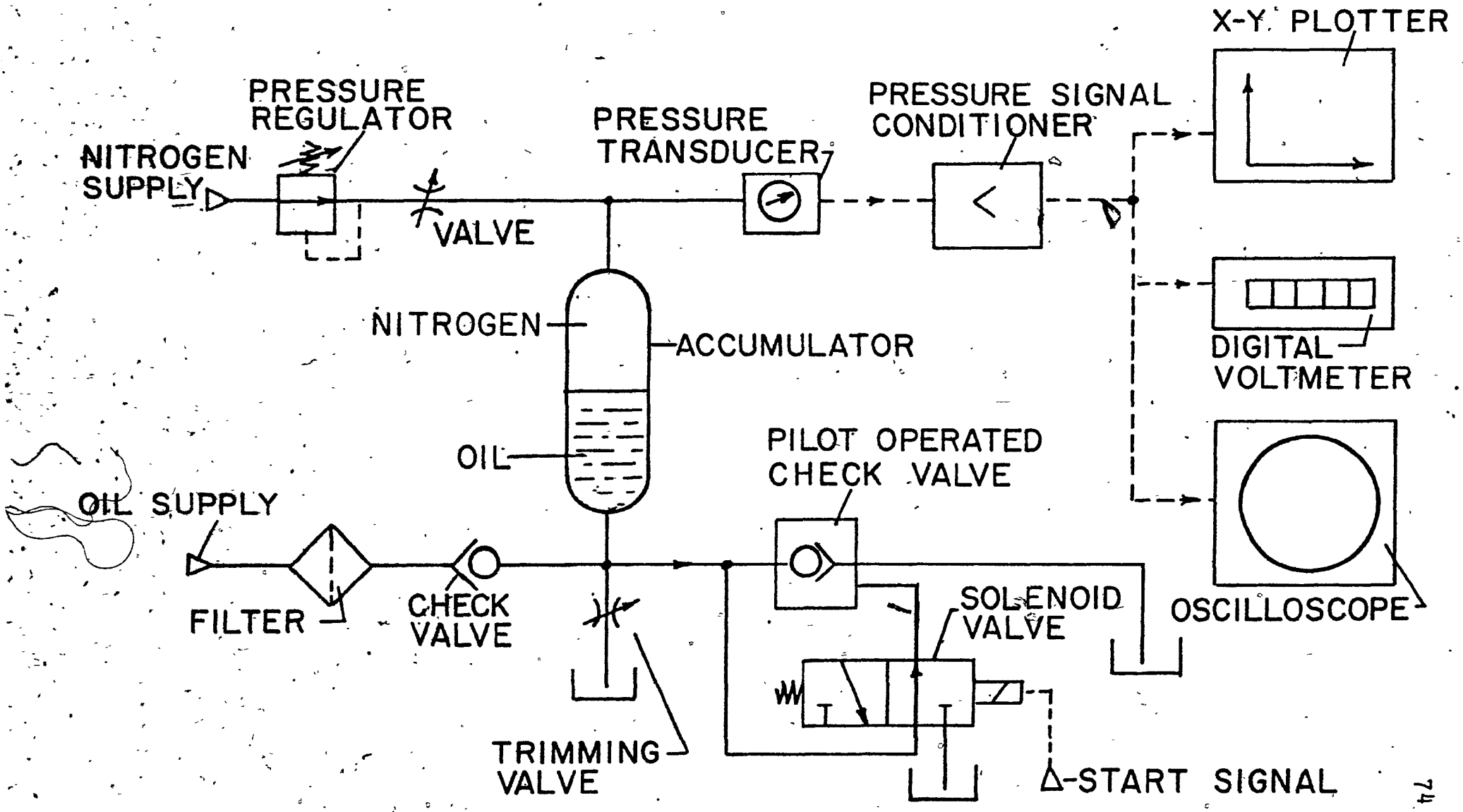

Fig. 4.1 Schematic of Experimental Set-Up

of the discharge speeds and to check for errors due to the response time of the x-y plotter. Since the x-y plotter response was found to be adequate, the oscilloscope was removed).

At the start of a series of tests, a deadweight tester was used to calibrate the pressure readout train (transducer, conditioner, x-y plotter, digital voltmeter and oscilloscope). This calibration was made for each instrument individually and for the readout train as an assembly. The digital voltmeter was calibrated for the highest pressure attained during the test while the x-y plotter was calibrated over the range of the transient only.

Initially the accumulator had neither nitrogen gas nor oil. The gas side is first precharged from the nitrogen bottle until the proper precharge pressure was reached. (For these experiments, absolute precharge pressures of 3.55, 7.00 and 10.44 MPa were used). Since the gas temperature dropped during charging, the gas pressure had to be stabilized after a charge and before a test.

Once the desired precharge pressure was attained and stabilized, the accumulator was loaded with oil. The oil isolation valve was opened, letting oil enter the accumulator from the supply unit. Gas pressure was monitored on the voltmeter. The oil supply was shut when gas pressure attai-

ned a level slightly higher than the desired initial pressure. Compression heated the gas and subsequent heat transfer to the walls cooled it back to ambient. The pressure was stabilized at the desired initial pressure using the trimming valve and the isolation valve. The set-up was then ready for testing.

The x-y plotter scan was started and the oscilloscope triggered. The solenoid valve was activated permitting fast discharge of the oil through the pilot operated check valve to the drain tank.

The time required for the oil to discharge depends on the pipe friction, the valve restriction and the initial pressure. This discharge time increases with initial pressure and with the volume of the accumulator. This is due to the increases of volume of oil to discharge. For the test runs, discharge times measured from 0.2 to 2.0 seconds.

Because of this short discharge period, the gas is expanded in a nearly adiabatic process. The low point of the expansion, (P_a), can be predicted using the ratio of specific heats, ($\gamma = 1.45$), as given for diatomic gases under adiabatic expansion, in the following equation, derived from Boyle's Law, applied for isothermal and for adiabatic processes (see equations (2.5) and (2.6)):

$$P_a = P_1 \left(\frac{P_o}{P_1} \right)^{\gamma} \qquad (4.1)$$

where (P_o) is the precharge pressure:

(P_1) is the initial pressure,

(P_a) is the pressure after adiabatic expansion of the gas, and

(γ) is the ratio of specific heats for the gas (here $\gamma = 1.45$).

Results of this prediction are shown in Table 4.1.

Table 4.1 is the test schedule used for the three accumulators. There were a total of 48 tests, 24 of which had the accumulator in a horizontal position, and 24 with the accumulator in a vertical position. The predicted (P_a) was required to permit rescaling of the x-y plotter before each test.

Table 4.1 Test Schedule

Test No	Precharge pressure, (P_o) MPa absolute	Initial pressure, (P_i) MPa absolute	$\frac{P_i}{P_o}$ ratio	Predicted (P_a) (eqn. 4.1) MPa absolute
1	3.55	3.89	1.1	3.41
2	3.55	5.27	1.5	2.97
3	3.55	10.44	3.0	2.19
4	6.996	7.68	1.1	6.71
5	6.996	10.44	1.5	5.84
6	6.996	20.79	3.0	4.29
7	10.44	11.48	1.1	10.00
8	10.44	15.61	1.5	8.71

4.2 Experimental Results

4.2.1 Calculation of Time Constant (τ) From Experiments

To determine the time constant (τ) from the experiments, the time constant of equation 2.22 was derived by solving for (τ) and:

$$\tau = \frac{-t}{\gamma \left[1 - \frac{P - P_a}{P_0 - P_a}\right]} \qquad (4.2)$$

where (t) is time, (P) is accumulator pressure at any instant of time; (P_0) is the precharge pressure and (P_a) is the lowest pressure attained after adiabatic discharge.

The time constants were calculated using equation (4.2) and the test data from the x-y recorder traces. The period is restricted to the initial time interval (less than 15 s), so that the time constant is based, toward neither the exponential nor the heat conduction distributions. The procedure is to select discrete times (i.e.: 5, 10, 15 s), and to find, by scaling the trace, the corresponding pressure. The trace also shows the adiabatic pressure and, after a long time, the precharge pressure. Thus for each time all the information is available to calculate the time constant from equation (4.2). This results in a set of calculated time constants for each test. At low values of time (less than 15 s), the constants always differ by less than 2 percent.

As time increases above 15 seconds, the calculated time constant becomes progressively longer. The time constant used to represent the test data is the average of values calculated from 0 to 15 seconds.

Table 4.2 shows the test results for the horizontal tests. The time constant follows a consistent pattern. It increases as precharge pressure increases. At any specific precharge pressure, the time constant decreases with increasing initial pressure. Figure 4.2 compares the normalized time parameter ($\alpha_e t/R^2$) from equation (2.5) (solid line), to the same parameter obtained from the experiments for the three L/D ratio. In each case the average of the 8 tests was taken. For L/D = 1.8, the % error is 3%; for L/D = 5.4, the % error is 1%, and for L/D = 13.6, the % error is -3%.

The ratio of specific heats given in Table 4.2 is calculated from the test data through the application of equation (4.1) solved for (γ).

$$\gamma = \frac{\log \frac{P_a}{P_1}}{\log \frac{P_0}{P_{-1}}} \qquad (4.3)$$

It can be observed from the ratio of specific heats obtained in the experiment that the use of (γ) = 1.45 to predict (P_a) as shown in Table 4.1 was adequate as a first order approximation since the average (γ) from data is = 1.46. The

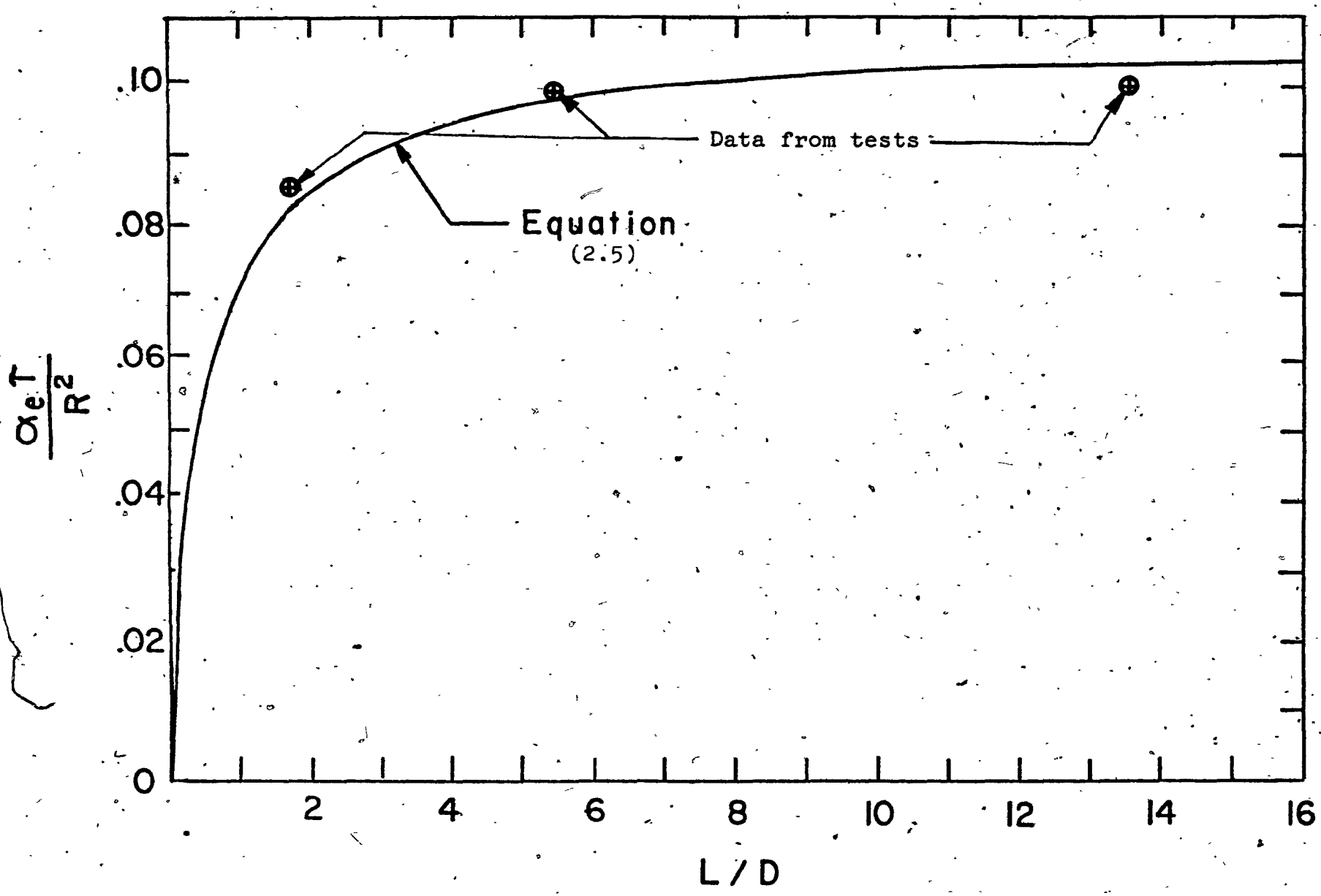

Fig. 4.2 Normalized Time Constant Equation (2.5) vs Data.

rapid discharge from initial pressure in the tests can therefore be considered adiabatic.

Table 4.2 Time Constants obtained from tests

Test No ↓	Ratio of Specific Heats, γ			Thermal Time Constants horizontal orientation					
acc.→	4 ℓ	28 ℓ	38 ℓ	4 litre		28 litre		38 litre	
				data	eqn. 3.10	data	eqn. 3.10	data	eqn. 3.10
1	1.45	1.47	1.45	21.5	20.1	38.1	32.2	32.4	26.2
2	1.47	1.44	1.43	15.5	14.0	25.5	22.4	19.1	18.2
3	1.49	1.40	1.38	12.9	10.9	18.7	17.5	16.0	14.2
4	1.43	1.43	1.40	27.0	28.0	48.0	45.1	29.6	36.5
5	1.50	1.45	1.44	18.9	19.4	30.8	31.3	22.6	25.3
6	1.53	1.44	1.42	14.7	15.2	22.7	24.5	18.0	19.8
7	1.58	1.49	1.50	28.9	34.0	47.7	54.8	35.0	44.0
8	1.47	1.49	1.52	21.7	23.7	32.8	38.2	26.1	30.9

4.2.2 Effect of Initial Pressure on Time Constant

The time constants for the horizontal tests are plotted against the initial pressure in figure (4.3a, b, c). The data appear as discrete points. Superimposed on the graph as lines are the time constants calculated from the empirical equations (3.10), (3.18), (3.19), (3.23). The empirical results may be observed to ge in good agreement with the data points.

The largest discrepancies occur when the precharge pressure is 10.44 MPa. In this case, the discrepancy can be reduced by using the specific heat ratio that was actually measured from the data (γ) = 1.49, at the 10.44 MPa precharge pressure instead of the average value.

4.2.3 Comparison of Test Results with Exponential Theory and with Heat Conduction Distribution Theory

Figures (4.4) and (4.5) show, in normalized form, the test data taken from the experimental traces for the 28 litre accumulator. These graphs are plotted on a semi-log scale.

The ordinate is: $1 - [(P-P_a)/(P_0-P_a)]$, and has the logarithmic scale. The abscissa is a normalized time parameter (t/τ). For each test the time constant used is the

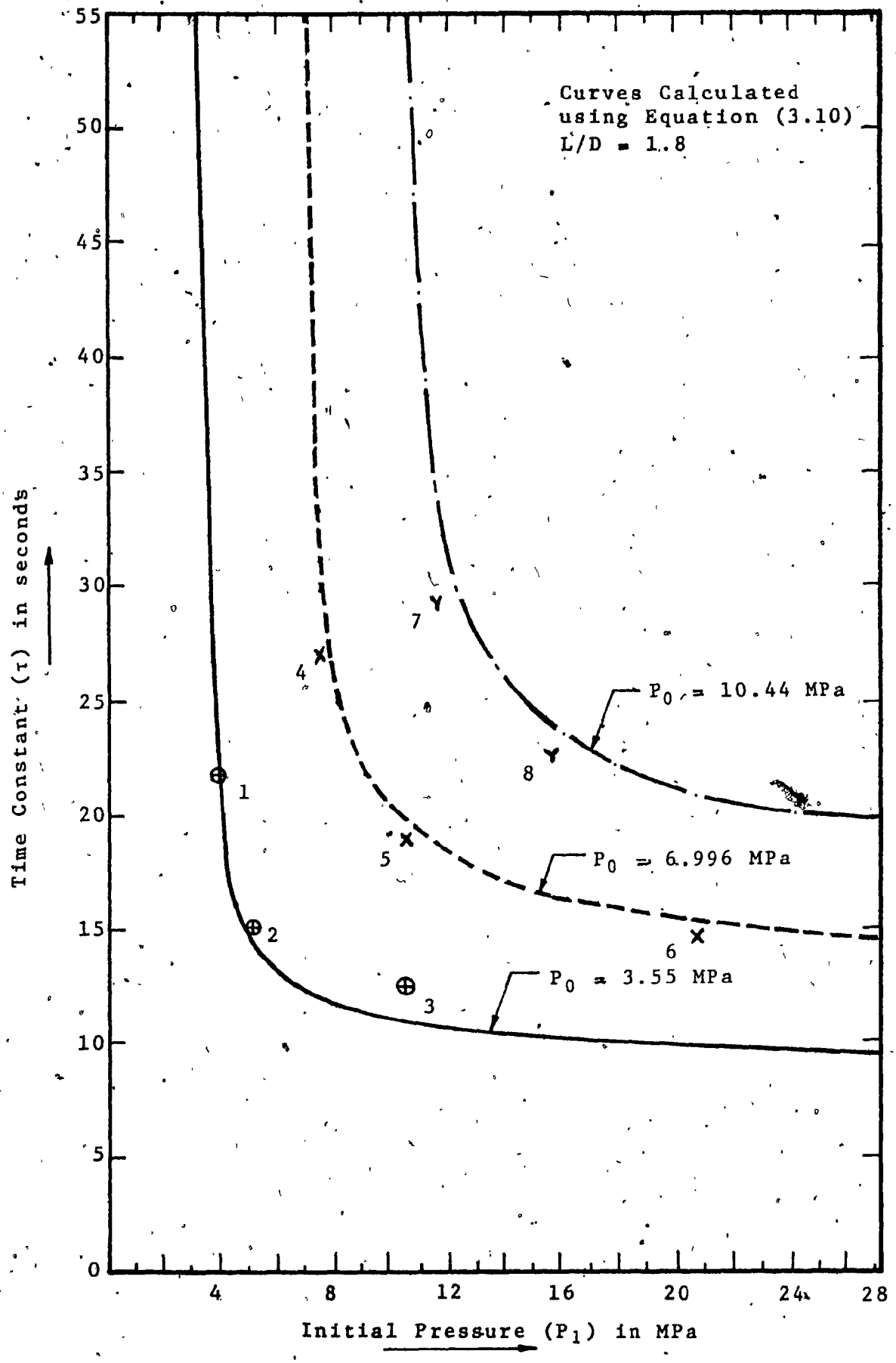

Fig. 4.3a Effect of Initial Pressure on Time Constant
4 Litre Accumulator

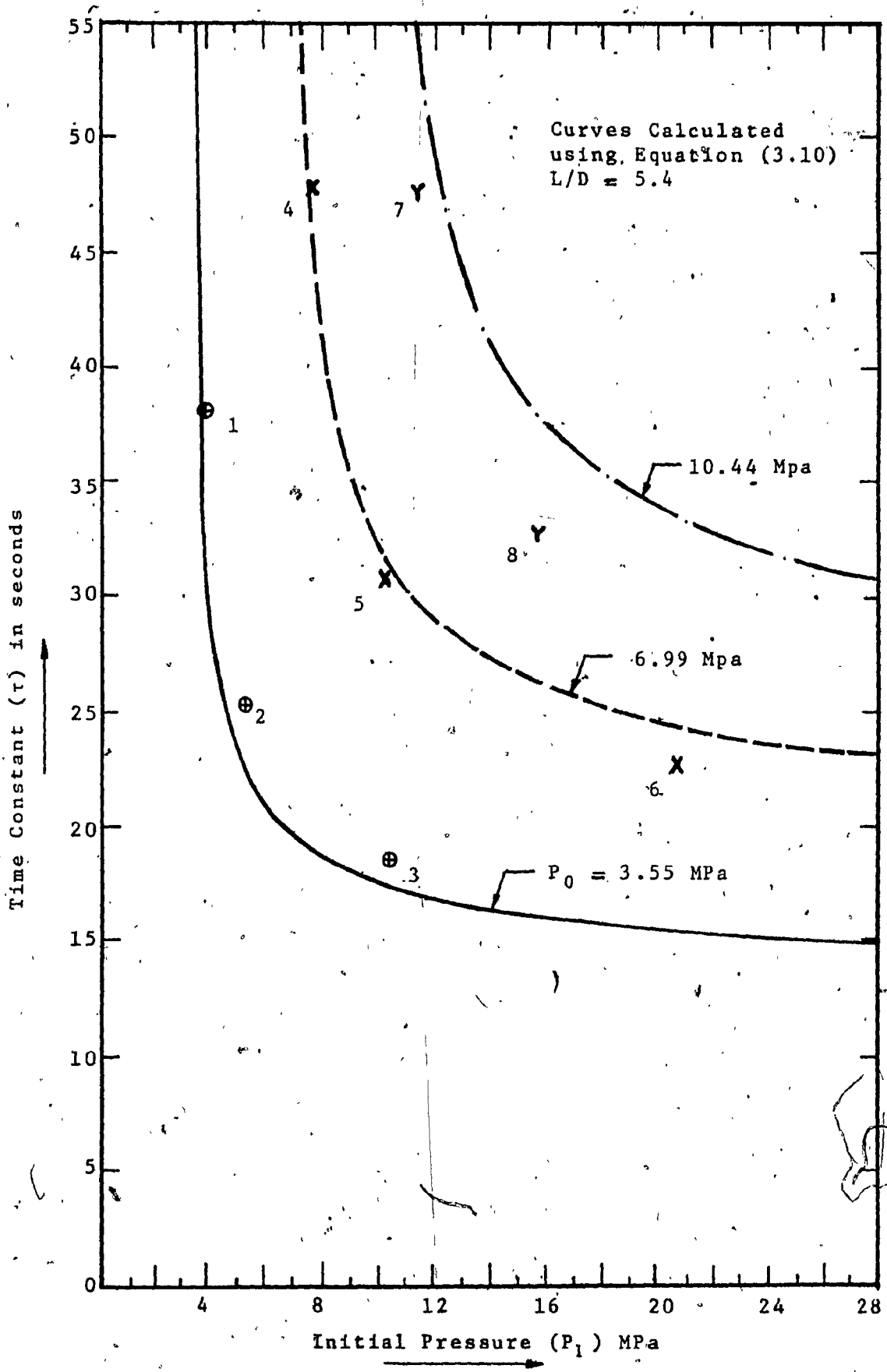

Fig. 4.3b Effect of Initial Pressure on Time Constant 28 Litre Accumulator.

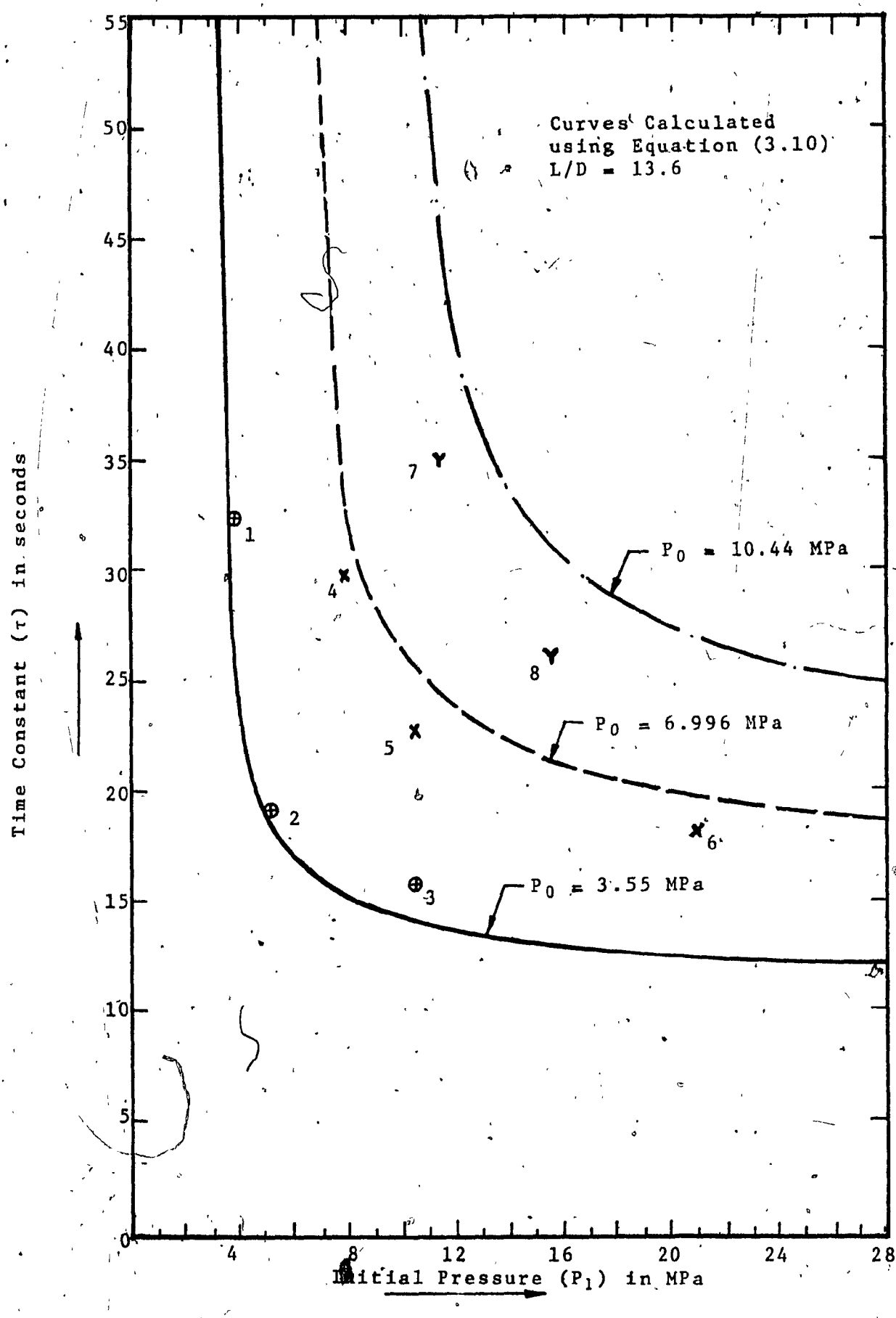

Fig. 4.3c Effect of Initial Pressure on Time Constant - 38 Litre Accumulator

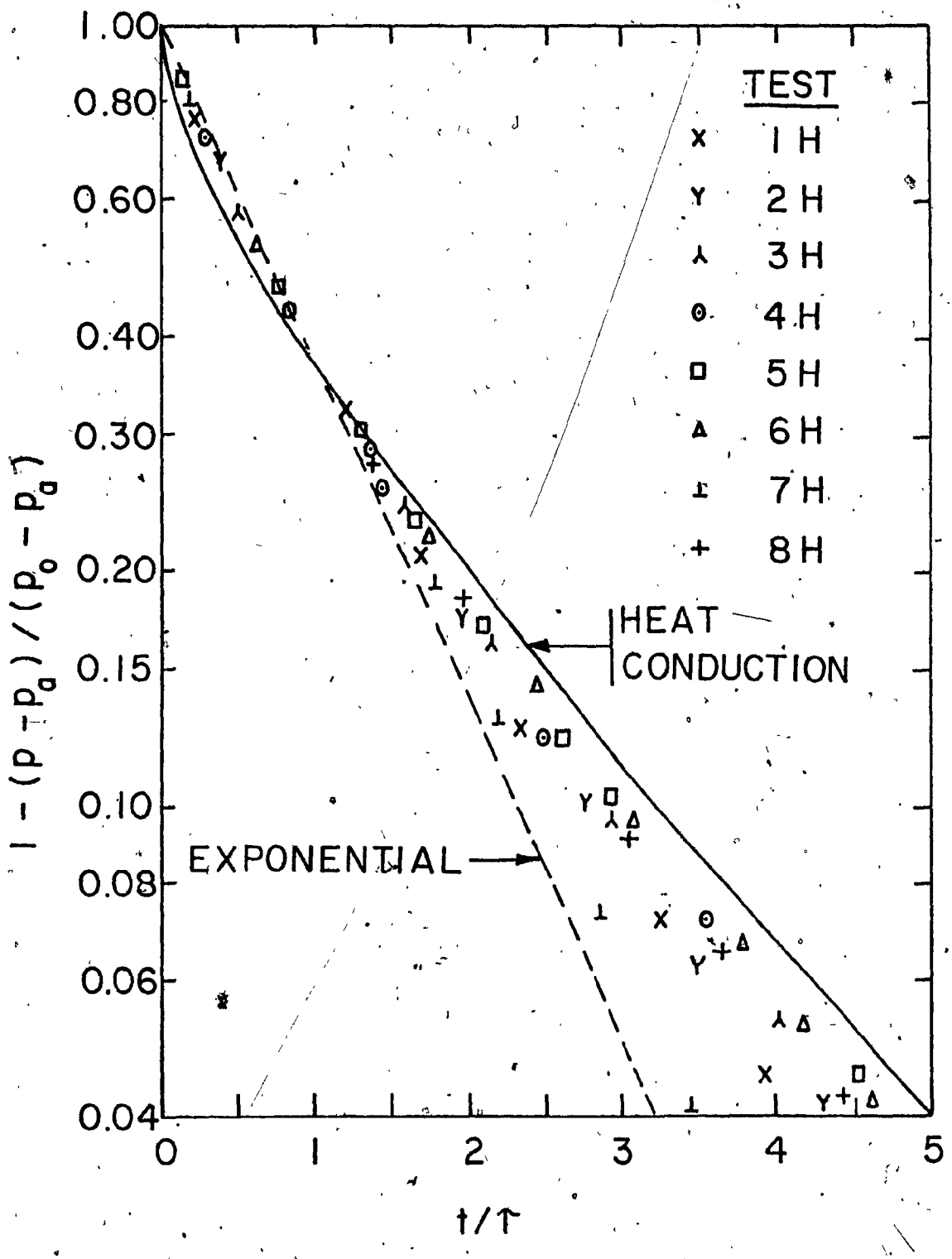

Fig. 4.4 Horizontal Test Results - 28 litre Accumulator

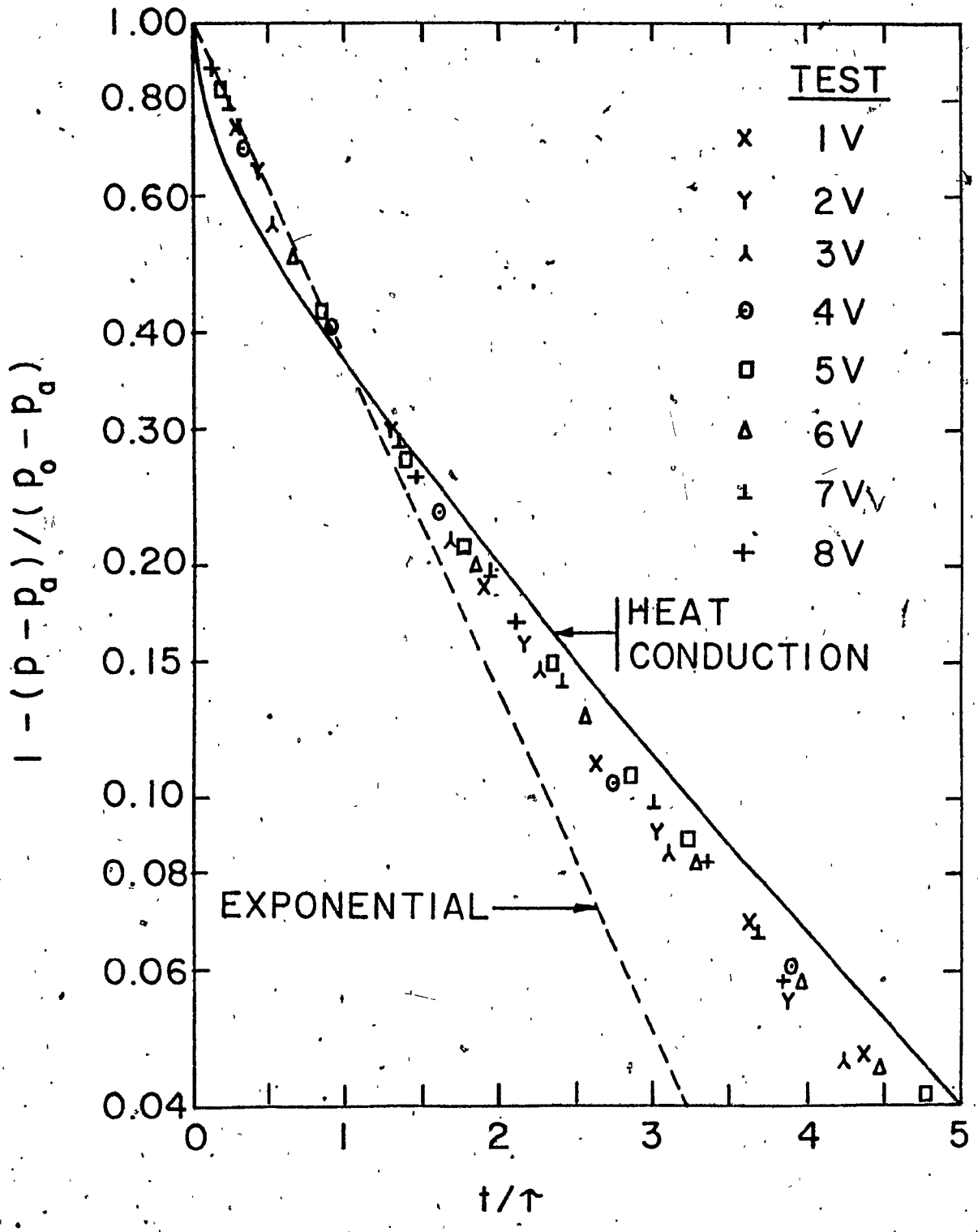

Fig. 4.5 Vertical Test Results - 28 litre Accumulator

one calculated for the test. The data are presented in this manner because the difference between the thermal models and the test data can be more readily observed. On these plots the exponential model (equation (2.22)) appears as a dashed straight line. The heat conduction model (equation 2.8)) is a curve with constantly decreasing negative slope and is shown by a solid line. The test data are represented by the discrete points scaled from the x-y recorder traces. The points selected for plotting are taken at irregular time intervals to present a clear indication of the trends in the data. Figure 4.4 represents the results of the horizontal tests and Figure 4.5, the results of the vertical tests. The data agree very well with the exponential model when the time is less than one time constant ($t/\tau<1$). For time greater than one time constant ($t/\tau>1$), the data always fall between the exponential and heat conduction models. In general the data for (t/τ) greater than unity are closer to the heat conduction model. This trend is more pronounced for the data from the vertical tests. In addition, the vertical test results show less scatter.

It can be observed here that the heat conduction model gives adequate overall results in predicting the thermodynamic phenomena. It is also capable of predicting the time constant with some accuracy. Therefore, the equations for time constant, (eqn. 2.5 and 3.10), derived from the heat conduction model are valid for use in the mathematical

model of this thesis.

4.2.4 Comparison of Experiments to the Models.

Since it was not possible to give a comparison of all the experiments to the models, three sample cases have been picked. These sample cases represent the three accumulators, the three pressure ratios and the three precharge pressures used throughout all the tests. Table 4.3 lists all the parameters for the sample comparisons shown in Figures 4.6, 4.7 and 4.8, for the 4, 28 & 38 litre accumulators respectively. These parameters were used in the pressure input computer model and a discharge of the accumulator was simulated. Actual output data is plotted on the figure corresponding to the equivalent test.

Table 4.3 List of Sample Conditions for Comparison of Model to Experiments

Test No	Accumulator			$\frac{P_1}{P_0}$ ratio	Precharge Pressure(P_0)	Initial Pressure(P_1)	See Figure No
	Capacity	D	L				
	litres	m	m		MPa	MPa	
1	4	.14605	.2602	1.1	3.55	3.891	4.6
6	28	.188	1.023	3	6.996	20.79	4.7
8	38	.14605	2.1534	1.5	10.44	15.61	4.8

Figures 4.6, 4.7 and 4.8 are reproduced from test data. Time is the abscissa and pressure of the charge-gas is the ordinate. The full line is the test data and represents the pressure transient after a complete discharge of the accumulator. The plotted symbols represent data at intervals from the computer simulation.

The correlation between computer model and experimental data is very high. In figure 4.8, the model data terminates 10kPa lower than the experimental data. This is probably due to the inaccuracy of the setting of the precharge pressure in the experiment.

In conclusion, it may be stated that the model accurately reproduces the thermal phenomena of a hydraulic accumulator.

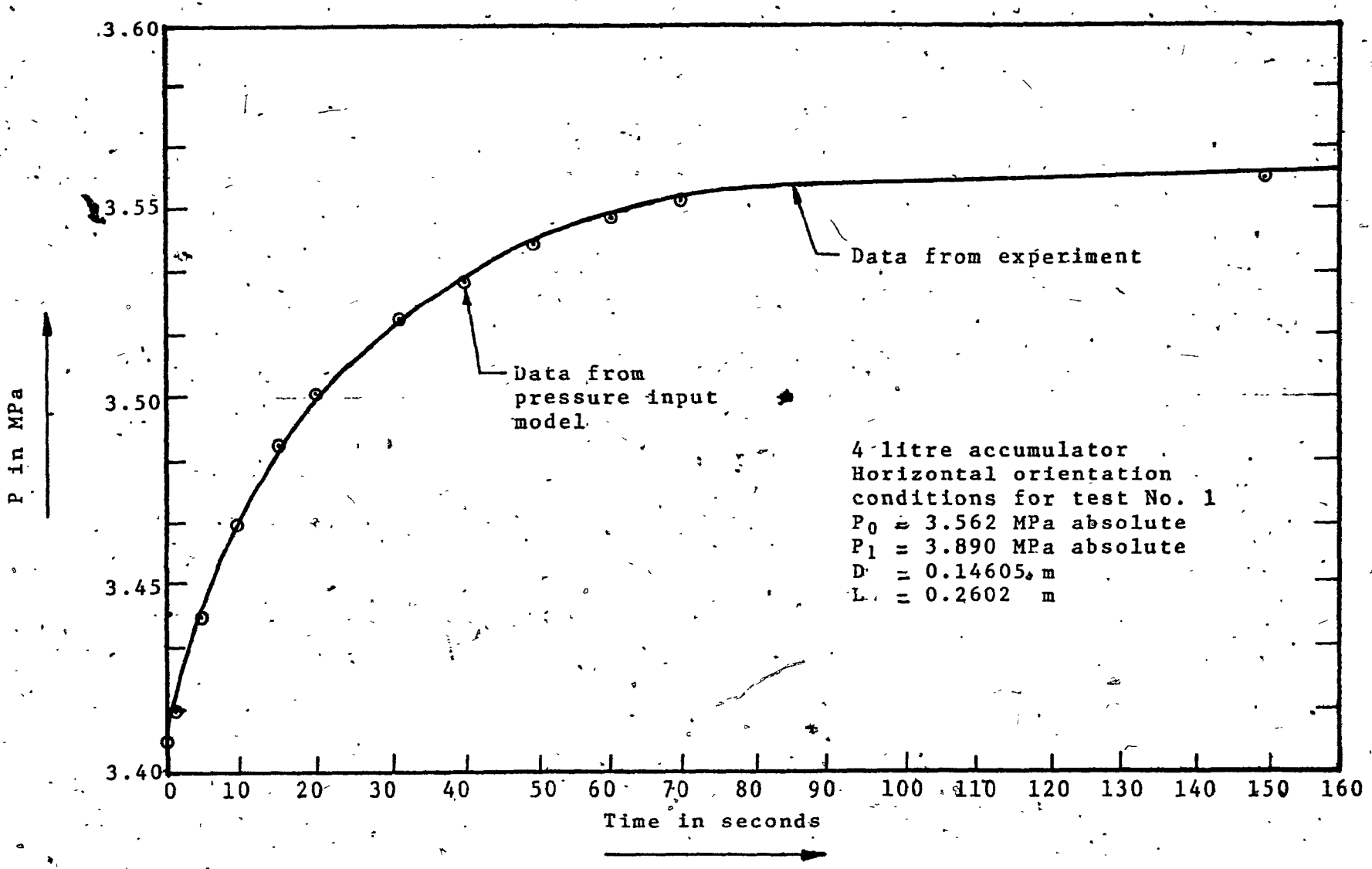

Figure 4.6 Comparison of Test Data to Model Output, Sample No. 1 - 4 liter accumulator

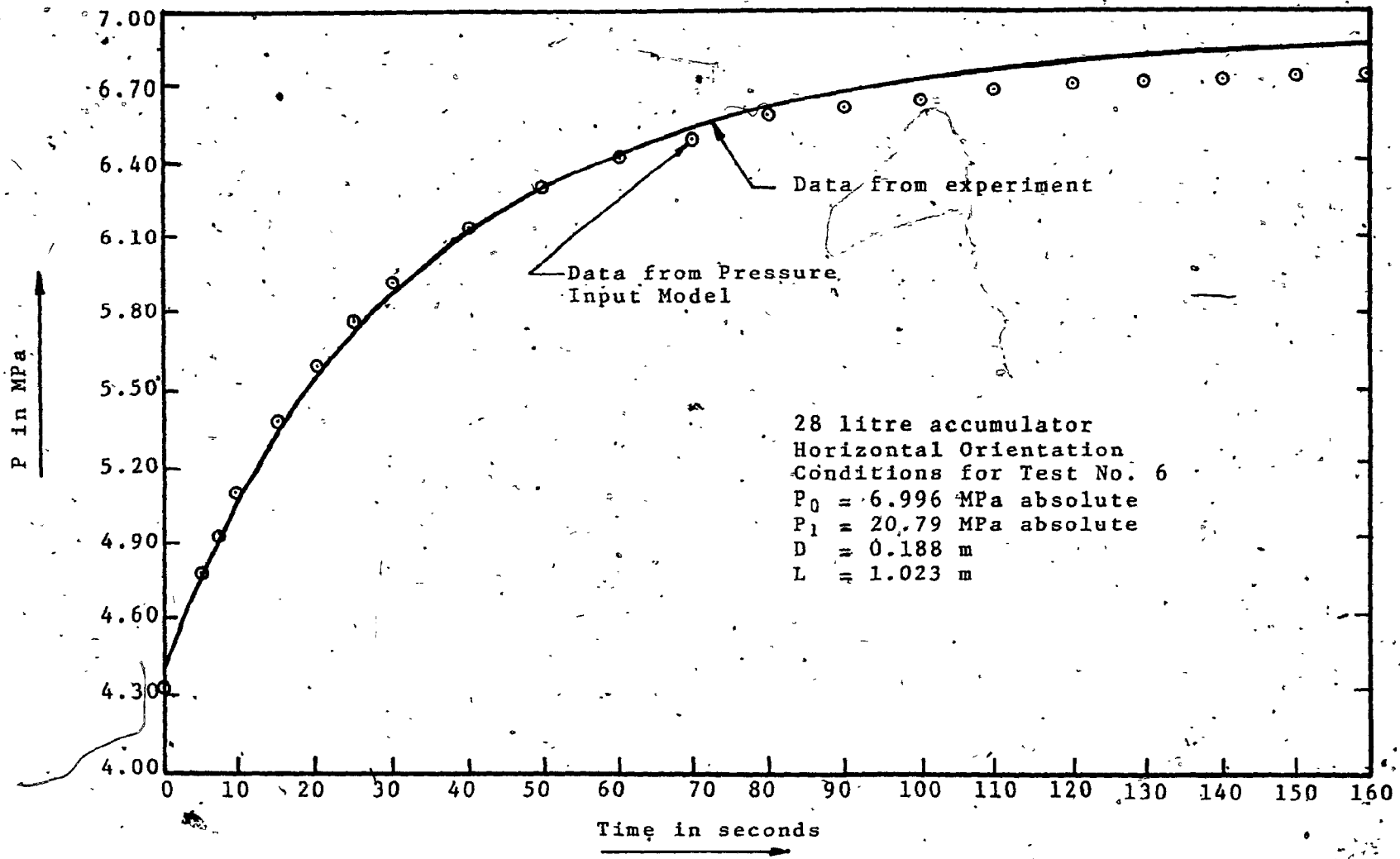

Fig. 4.7 Comparison of Test Data to Model Output, Sample No. 2 - 28 litre accumulator

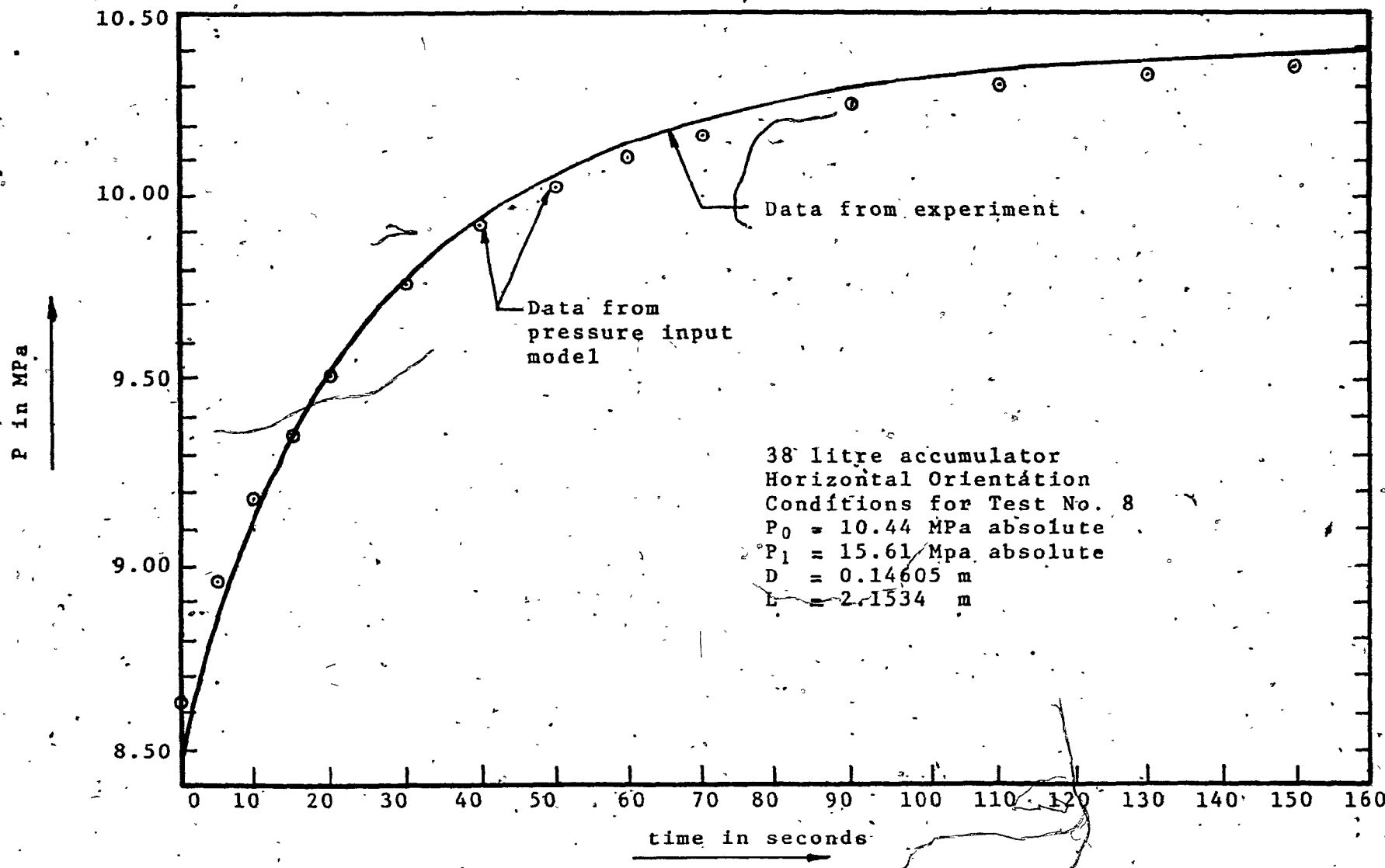

Fig. 4.8 Comparison of Test Data to Model Output, Sample No. 3 - 38 litre accumulator

CHAPTER 5

CONCLUSIONS

5.1 Summary

The purpose of this thesis is to derive the thermodynamics of gas-charged hydraulic accumulators from basic principles. To develop an accurate mathematical model for these accumulators from the derived theory; and, to prove both the derived theory and the developed models by experiments.

The thermodynamic equations were derived from the heat conduction distribution equations suggested by Carslaw and Jaeger |13|, further developed by Svoboda, Bouchard and Katz |14|. In this work, these equations are adapted for use in iterative mathematical models.

The base for the models was first developed by Otis |9|, |10| and |11|. His models, along with Green |8| assume the solution to be that of an exponential decay curve with a time constant. Both Otis and Green suggest that this time constant should be found by experiments for each accumulator. This approach is not practical as the models are used, for the main part, to optimize hydraulic systems and thus to size the accumulators. In the two models developed

in this thesis, all the parameters can be calculated from the geometry of a desired accumulator and from the desired operating conditions. They can be considered, therefore, as a pure design tool.

An extensive series of tests on three accumulators under different operating conditions has shown that the models proposed correlate to a high degree with actual operation. The models will therefore improve the accuracy of simulations of systems where accumulators are used. They will permit proper sizing both of the accumulator and of the system in general. This will effectively reduce the cost of hardware and energy in hydraulic power transmission systems.

5.2 Suggested Further Work

Following are summarized suggestions for improvement of the models:

1) The next logical step, after developing models for piston accumulators should be to develop, through experimentation, parameters which would modify the model equations for use with other types of accumulators, particularly the diaphragm accumulator.
2) In order to improve stability, the Euler numerical method should be replaced by a fourth-order Runge-Kutta scheme.
3) Theory should be derived to account for the variation of the time constant due to vertical orientation. This theory would be related to the characteristic dimension, δ, for different orientation.

REFERENCES AND BIBLIOGRAPHY

List of References

1. Shearer, J.L.; Murphy, A.T.; and Richardson, H.H. Introduction to System Dynamics. Reading, Mass: Addison-Wesley Publishing, 1967, pp. 61-65, 83-84.

2. Lindsay, J.F., and Katz, S. Dynamics of Physical Circuits and Systems. Champaign, Ill.: Matrix Publishers, 1978, pp. 89-95.

3. Graze, H.R. "A Rational Thermodynamic Equation for Air Chamber Design". Third Australasian Conference on Hydraulics and Fluid Mechanics. Nov. 25 to 29, 1968. Sydney, Australia.

4. Graze, H.R. and Forrest, J.A. "New Design Charts for Air Chambers". Fifth Australasian Conference on Hydraulics and Fluid Mechanics. Dec. 9 to 13, 1974, University of Canterbury, Christchurch, New Zealand.

5. Gangnath, R.B. and White, H.W. "Optimization of Hydraulic Accumulators for Low Temperature Applications". Society of Automotive Engineers, Issue 711B, Montreal, June, 1963.

6. Klein, H. Ch. "Amvendung Hydropneumatischer Energispeicher Inder Olhydraulic". Konstruction, Vol. 16, No. 1, January 1964, pp. 12-21.

7. Röper, R. "Die Dynamik des Hydro-Speicher Kreislaufes". Konstruction, 20, 1968, Heft 9, pp. 341-349.

8. Green, W.L. "The Effects of Discharge Times on the Selection of Gas-Charged Hydraulic Accumulators". Paper D1. 3rd International Fluid Power Symposium. Turin, Italy, 9th - 11th May, 1973, pp. D1-1 - D1-15.

9. Otis, David R. "Predicting Performance of Gas Charged Accumulators". Presented at First Fluid Power Controls & Systems Conference. University of Wisconsin, Madison, May 23-25, 1973, 12 p. 5 fig.

10. Otis, David R. "Thermal Losses in Gas-Charged Hydraulic Accumulators". Intersociety Energy Conversion Engineering Conference. 8th Proceedings pap. University of PA., Philadelphia. Aug. 13-17, 1973, pp. 198-201. Published by AIAA. Paper No. 739093.

11. Otis, David R. "New Developments in Predicting and Modifying Performance of Hydraulic Accumulators". National Conference on Fluid Power, 1974, pp. 473-489.

12. Elder, F.T. and Otis, David R. "Accumulators: The Role of Heat Transfer in Fluid Power Losses". 4th International Fluid Power Symposium. Sheffield England by BHRA Fluid Engineering. April 16-18, 1975, Paper D2, pp. D2-27 to 37.

13. Carslaw, H.S., and Jaeger, J.C. Conduction of Heat in Solids. 2nd ed. Oxford: Clarendon Press, 1959, pp. 226-227.

14. Svoboda, J.; Bouchard, G.; and Katz, S. "A Thermal Model for Gas-Charged Accumulators Based on the Heat Conduction Distribution". Fluid Transients and Acoustics in the Power Industry. New York: American Society for Mechanical Engineering, 1978, pp. 161-167.

15. Holman, J.P. Heat Transfer. 4th. ed. New York: McGraw Hill Book Co., 1976, pp. 255-260.

16. Jakob, Max. Heat Transfer. Vol. I & II. New York: John Wiley & Sons, Vol. I, 1949; Vol. II, 1965. Vol. I, pp. 522-542. Vol II, pp. 577-579.

17. Welty, James R.; Wicks, Charles E.; and Wilson, Robert E. Fundamental of Momentum, Heat and Mass Transfer. New York: John Wiley & Sons, 1969, pp. 338-342, 220, 313, 215, 654.

18. Jones, James B. and Hawkins, George A. Engineering Thermodynamics. An Introductory Textbook. New York: John Wiley & Sons, 1960, pp. 201-203, 164.

19. Hornbeck, Robert W. Numerical Methods. New York: Quantum Publishers, 1975, pp. 192-194.

Suggested Reading

20. Dewey, C., Elder, F.T., Otis, D.R. "Accumulator-Charged Hydrostatic Drive for Cars Saves Energy". Hydraulics and Pneumatics, October 1974, pp. 180-183.

21. Dunn, H.S. and Wojciechowski, P.H. "Energy Storage and Conversion Efficiency in a Hydraulic / Gas-Turbine Hybrid". The Amercian Society of Mechanical Engineers. Contributed by the Gas Turbine Division of the A.S.M.E. for Presentation at the Gas Turbine Conference & Products Show, Zurich, Switzerland, March 30 - April 4, 1974.

22. Gottschald, Dr. L. "Criteria for the Discharge of Hydropneumatic Accumulators". Paper No. 27. First European Fluid Power Conference, Glascow 10-12, September 1973.

23. Korkmaz, F.; und Walz, L. "Hydrospeicher als Energeispeicher Ideales und Reales Verhalten des Energieträgers". Oilhydraulik und Pneumatik, 18, 1974, Nr 2, pp. 132-140.

24. Lewis, Michael A. "Accumulators Review. Making the Right Choice". Fluid Power International, May 1973, pp. 27-29, 31.

25. MacArthur, Douglas Scott. Churchill College. Energy Storing Hydrostatic Transmission for Urban Vehicles. A Thesis Submitted to the University of Cambridge for the Degree of Doctor of Philosophy. April 1977. Chapter 5, Accumulators, pp. 66-84, 158-160, 152-153, 215.

26. Otis, D.R. "The use of Flexible, Gas-Filled Composites as the Medium of Compression in Pneumatic Systems". In Thermal Losses in Gas-Charged Hydraulic Accumulators. June 19, 1968.

27. Otis, D.R. "Plastic Foams Reduce Heating in Gas-Charged Accumulators". Hydraulics and Pneumatics, February 1975, pp. 56-57.

28. Otis, D.R. "Getting Maximum Energy-Savings from your Accumulators". Hydraulics and Pneumatics, December 1979, pp. 57-60.

29. Sherman, M.P. and Karlekar, B.V. "Improving the Energy Storage Capacity of Hydraulic Accumulators". Inter-Society Energy Conversion Engineering Conference, 8th Proceedings pap. University of Pensylvania, Philadelphia, August 13-17, 1973, pp. 202-207. Paper No. 739094.

30. Svoboda, Jaroslav. Hydraulic Hybrid Vehicular Drive Employing Regenerating Braking. A Thesis in the Faculty of Engineering Concordia University, November 1975.

31. Toft Fensvic, A. Nielsen, T.H., Ovesen, T.B. "On the Dynamics of Rubber Bag Accumulators - Analytical and Experimental Modelling". Paper D1. 4th International Fluid Power Symposium. Sheffield, England, April 16-18, 1975.

32. White, Roy. "Accumulator Applications in the Mobile Machinery Industry". Hydraulic Pneumatic Power, November 1973, pp. 419-422.

33. Wingate, I. "A Simplified Calculation Method for Hydraulic Accumulator Selection". Power, October 1975, pp. 361-365.

34. Wingate, I. "Accumulators Review. Design and Application Trends". Fluid Power International, May 1973, pp. 23, 25.

35. Wolfe, Gene. "A Plant Engineers Guide to Hydraulic Accumulators". Plant Engineering, November 14, 1974, pp. 120-126.

36. Zahid, Abduz. "Accumulators and their Applications". Annual Southern Industry Fluid Power Conference and Exhibit. Huntsville, Alabama, November 1966. In Otis, D.R. "Predicting Performance of Gas Charged Accumulators".

37. Zahid, Abduz. "No More Shake, Rattle, and Roll. An Hydropneumatic Accumulator can Effectively Reduce Shock and Vibration in Hydraulic Pipe Lines". Hydraulics and Pneumatics, May 1970, pp. 84-86.

38. Zahid, Abduz. "Sizing Hydraulic Accumulators". Plant Engineering, October 28, 1971, pp. 47-49.

39. Zahid, Abduz. "Accumulators for Closed-Center Mobile Hydraulic Systems". Hydraulics and Pneumatics, Vol. 25, No. 6, June 1974, pp. 80-83.

40. Zahid, Abduz. "Can an Accumulator Save Hydraulic Energy". Hydraulics and Pneumatics, 28, 7, July 1975, pp. 82-84.

41. Zahid, Abduz. "Can an Accumulator Save Hydraulic Energy". Hydraulics and Pneumatics, 28, 7, July 1975, pp. 82-84.

42. Zahid, Abduz. "Computer Sizes Accumulators to Control Surge and Pulsation". Hydraulics and Pneumatics, June 1977, pp. 64-66.

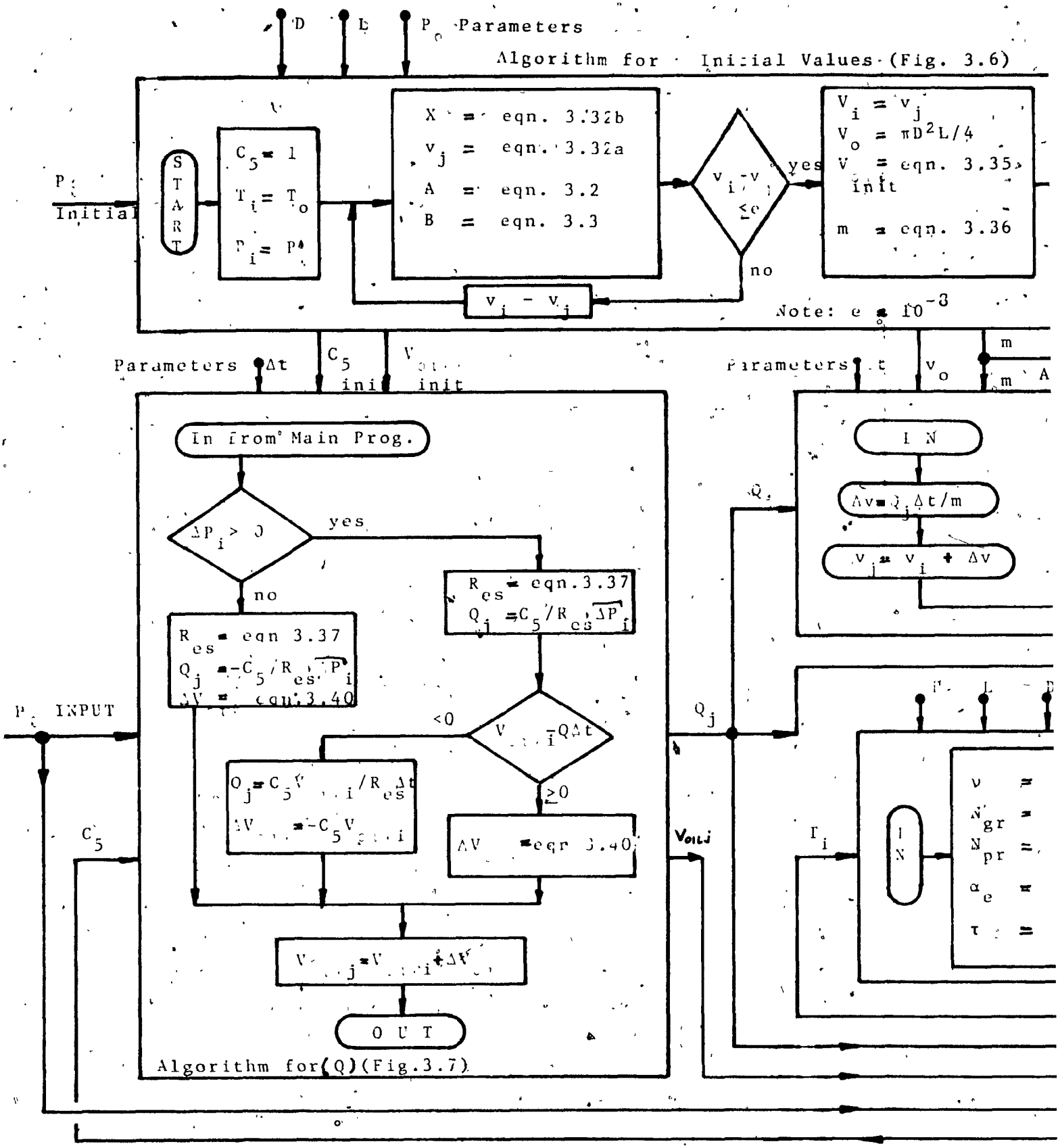
D
L
P_o Parameters
Algorithm for Initial Values (Fig. 3.6)
START
$C_5 = 1$
$T_i = T_o$
$P_i = P_o$
X = eqn. 3.32b
v_j = eqn. 3.32a
A = eqn. 3.2
B = eqn. 3.3
$v_i - v_j \leq e$
yes
no
$v_j - v_i$
$V_i = v_j$
$V_o = \pi D^2 L/4$
V_{init} = eqn. 3.35
m = eqn. 3.36
Note: $e = 10^{-3}$
Parameters Δt
C_5 init
V_{oil} init
Parameters t
v_o
m
A
In from Main Prog.
$\Delta P_i > 0$
yes
no
R_{es} = eqn.3.37
$Q_j = C_5/R_{es}\sqrt{\Delta P_i}$
R_{es} = eqn 3.37
$Q_j = -C_5/R_{es}\sqrt{P_i}$
ΔV = eqn.3.40
$V_{oil_i} - Q\Delta t$
<0
≥0
$Q_j = C_5 V_{oil_i}/R_{es}\Delta t$
$\Delta V = -C_5 V_{oil_i}$
ΔV = eqn 3.40
$V_{oil_j} = V_{oil_i} + \Delta V$
OUT
Algorithm for (Q) (Fig.3.7)
P_i INPUT
C_5
Q_j
V_{oil_j}
IN
$\Delta v = Q_j \Delta t/m$
$v_j = v_i + \Delta v$
Γ_i
IN
ν =
N_{gr} =
N_{pr} =
α_e =
τ =

(Fig. 3.6)

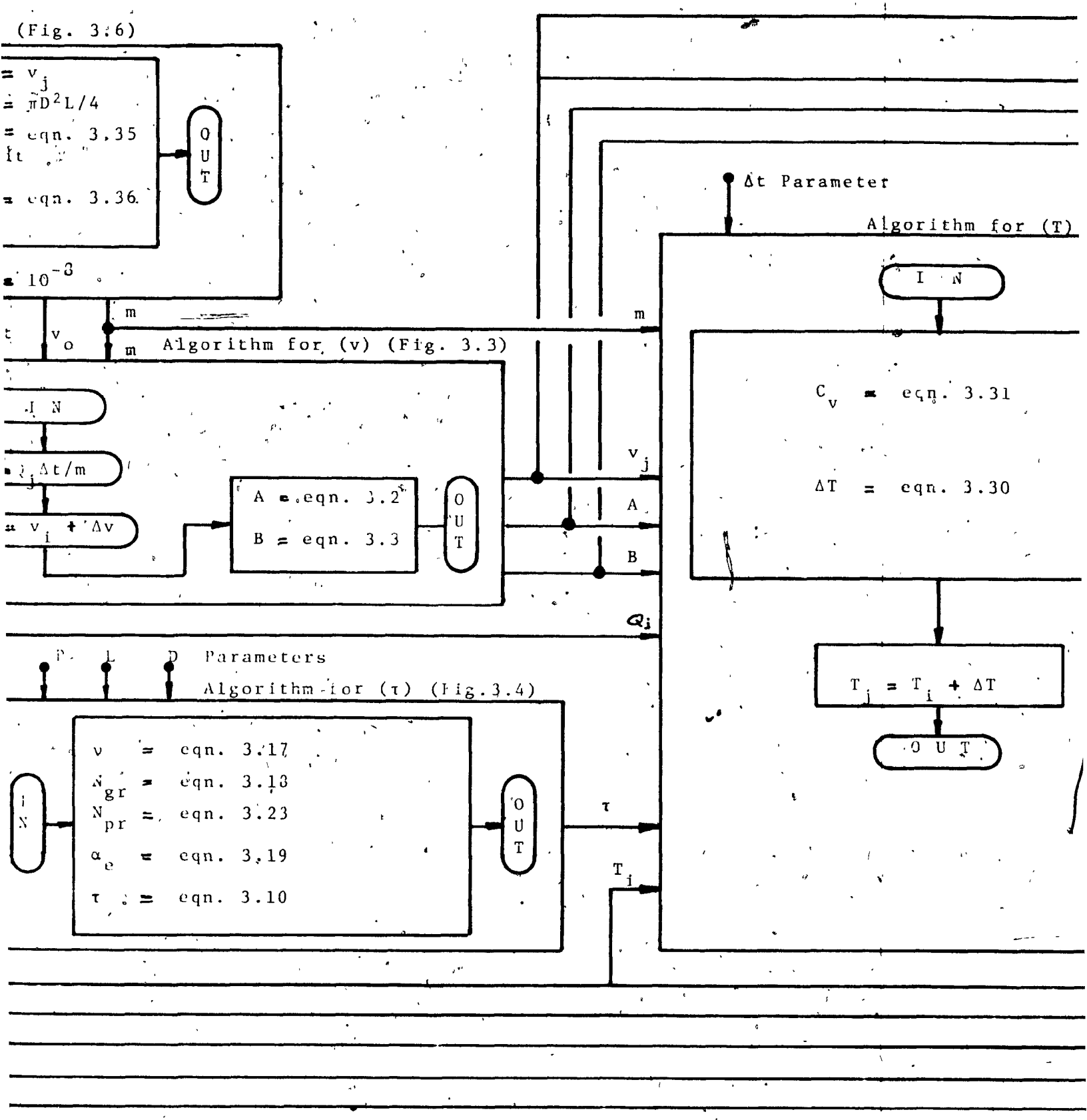
= v_j
= $\pi D^2 L/4$
= eqn. 3.35
= eqn. 3.36
OUT
10^{-3}
v_o
m
m
Algorithm for (v) (Fig. 3.3)
IN
$\Delta t/m$
$v_i + \Delta v$
A = eqn. 3.2
B = eqn. 3.3
OUT
v_j
A
B
Q_j
P L D Parameters
Algorithm for (τ) (Fig. 3.4)
IN
ν = eqn. 3.17
N_{gr} = eqn. 3.18
N_{pr} = eqn. 3.23
α_e = eqn. 3.19
τ = eqn. 3.10
OUT
τ
T_i
Δt Parameter
Algorithm for (T)
IN
C_v = eqn. 3.31
ΔT = eqn. 3.30
$T_j = T_i + \Delta T$
OUT

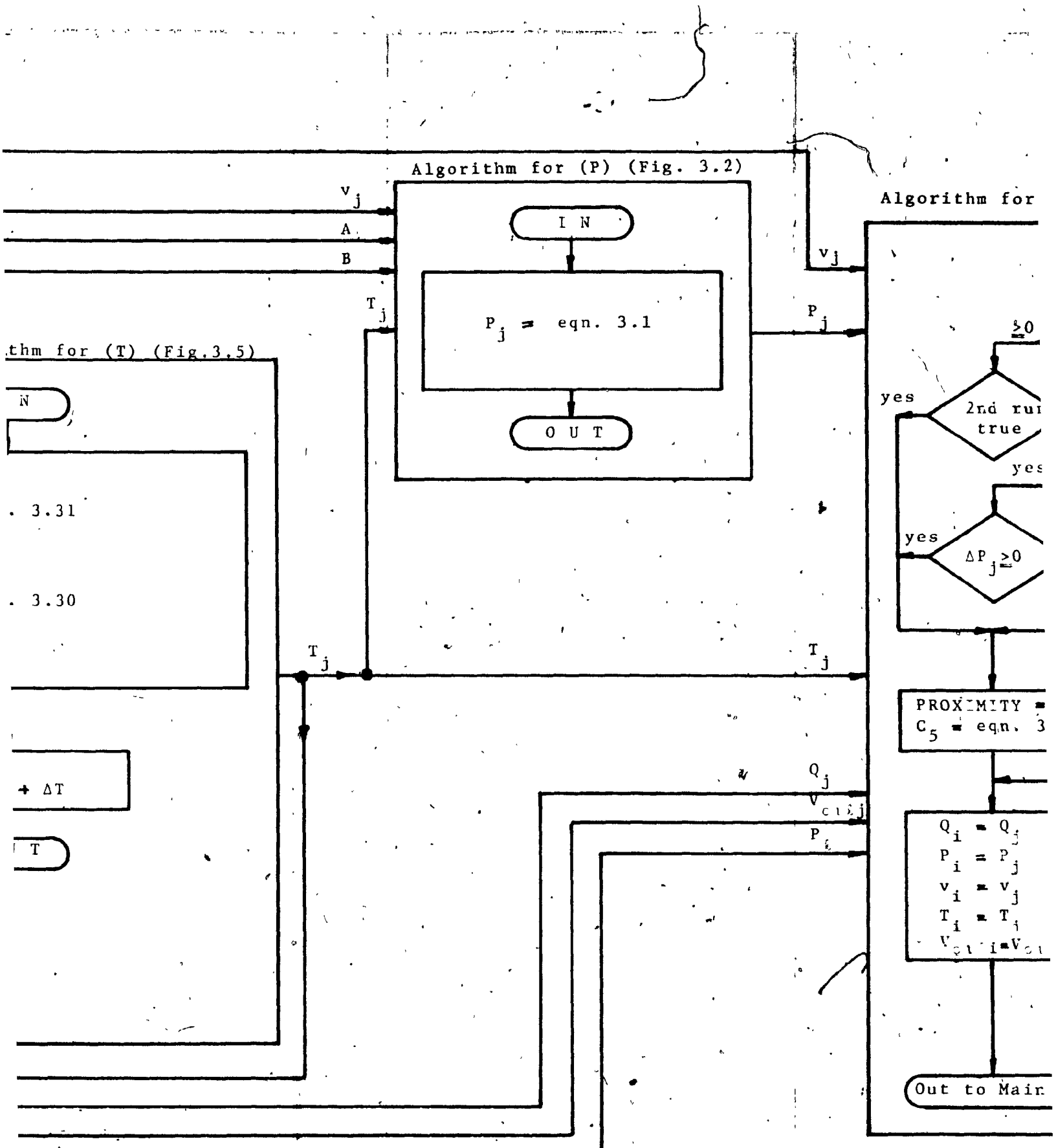

Note: The subscript i corresponds
The subscript j corresponds

) (Fig. 3.2)

3.1

Algorithm for Correction of Instability (Fig.3.10)

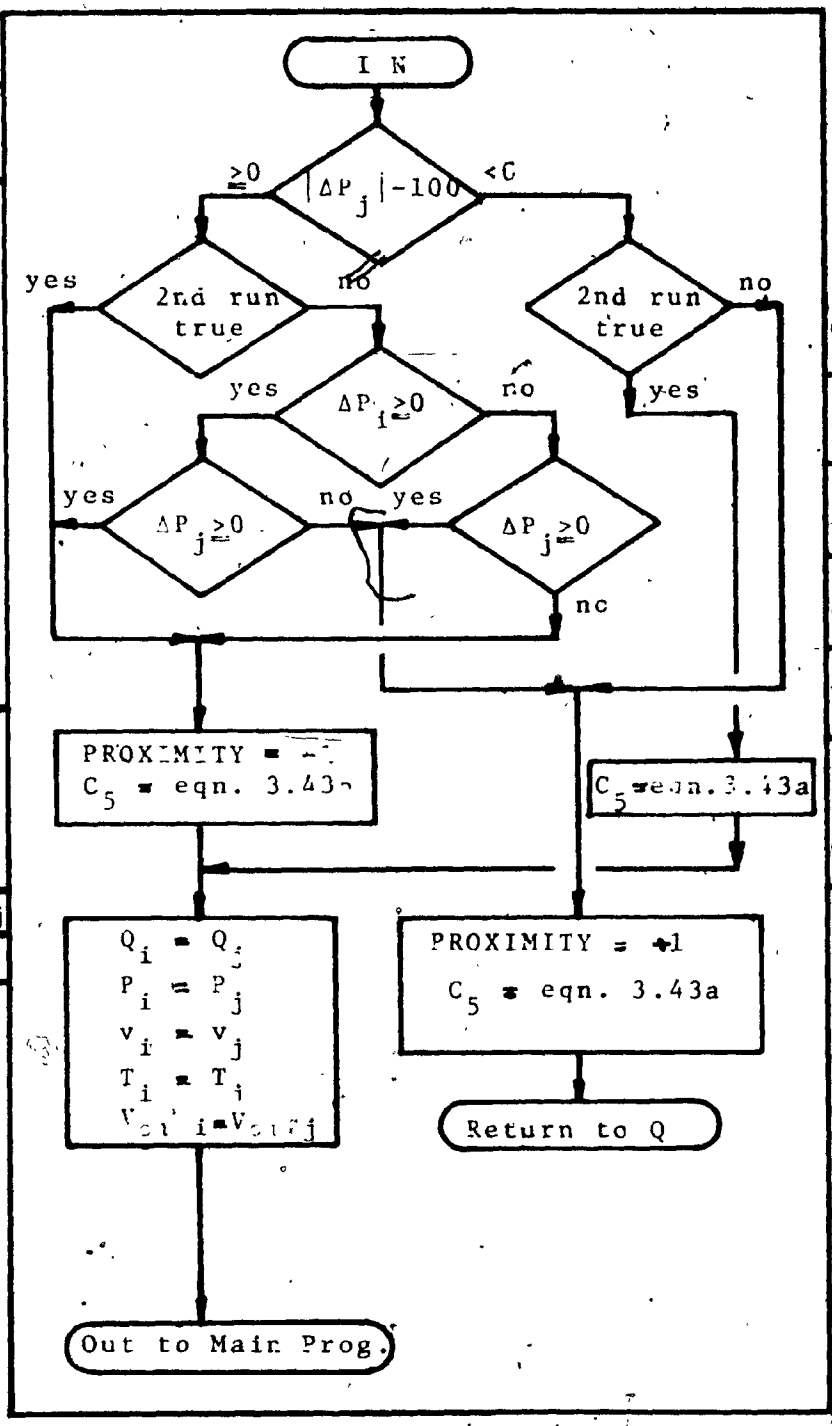

Note: The subscript i corresponds to the correct value.
The subscript j corresponds to the suggested value.

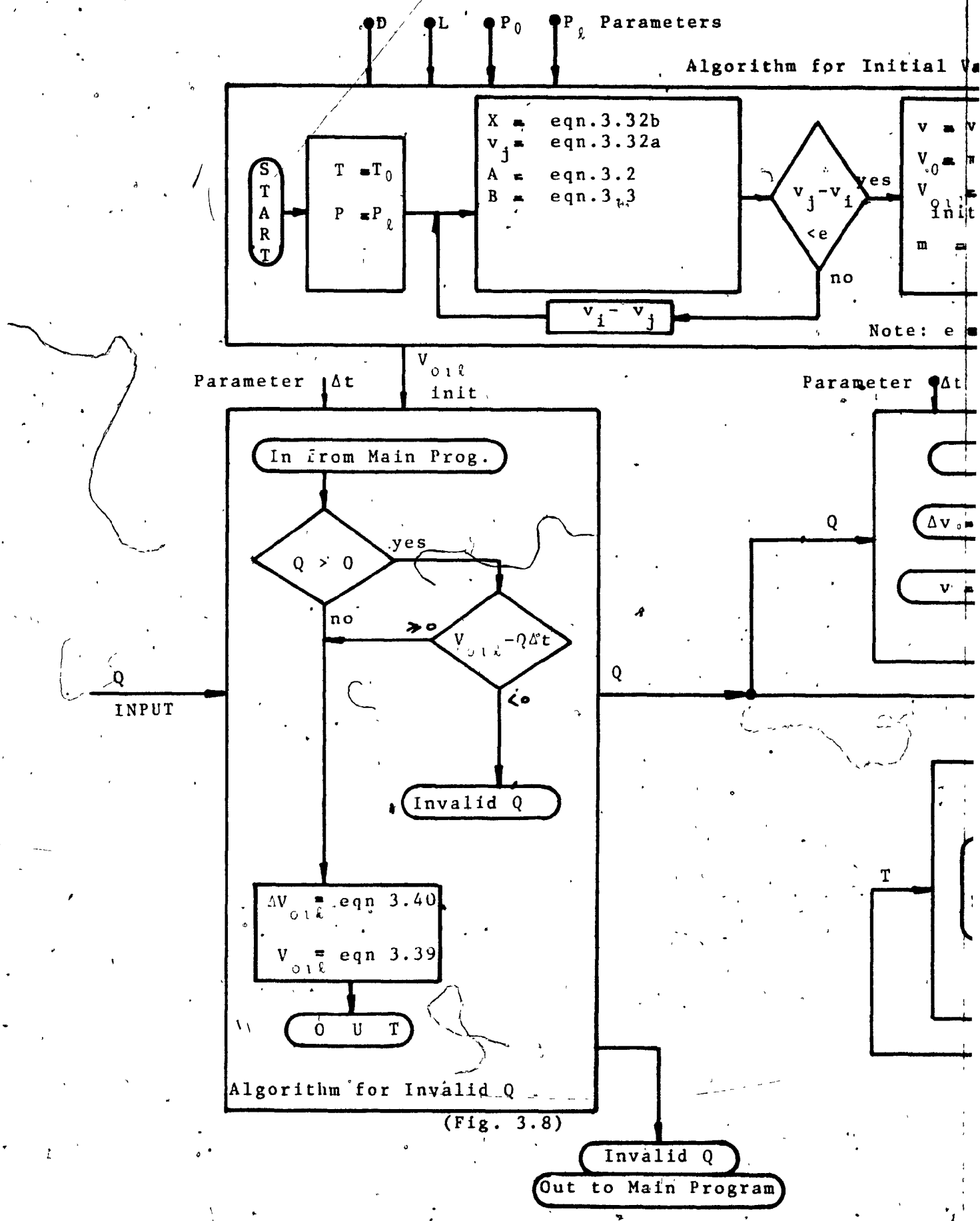
D
L
P_0
P_ℓ Parameters
Algorithm for Initial V
START
T = T_0
P = P_ℓ
X = eqn.3.32b
v_j = eqn.3.32a
A = eqn.3.2
B = eqn.3.3
$v_j - v_i$ <e
yes
no
$v_i - v_j$
v =
V_0 =
$V_{o\ell}$ init
m =
Note: e
Parameter Δt
$V_{o\ell}$ init
Parameter Δt
In from Main Prog.
Q > 0
yes
no
≥0
$V_{o\ell} - Q\Delta t$
<0
Q
INPUT
Invalid Q
$\Delta V_{o\ell}$ = eqn 3.40
$V_{o\ell}$ = eqn 3.39
O U T
Algorithm for Invalid Q
(Fig. 3.8)
Invalid Q
Out to Main Program
Q
Δv_o =
v =
T

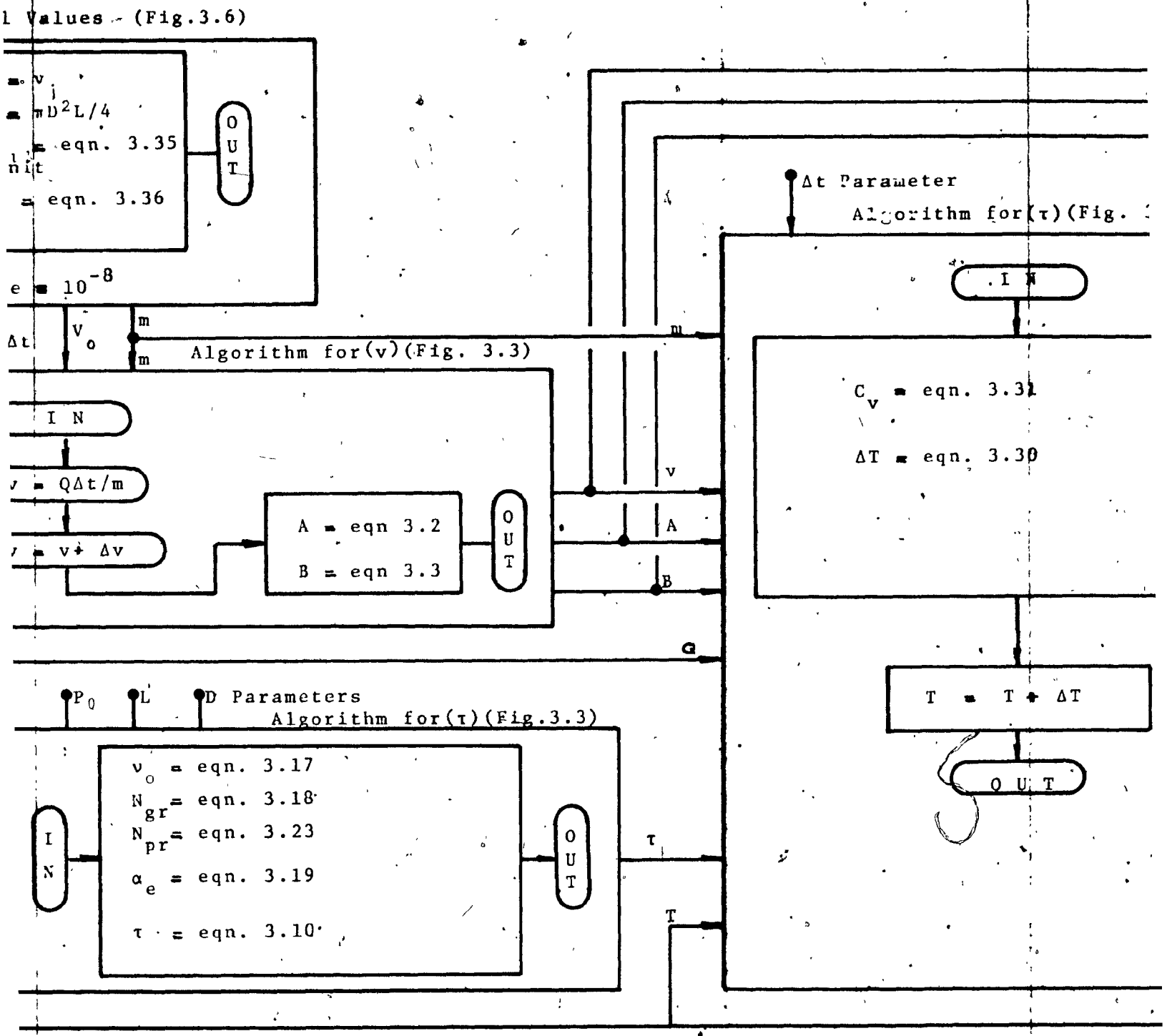
l Values (Fig.3.6)
= v
= πD²L/4
= eqn. 3.35
nit
= eqn. 3.36
OUT
e = 10⁻⁸
Δt
V₀
m
m
Algorithm for(v)(Fig. 3.3)
I N
v = QΔt/m
v = v + Δv
A = eqn 3.2
B = eqn 3.3
OUT
v
A
B
m
Δt Parameter
Algorithm for(τ)(Fig.
I N
C_v = eqn. 3.31
ΔT = eqn. 3.30
T = T + ΔT
OUT
Q
P₀
L
D Parameters
Algorithm for(τ)(Fig.3.3)
I N
ν₀ = eqn. 3.17
N_gr = eqn. 3.18
N_pr = eqn. 3.23
α_e = eqn. 3.19
τ = eqn. 3.10
OUT
τ
T

APPENDIX

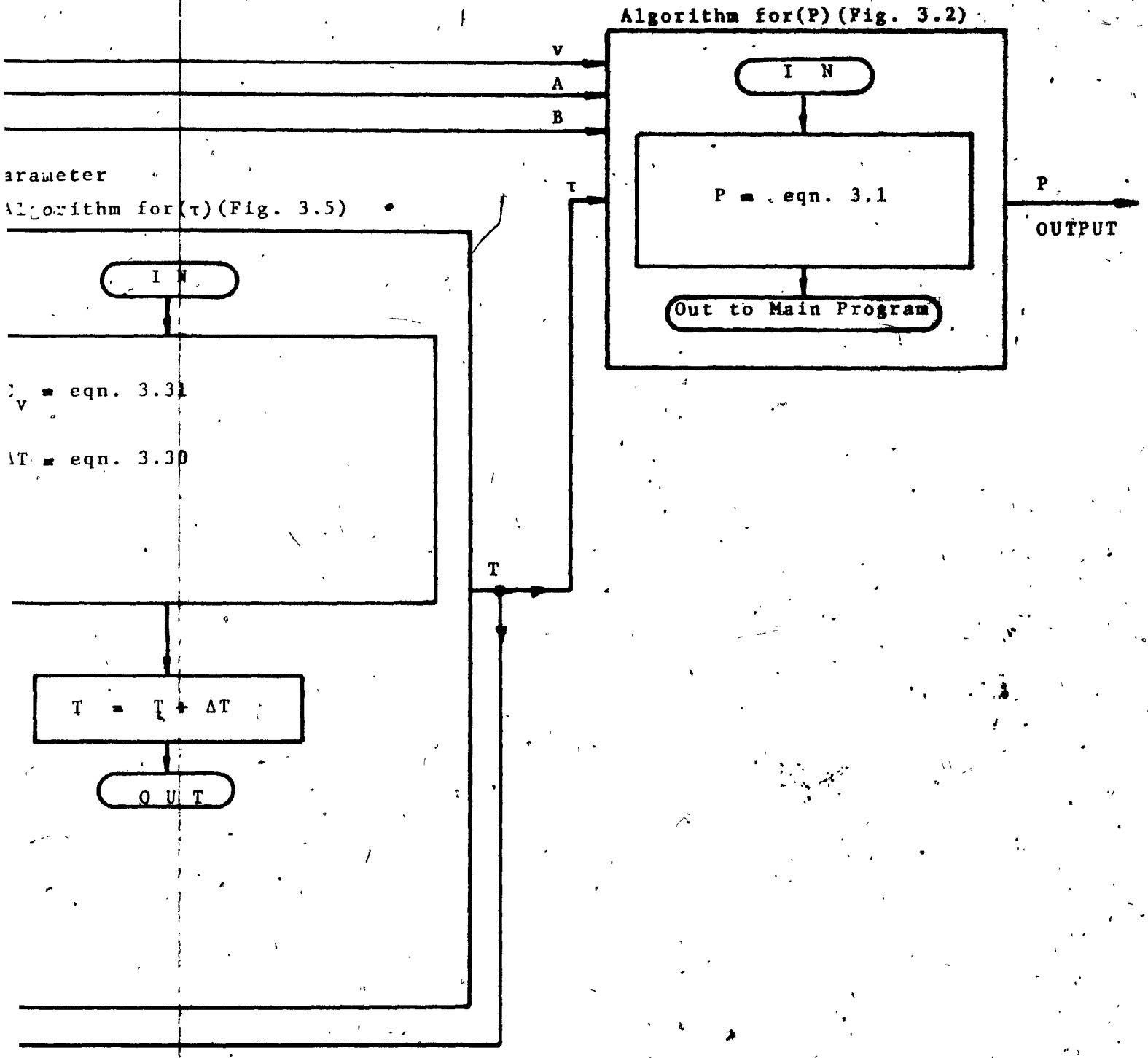

APPENDIX B The Complete Flow Input Model

APPENDIX C

Flow Input Model FORTRAN

```
      PROGRAM FLOWIN(INPUT,OUTPUT)
C     PARAMETERS AND CONSTANTS
50    FORMAT(5F15.7)
      READ50,PIE,C1,C2,C3,C10
      READ50,AL,AO,BL,BO,G
      READ50,CK1,CK3,CK10,CK11,PS
      READ50,RU,SVS,ALPHS,CNUS,C5
      READ50,CL,PO,TO,D,DELT
      READ50,PL,A,B,SVI,TIM
C
C   INITIAL VALUES ALGORITHM
C
      T     =TO
      PA    =PL
      J     =(1.0/DELT)+DELT
      X     =RU*T/PA
100   SV    =0.5*(X+((X**2.-(4.*A/PA)+4.*X*B)**.5))
      A     =AO*(1.-(AL/SV))
      B     =BO*(1.-(BL/SV))
      IF(ABS(SV-SVI)-1.0E-6)120,120,110
110   SVI   =SV
      GO TO 100
120   VOL   =(D**2.)*CL*PIE/4.
      VOIL  =VOL*(1.-(PO/PA))
      CMASS =(VOL*PO)/(SVS*PS)
130   FORMAT(F8.2,2F10.8)
      PRINT130,TIM,VOIL,SV
140   FORMAT(3X,*TIME*,6X,*PRESSURE*,8X,*FLOW*,8X,*TEMP.*)
      PRINT 140
      PRINT220,TIM,PA,Q,T
C
C     MAIN CONTROL PROGRAM
200   DO1300 I=1,J
      TIM   =TIM+DELT
      IF(TIM-200.)230,300,300
230   IF(TIM-2.0)240,250,250
240   Q     =(-0.001)
      GO TO 260
250   Q     =0.00
      GO TO 260
C     ACCUMULATOR MODEL Q INPUT
260   IF(Q)400,400,270
270   IF(VOIL-(Q*DELT))280,400,400
280   PRINT290
290   FORMAT(1X,*INVALID Q*)
300   CONTINUE
      STOP1
```

```
400   DELVOL =(-Q*DELT)
      VOIL   =VOIL+DELVOL
C     ALGORITHM FOR SV
      DELSV  =Q*DELT/CMASS
      SV     =SV+DELSV
      A      =AO*(1.-(AL/SV))
      B      =BO*(1.-(BL/SV))
C     ALGORITHM FOR TAU
      CNUO   =CNUS*PS/PO
      CNGR   =ABS((G/(CNUO**2.))*((D/2.)**3.)*((TO-T)/TO))
      CNPR   =0.71
      ALPHE  =(ALPHS*PS/PO)*CK3*((CNGR*CNPR)**.25)
      IF(ALPHE)510,500,510
500   TAU    =(1.0E70)
      GO TO 520
510   TAU    =(CK1/ALPHE)*((D/2.)**2.)*((CL/D)/(2.+(4.*(CL/D))))
C     ALGORITHM FOR T
520   CV     =C1*(T**2.)+(C2*T)+C3
      DELTEM =DELT*(((TO-T)/TAU)-((Q/(CMASS*CV))*((RU*T*((SV+B)/
     *(SV**2.)))-(A/(SV**2.)))))
      T      =T+DELTEM
C     ALGORITHM FOR PA
      PA     =(RU*T*((SV+B)/(SV**2.)))-(A/(SV**2.))
1300  CONTINUE
220   FORMAT(1X,F8.2,2X,F12.2,2X,F10.8,2X,F10.2)
      PRINT220,TIM,PA,Q,T
      GO TO 200
      END
```

APPENDIX D

Flow Input Model FORTRAN, results from typical step response test, 4 litre accumulator

0.00 .00048425 .02222324

TIME	PRESSURE	FLOW	TEMP.
0.00	4000000.00	0.00000000	300.00
1.00	6153988.04	-.00100000	337.55
2.00	11520017.45	-.00100000	397.87
3.00	11268467.20	0.00000000	390.11
4.00	11041402.38	0.00000000	383.10
5.00	10836015.70	0.00000000	376.75
6.00	10649868.55	0.00000000	371.01
7.00	10480836.65	0.00000000	365.79
8.00	10327064.52	0.00000000	361.04
9.00	10186927.34	0.00000000	356.72
10.00	10058998.71	0.00000000	352.77
11.00	9942023.42	0.00000000	349.15
12.00	9834894.36	0.00000000	345.85
13.00	9736632.86	0.00000000	342.81
14.00	9646371.96	0.00000000	340.03
15.00	9563342.04	0.00000000	337.46
16.00	9486858.53	0.00000000	335.10
17.00	9416311.32	0.00000000	332.92
18.00	9351155.68	0.00000000	330.91
19.00	9290904.33	0.00000000	329.05
20.00	9235120.61	0.00000000	327.33
21.00	9183412.61	0.00000000	325.73
22.00	9135427.95	0.00000000	324.25
23.00	9090849.30	0.00000000	322.88
24.00	9049390.45	0.00000000	321.60
25.00	9010792.90	0.00000000	320.41
26.00	8974822.79	0.00000000	319.29
27.00	8941268.26	0.00000000	318.26
28.00	8909937.14	0.00000000	317.29
29.00	8880654.86	0.00000000	316.39
30.00	8853262.65	0.00000000	315.54
31.00	8827615.90	0.00000000	314.75
32.00	8803582.78	0.00000000	314.01
33.00	8781042.89	0.00000000	313.31
34.00	8759886.24	0.00000000	312.66
35.00	8740012.14	0.00000000	312.05
36.00	8721328.38	0.00000000	311.47
37.00	8703750.36	0.00000000	310.93
38.00	8687200.46	0.00000000	310.41
39.00	8671607.30	0.00000000	309.93
40.00	8656905.26	0.00000000	309.48
41.00	8643033.89	0.00000000	309.05
42.00	8629937.47	0.00000000	308.65
43.00	8617564.61	0.00000000	308.27
44.00	8605867.83	0.00000000	307.90
45.00	8594803.27	0.00000000	307.56

46.00	8584330.34	0.00000000	307.24
47.00	8574411.47	0.00000000	306.93
48.00	8565011.84	0.00000000	306.64
49.00	8556099.15	0.00000000	306.37
50.00	8547643.44	0.00000000	306.11
51.00	8539616.86	0.00000000	305.86
52.00	8531993.53	0.00000000	305.62
53.00	8524749.37	0.00000000	305.40
54.00	8517861.96	0.00000000	305.19
55.00	8511310.43	0.00000000	304.98
56.00	8505075.30	0.00000000	304.79
57.00	8499138.39	0.00000000	304.61
58.00	8493482.76	0.00000000	304.43
59.00	8488092.55	0.00000000	304.27
60.00	8482952.95	0.00000000	304.11
61.00	8478050.09	0.00000000	303.96
62.00	8473371.02	0.00000000	303.81
63.00	8468903.58	0.00000000	303.68
64.00	8464636.38	0.00000000	303.54
65.00	8460558.74	0.00000000	303.42
66.00	8456660.65	0.00000000	303.30
67.00	8452932.69	0.00000000	303.18
68.00	8449366.03	0.00000000	303.07
69.00	8445952.37	0.00000000	302.97
70.00	8442683.89	0.00000000	302.87
71.00	8439553.25	0.00000000	302.77
72.00	8436553.52	0.00000000	302.68
73.00	8433678.19	0.00000000	302.59
74.00	8430921.11	0.00000000	302.50
75.00	8428276.50	0.00000000	302.42
76.00	8425738.90	0.00000000	302.34
77.00	8423303.14	0.00000000	302.27
78.00	8420964.36	0.00000000	302.20
79.00	8418717.97	0.00000000	302.13
80.00	8416559.61	0.00000000	302.06
81.00	8414485.18	0.00000000	302.00
82.00	8412490.79	0.00000000	301.93
83.00	8410572.76	0.00000000	301.87
84.00	8408727.60	0.00000000	301.82
85.00	8406952.03	0.00000000	301.76
86.00	8405242.91	0.00000000	301.71
87.00	8403597.28	0.00000000	301.66
88.00	8402012.33	0.00000000	301.61
89.00	8400485.40	0.00000000	301.56
90.00	8399013.95	0.00000000	301.52
91.00	8397595.58	0.00000000	301.47
92.00	8396228.01	0.00000000	301.43
93.00	8394909.07	0.00000000	301.39
94.00	8393636.70	0.00000000	301.35
95.00	8392408.94	0.00000000	301.31
96.00	8391223.93	0.00000000	301.28
97.00	8390079.89	0.00000000	301.24
98.00	8388975.13	0.00000000	301.21
99.00	8387908.04	0.00000000	301.17

100.00	8386877.10	0.00000000	301.14
101.00	8385880.84	0.00000000	301.11
102.00	8384917.88	0.00000000	301.08
103.00	8383986.88	0.00000000	301.05
104.00	8383086.58	0.00000000	301.03
105.00	8382215.78	0.00000000	301.00
106.00	8381373.31	0.00000000	300.97
107.00	8380558.09	0.00000000	300.95
108.00	8379769.06	0.00000000	300.92
109.00	8379005.21	0.00000000	300.90
110.00	8378265.60	0.00000000	300.88
111.00	8377549.29	0.00000000	300.86
112.00	8376855.42	0.00000000	300.83
113.00	8376183.15	0.00000000	300.81
114.00	8375531.67	0.00000000	300.79
115.00	8374900.22	0.00000000	300.77
116.00	8374288.06	0.00000000	300.75
117.00	8373694.50	0.00000000	300.74
118.00	8373118.85	0.00000000	300.72
119.00	8372560.47	0.00000000	300.70
120.00	8372018.75	0.00000000	300.68
121.00	8371493.08	0.00000000	300.67
122.00	8370982.91	0.00000000	300.65
123.00	8370487.68	0.00000000	300.64
124.00	8370006.88	0.00000000	300.62
125.00	8369540.01	0.00000000	300.61
126.00	8369086.57	0.00000000	300.59
127.00	8368646.12	0.00000000	300.58
128.00	8368218.20	0.00000000	300.57
129.00	8367802.40	0.00000000	300.55
130.00	8367398.30	0.00000000	300.54
131.00	8367005.50	0.00000000	300.53
132.00	8366623.64	0.00000000	300.52
133.00	8366252.34	0.00000000	300.51
134.00	8365891.27	0.00000000	300.50
135.00	8365540.07	0.00000000	300.48
136.00	8365198.44	0.00000000	300.47
137.00	8364866.06	0.00000000	300.46
138.00	8364542.62	0.00000000	300.45
139.00	8364227.86	0.00000000	300.44
140.00	8363921.47	0.00000000	300.43
141.00	8363623.21	0.00000000	300.43
142.00	8363332.80	0.00000000	300.42
143.00	8363050.02	0.00000000	300.41
144.00	8362774.61	0.00000000	300.40
145.00	8362506.34	0.00000000	300.39
146.00	8362245.00	0.00000000	300.38
147.00	8361990.38	0.00000000	300.37
148.00	8361742.26	0.00000000	300.37
149.00	8361500.44	0.00000000	300.36
150.00	8361264.74	0.00000000	300.35
151.00	8361034.98	0.00000000	300.35
152.00	8360810.98	0.00000000	300.34
153.00	8360592.53	0.00000000	300.33

154.00	8360379.51	0.00000000	300.33
155.00	8360171.75	0.00000000	300.32
156.00	8359969.09	0.00000000	300.31
157.00	8359771.37	0.00000000	300.31
158.00	8359578.47	0.00000000	300.30
159.00	8359390.23	0.00000000	300.29
160.00	8359206.52	0.00000000	300.29
161.00	8359027.21	0.00000000	300.28
162.00	8358852.18	0.00000000	300.28
163.00	8358681.30	0.00000000	300.27
164.00	8358514.45	0.00000000	300.27
165.00	8358351.53	0.00000000	300.26
166.00	8358192.42	0.00000000	300.26
167.00	8358037.02	0.00000000	300.25
168.00	8357885.21	0.00000000	300.25
169.00	8357736.91	0.00000000	300.24
170.00	8357592.02	0.00000000	300.24
171.00	8357450.44	0.00000000	300.23
172.00	8357312.08	0.00000000	300.23
173.00	8357176.85	0.00000000	300.23
174.00	8357044.67	0.00000000	300.22
175.00	8356915.46	0.00000000	300.22
176.00	8356789.14	0.00000000	300.21
177.00	8356665.63	0.00000000	300.21
178.00	8356544.86	0.00000000	300.21
179.00	8356426.75	0.00000000	300.20
180.00	8356311.23	0.00000000	300.20
181.00	8356198.24	0.00000000	300.20
182.00	8356087.70	0.00000000	300.19
183.00	8355979.56	0.00000000	300.19
184.00	8355873.76	0.00000000	300.19
185.00	8355770.23	0.00000000	300.18
186.00	8355668.91	0.00000000	300.18
187.00	8355569.75	0.00000000	300.18
188.00	8355472.70	0.00000000	300.17
189.00	8355377.69	0.00000000	300.17
190.00	8355284.68	0.00000000	300.17
191.00	8355193.62	0.00000000	300.17
192.00	8355104.46	0.00000000	300.16
193.00	8355017.15	0.00000000	300.16
194.00	8354931.65	0.00000000	300.16
195.00	8354847.91	0.00000000	300.15
196.00	8354765.89	0.00000000	300.15
197.00	8354685.54	0.00000000	300.15
198.00	8354606.82	0.00000000	300.15
199.00	8354529.71	0.00000000	300.14
200.00	8354454.14	0.00000000	300.14

APPENDIX E

Pressure Input Model FORTRAN

```
      PROGRAM PRESIN(INPUT,OUTPUT)
C     CONSTANTS AND PARAMETERS
50    FORMAT(5E15.7)
      READ50,PIE,C1,C2,C3,C10
      READ50,AL,AO,BL,BO,G
      READ50,CK1,CK3,CK10,CK11,PS
      READ50,RU,SVS,ALPHS,CNUS,C5
      READ50,CL,PO,TO,D,DELT
      READ50,PL,A,B,SVI,TIM
      READ50,RES
C
C     INITIAL VALUES ALGORITHM
C
      TI      =TO
      PAI     =PL
      PROX    =(-1.0)
      J       =(1.0/DELT)+DELT
C     SVJ
      X       =RU*TI/PAI
100   SVJ     =0.5*(X+((X**2.-(4.*A/PAI)+4.*X*B)**0.5))
      A       =AO*(1.-(AL/SVJ))
      B       =BO*(1.-(BL/SVJ))
      IF(ABS(SVJ-SVI)-1.0E-6)120,120,110
110   SVI     =SVJ
      GO TO 100
120   VOL     =(D**2.)*CL*PIE/4.
      VOILI   =VOL*(1.-(PO/PAI))
      CMASS   =(VOL*PO)/(SVS*PS)
130   FORMAT(F8.2,2F10.8)
      PRINT130,TIM,VOILI,SVI
140   FORMAT(3X,*TIME*,6X,*PRESSURE*,8X,*FLOW*,8X,*TEMP.*)
      PRINT 140
      PRINT220,TIM,PAI,QI,TI
C     MAIN CONTROL PROGRAM
200   DO1300 I=1,J
      TIM     =TIM+DELT
      IF(TIM-200.)230,300,300
230   IF(TIM-1.0)240,250,250
240   PL      =PL
      GO TO 260
250   PL      =PS
      GO TO 260
C     ACCUMULATOR MODEL PL INPUT
260   IF(PAI-PL)290,290,270
270   QJ      =(C5/RES)*((PAI-PL)**0.5)
      IF(VOILI-(QJ*DELT))280,400,400
```

```
280   QJ      =C5*VOILI/DELT
      DELVOL  =(-C5*VOILI)
      GO TO 410
290   QJ      =(-C5/RES)*((ABS(PAI-PL))**0.5)
400   DELVOL  =(-QJ*DELT)
410   VOILJ   =VOILI+DELVOL
C     ALGORITHM FOR SVI
      DELSV   =QJ*DELI/CMASS
      SVJ     =SVI+DELSV
      A       =A0*(1.-(AL/SVJ))
      B       =B0*(1.-(BL/SVJ))
C     ALGORITHM FOR TAU
      CNUO    =CNUS*PS/PO
      CNGR    =ABS((G/(CNUO**2.))*((D/2.)**3.)*((TO-TI)/TO))
      CNPR    =0.71
      ALPHE   =(ALPHS*PS/PO)*CK3*((CNGR*CNPR)**0.25)
      IF(ALPHE)510,500,510
500   TAU     =(1.0E70)
      GO TO 520
510   TAU     =(CK1/ALPHE)*((D/2.)**2.)*((CL/D)/(2.+(4.*(CL/D))))
C     ALGORITHM FOR TJ
520   CV      =C1*(TI**2.)+(C2*TI)+C3
      DELTEM  =DELT*(((TO-TI)/TAU)-((QJ/(CMASS*CV))*((RU*TI*((SVJ+B)/
     *(SVJ**2.)))-(A/(SVJ**2.)))))
      TJ      =TI+DELTEM
C     ALGORITHM FOR PAJ
      PAJ     =(RU*TJ*((SVJ+B)/(SVJ**2.)))-(A/(SVJ**2.))
C     ALGORITHM FOR CORRECTION OF INSTABILITY
      IF(ABS(PAI-PL)-100.)1010,1020,1020
1010  IF(PROX)1200,1200,1100
1020  IF(PROX)1050,1050,1090
1050  IF(PAI-PL)1070,1080,1080
1070  IF(PAJ-PL)1090,1200,1200
1080  IF(PAJ-PL)1200,1090,1090
1090  PROX    =(-1.0)
      C5      =1.0
1100  QI      =QJ
      PAI     =PAJ
      SVI     =SVJ
      TI      =TJ
      VOILI   =VOILJ
      GO TO 1300
1200  PROX    =1.0
      C5      =(0.0003)*((ABS(PAI-PL))**0.5)
      GO TO 260
1300  CONTINUE
220   FORMAT(1X,F8.2,2X,F12.2,2X,F10.8,2X,F10.2)
      PRINT220,TIM,PAI,QI,TI
      GO TO 200
300   STOP2
      END
```

APPENDIX F

Pressure Input Model FORTRAN, results from test conditions No. 1 for 4 litre accumulator

0.00 .00037571 .02284389

TIME	PRESSURE	FLOW	TEMP.
0.00	3891000.00	0.00000000	300.00
1.00	3891025.86	0.00000000	300.00
2.00	3427072.41	0.00000000	289.99
3.00	3432888.04	0.00000000	290.45
4.00	3438375.59	0.00000000	290.88
5.00	3443557.03	0.00000000	291.29
6.00	3448452.63	0.00000000	291.67
7.00	3453081.10	0.00000000	292.04
8.00	3457459.75	0.00000000	292.38
9.00	3461604.57	0.00000000	292.71
10.00	3465530.40	0.00000000	293.01
11.00	3469250.97	0.00000000	293.31
12.00	3472779.04	0.00000000	293.58
13.00	3476126.42	0.00000000	293.85
14.00	3479304.12	0.00000000	294.10
15.00	3482322.34	0.00000000	294.33
16.00	3485190.60	0.00000000	294.56
17.00	3487917.75	0.00000000	294.77
18.00	3490512.04	0.00000000	294.98
19.00	3492981.16	0.00000000	295.17
20.00	3495332.29	0.00000000	295.36
21.00	3497572.14	0.00000000	295.53
22.00	3499706.95	0.00000000	295.70
23.00	3501742.60	0.00000000	295.86
24.00	3503684.55	0.00000000	296.01
25.00	3505537.93	0.00000000	296.16
26.00	3507307.55	0.00000000	296.30
27.00	3508997.90	0.00000000	296.43
28.00	3510613.22	0.00000000	296.56
29.00	3512157.46	0.00000000	296.68
30.00	3513634.34	0.00000000	296.79
31.00	3515047.36	0.00000000	296.90
32.00	3516399.81	0.00000000	297.01
33.00	3517694.77	0.00000000	297.11
34.00	3518935.14	0.00000000	297.21
35.00	3520123.68	0.00000000	297.30
36.00	3521262.96	0.00000000	297.39
37.00	3522355.40	0.00000000	297.48
38.00	3523403.29	0.00000000	297.56
39.00	3524408.81	0.00000000	297.64
40.00	3525373.99	0.00000000	297.71
41.00	3526300.75	0.00000000	297.79
42.00	3527190.93	0.00000000	297.86
43.00	3528046.22	0.00000000	297.92
44.00	3528868.28	0.00000000	297.99
45.00	3529658.62	0.00000000	298.05

46.00	3530418.71	0.00000000	298.11
47.00	3531149.93	0.00000000	298.17
48.00	3531853.59	0.00000000	298.22
49.00	3532530.92	0.00000000	298.28
50.00	3533183.09	0.00000000	298.33
51.00	3533811.21	0.00000000	298.38
52.00	3534416.36	0.00000000	298.42
53.00	3534999.52	0.00000000	298.47
54.00	3535561.64	0.00000000	298.51
55.00	3536103.64	0.00000000	298.56
56.00	3536626.36	0.00000000	298.60
57.00	3537130.63	0.00000000	298.64
58.00	3537617.23	0.00000000	298.68
59.00	3538086.88	0.00000000	298.71
60.00	3538540.30	0.00000000	298.75
61.00	3538978.15	0.00000000	298.78
62.00	3539401.07	0.00000000	298.82
63.00	3539809.67	0.00000000	298.85
64.00	3540204.52	0.00000000	298.88
65.00	3540586.18	0.00000000	298.91
66.00	3540955.16	0.00000000	298.94
67.00	3541311.98	0.00000000	298.97
68.00	3541657.12	0.00000000	298.99
69.00	3541991.01	0.00000000	299.02

Pressure Input Model FORTRAN, results from test conditions No. 6 for 28 litre accumulator

0.00 .01884156 .00460952

TIME	PRESSURE	FLOW	TEMP.
0.00	20790000.00	0.00000000	300.00
1.00	20789999.89	.00000003	300.01
2.00	4325750.50	0.00000000	203.06
3.00	4416067.01	0.00000000	206.55
4.00	4502363.87	0.00000000	209.87
5.00	4584853.85	0.00000000	213.05
6.00	4663736.73	0.00000000	216.10
7.00	4739200.12	0.00000000	219.01
8.00	4811420.38	0.00000000	221.79
9.00	4880563.33	0.00000000	224.46
10.00	4946785.00	0.00000000	227.01
11.00	5010232.24	0.00000000	229.46
12.00	5071043.38	0.00000000	231.80
13.00	5129348.77	0.00000000	234.05
14.00	5185271.29	0.00000000	236.21
15.00	5238926.86	0.00000000	238.27
16.00	5290424.86	0.00000000	240.26
17.00	5339868.57	0.00000000	242.17
18.00	5387355.56	0.00000000	244.00
19.00	5432978.01	0.00000000	245.76
20.00	5476823.09	0.00000000	247.45
21.00	5518973.24	0.00000000	249.07
22.00	5559506.50	0.00000000	250.64
23.00	5598496.72	0.00000000	252.14
24.00	5636013.86	0.00000000	253.59
25.00	5672124.20	0.00000000	254.98
26.00	5706890.58	0.00000000	256.32
27.00	5740372.56	0.00000000	257.61
28.00	5772626.68	0.00000000	258.85
29.00	5803706.58	0.00000000	260.05
30.00	5833663.17	0.00000000	261.21
31.00	5862544.84	0.00000000	262.32
32.00	5890397.53	0.00000000	263.39
33.00	5917264.93	0.00000000	264.43
34.00	5943188.56	0.00000000	265.43
35.00	5968207.94	0.00000000	266.39
36.00	5992360.64	0.00000000	267.33
37.00	6015682.45	0.00000000	268.22
38.00	6038207.44	0.00000000	269.09
39.00	6059968.04	0.00000000	269.93
40.00	6080995.19	0.00000000	270.74
41.00	6101318.34	0.00000000	271.53
42.00	6120965.58	0.00000000	272.28
43.00	6139963.73	0.00000000	273.02
44.00	6158338.34	0.00000000	273.73
45.00	6176113.81	0.00000000	274.41

46.00	6193313.43	0.00000000	275.07
47.00	6209959.44	0.00000000	275.72
48.00	6226073.10	0.00000000	276.34
49.00	6241674.69	0.00000000	276.94
50.00	6256783.62	0.00000000	277.52
51.00	6271418.45	0.00000000	278.09
52.00	6285596.92	0.00000000	278.63
53.00	6299335.99	0.00000000	279.16
54.00	6312651.91	0.00000000	279.68
55.00	6325560.21	0.00000000	280.17
56.00	6338075.79	0.00000000	280.66
57.00	6350212.89	0.00000000	281.12
58.00	6361985.17	0.00000000	281.58
59.00	6373405.70	0.00000000	282.02
60.00	6384487.02	0.00000000	282.45
61.00	6395241.15	0.00000000	282.86
62.00	6405679.62	0.00000000	283.26
63.00	6415813.47	0.00000000	283.65
64.00	6425653.33	0.00000000	284.03
65.00	6435209.35	0.00000000	284.40
66.00	6444491.31	0.00000000	284.76
67.00	6453508.58	0.00000000	285.11
68.00	6462270.18	0.00000000	285.44
69.00	6470784.76	0.00000000	285.77
70.00	6479060.61	0.00000000	286.09
71.00	6487105.74	0.00000000	286.40

Pressure Input Model FORTRAN, results from test conditions No. 8 for 38 litre accumulator

0.00 .01253619 .00593559

TIME	PRESSURE	FLOW	TEMP.
0.00	15610000.00	0.00000000	300.00
1.00	15610000.00	.00000001	299.99
2.00	8572974.22	0.00000000	257.84
3.00	8624185.72	0.00000000	259.09
4.00	8673516.36	0.00000000	260.29
5.00	8721048.45	0.00000000	261.45
6.00	8766860.09	0.00000000	262.57
7.00	8811025.48	0.00000000	263.64
8.00	8853615.10	0.00000000	264.68
9.00	8894695.94	0.00000000	265.68
10.00	8934331.68	0.00000000	266.65
11.00	8972582.91	0.00000000	267.58
12.00	9009507.25	0.00000000	268.48
13.00	9045159.55	0.00000000	269.35
14.00	9079592.05	0.00000000	270.19
15.00	9112854.47	0.00000000	271.00
16.00	9144994.22	0.00000000	271.78
17.00	9176056.46	0.00000000	272.54
18.00	9206084.25	0.00000000	273.27
19.00	9235118.65	0.00000000	273.98
20.00	9263198.84	0.00000000	274.66
21.00	9290362.21	0.00000000	275.32
22.00	9316644.45	0.00000000	275.96
23.00	9342079.63	0.00000000	276.58
24.00	9366700.30	0.00000000	277.18
25.00	9390537.57	0.00000000	277.76
26.00	9413621.15	0.00000000	278.33
27.00	9435979.47	0.00000000	278.87
28.00	9457639.69	0.00000000	279.40
29.00	9478627.81	0.00000000	279.91
30.00	9498968.70	0.00000000	280.41
31.00	9518686.17	0.00000000	280.89
32.00	9537803.01	0.00000000	281.35
33.00	9556341.03	0.00000000	281.80
34.00	9574321.14	0.00000000	282.24
35.00	9591763.37	0.00000000	282.67
36.00	9608686.91	0.00000000	283.08
37.00	9625110.16	0.00000000	283.48
38.00	9641050.77	0.00000000	283.87
39.00	9656525.66	0.00000000	284.25
40.00	9671551.05	0.00000000	284.61
41.00	9686142.54	0.00000000	284.97
42.00	9700315.06	0.00000000	285.31
43.00	9714082.97	0.00000000	285.65
44.00	9727460.05	0.00000000	285.97
45.00	9740459.54	0.00000000	286.29

46.00	9753094.16	0.00000000	286.60
47.00	9765376.13	0.00000000	286.90
48.00	9777317.20	0.00000000	287.19
49.00	9788928.65	0.00000000	287.47
50.00	9800221.35	0.00000000	287.75
51.00	9811205.74	0.00000000	288.01
52.00	9821891.86	0.00000000	288.27
53.00	9832289.39	0.00000000	288.53
54.00	9842407.61	0.00000000	288.77
55.00	9852255.50	0.00000000	289.01
56.00	9861841.66	0.00000000	289.25
57.00	9871174.41	0.00000000	289.48
58.00	9880261.74	0.00000000	289.70
59.00	9889111.35	0.00000000	289.91
60.00	9897730.67	0.00000000	290.12
61.00	9906126.85	0.00000000	290.33
62.00	9914306.78	0.00000000	290.53
63.00	9922277.12	0.00000000	290.72
64.00	9930044.28	0.00000000	290.91
65.00	9937614.44	0.00000000	291.09
66.00	9944993.57	0.00000000	291.27
67.00	9952187.42	0.00000000	291.45
68.00	9959201.55	0.00000000	291.62
69.00	9966041.32	0.00000000	291.79
70.00	9972711.90	0.00000000	291.95

APPENDIX G

Pressure Input Model, TI-59
Initial Value Calculations

```
000  76 LBL     045  55  ÷     090  42 STO     135  43 RCL
001  11  A      046  02  2     091  50  50     136  24  24
002  43 RCL     047  95  =     092  43 RCL     137  55  ÷
003  46  46     048  42 STO     093  49  49     138  43 RCL
004  42 STO     049  49  49     094  42 STO     139  21  21
005  34  34     050  35 1/X     095  40  40     140  33  X²
006  76 LBL     051  65  ×     096  43 RCL     141  95  =
007  15  E      052  43 RCL     097  50  50     142  42 STO
008  43 RCL     053  05  05     098  23 LNX     143  37  37
009  16  16     054  94 +/-     099  67  EQ     144  00  0
010  65  ×      055  85  +     100  15  E      145  42 STO
011  43 RCL     056  01  1     101  43 RCL     146  38  38
012  26  26     057  95  =     102  27  27     147  43 RCL
013  55  ÷      058  65  ×     103  42 STO     148  15  15
014  43 RCL     059  43 RCL     104  51  51     149  55  ÷
015  34  34     060  06  06     105  43 RCL     150  43 RCL
016  95  =      061  95  =     106  26  26     151  25  25
017  42 STO     062  42 STO     107  42 STO     152  95  =
018  28  28     063  30  30     108  39  39     153  42 STO
019  85  +      064  43 RCL     109  42 RCL     154  35  35
020  52  (      065  00  00     110  20  20     155  35 1/X
021  53  (      066  65  ×     111  32 X↑T     156  65  ×
022  43 RCL     067  53  (     112  65  ×     157  43 RCL
023  28  28     068  01  1     113  43 RCL     158  41  41
024  33 X²      069  75  -     114  23  23     159  55  ÷
025  75  -      070  43 RCL     115  65  ×     160  43 RCL
026  04  4      071  07  07     116  89  π     161  17  17
027  65  ×      072  55  ÷     117  55  ÷     162  95  =
028  43 RCL     073  43 RCL     118  04  4     163  42 STO
029  30  30     074  49  49     119  95  =     164  28  28
030  55  ÷      075  54  )     120  42 STO     165  43 RCL
031  43 RCL     076  95  =     121  41  41     166  42  42
032  24  24     077  42 STO     122  55  ÷     167  99 PRT
033  65  ×      078  31  31     123  53  (     168  01  R/S
034  04  4      079  43 RCL     124  01  1     169  76 LBL
035  85  +      080  49  49     125  75  -     170  14  D
036  53  (      081  54  )     126  43 RCL     171  43 RCL
037  43 RCL     082  42 STO     127  50  50     172  42  42
038  28  28     083  32 X↑T     128  85  +     173  99 PRT
039  65  ×      084  43 RCL     129  53  (     174  01  R/S
040  43 RCL     085  50  50     130  43 RCL     175  76 LBL
041  31  31     086  23 LNX     131  40  40     176  15  E
042  54  )      087  42 STO     132  54  )     177  43 RCL
043  54  )      088  51  51     133  95  =     178  51  51
044  95  =      089  43 RCL     134  42 STO     179  99 PRT
                090  51  51     135  43  43    180  01  R/S
                091  54  )     136  43 RCL     181  76 LBL
                092  95  =     137  43  43    182  16 A'
                                138  95  =     183  43 RCL
                                139  42 STO     184  51  51
                                140  44  44    185  99 PRT
                                141  43 RCL     186  01  R/S
                                142  24  24
                                143  55  ÷
                                144  43 RCL
                                145  21  21
                                146  33  X²
                                147  95  =
                                148  42 STO
                                149  37  37
                                150  00  0
                                151  42 STO
                                152  38  38
                                153  43 RCL
                                154  15  15
                                155  55  ÷
                                156  43 RCL
                                157  25  25
                                158  95  =
                                159  42 STO
                                160  35  35
                                161  35 1/X
                                162  65  ×
                                163  43 RCL
                                164  41  41
                                165  55  ÷
                                166  43 RCL
                                167  17  17
                                168  95  =
                                169  42 STO
                                170  28  28
                                171  43 RCL
                                172  42  42
                                173  99 PRT
                                174  01  R/S
```

Pressure Input Model, TI-59.

Main Program.

000	76	LBL	045	43	RCL	090	65	×	135	39	39				
001	11	A	046	43	43	091	43	RCL	136	33	X²				
002	43	RCL	047	50	I×I	092	51	51	137	65	×				
003	34	34	048	34	ΓX	093	55	÷	138	43	RCL				
004	75	-	049	95	=	094	43	RCL	139	00	00				
005	43	RCL	050	42	STO	095	29	29	140	85	+				
006	46	46	051	36	36	096	95	=	141	43	RCL				
007	95	=	052	61	GTO	097	42	STO	142	39	39				
008	42	STO	053	12	B	098	44	44	143	65	×				
009	43	43	054	76	LBL	099	85	+	144	43	RCL				
010	87	IFF	055	16	A'	100	43	RCL	145	01	01				
011	00	00	056	43	RCL	101	40	40	146	85	+				
012	17	B'	057	03	03	102	95	=	147	43	RCL				
013	01	1	058	55	÷	103	42	STO	148	02	02				
014	42	STO	059	43	RCL	104	49	49	149	95	=				
015	03	03	060	37	37	105	35	1/X	150	42	STO				
016	61	GTO	061	65	×	106	65	×	151	32	32				
017	15	E	062	43	RCL	107	43	RCL	152	43	RCL				
018	76	LBL	063	43	43	108	05	05	153	11	11				
019	17	B'	064	34	ΓX	109	92	RTN	154	65	×				
020	50	I×I	065	95	=	110	05	5	155	43	RCL				
021	34	ΓX	066	42	STO	111	01	1	156	20	20				
022	65	×	067	36	36	112	95	=	157	45	Y^X				
023	43	RCL	068	92	RTN	113	45	Y^X	158	03	3				
024	51	51	069	65	×	114	43	RCL	159	55	÷				
025	45	Y^X	070	43	RCL	115	06	06	160	53	(				
026	03	3	071	51	51	116	95	=	161	43	RCL				
027	92	RTN	072	85	+	117	42	STO	162	35	35				
028	05	5	073	43	RCL	118	30	30	163	65	×				
029	95	=	074	42	42	119	43	RCL	164	43	RCL				
030	42	STO	075	95	=	120	08	08	165	19	19				
031	03	03	076	71	GE	121	55	÷	166	54	)				
032	76	LBL	077	12	B	122	53	(	167	33	X²				
033	15	E	078	43	RCL	123	01	1	168	65	×				
034	43	RCL	079	42	42	124	75	-	169	53	(				
035	43	43	080	55	÷	125	43	RCL	170	43	RCL				
036	71	GE	081	43	RCL	126	07	07	171	00	00				
037	16	A'	082	51	51	127	65	×	172	75	-				
038	71	PFL	083	95	=	128	43	RCL	173	43	RCL				
039	03	03	084	42	STO	129	49	49	174	39	39				
040	55	÷	085	36	36	130	54	)	175	54	)				
041	43	RCL	086	76	LBL	131	95	=	176	35	1/X				
042	37	37	087	12	B	132	42	STO	177	53	(				
043	94	+/-	088	43	RCL	133	31	31	178	43	RCL				
044	65	×	089	36	36	134	43	RCL	179	26	26				

180	85	+
181	43	RCL
182	39	39
183	54	)
184	95	=
185	67	EQ
186	18	C'
187	50	I"I
188	65	×
189	43	RCL
190	14	14
191	95	=
192	34	FX
193	34	FX
194	65	×
195	43	RCL
196	18	18
197	65	×
198	43	RCL
199	13	13
200	65	×
201	43	RCL
202	35	35
203	95	=
204	35	1/X
205	65	×
206	43	RCL
207	12	12
208	65	×
209	53	(
210	43	RCL
211	20	20
212	33	X²
213	55	÷
214	53	(
215	43	RCL
216	20	20
217	55	÷
218	43	RCL
219	23	23
220	85	+
221	02	2
222	54	)
223	54	)
224	95	=

225	61	GTO
226	13	C
227	76	LBL
228	18	C'
229	43	RCL
230	04	04
231	76	LBL
232	13	C
233	35	1/X
234	65	×
235	43	RCL
236	10	10
237	65	×
238	53	(
239	43	RCL
240	26	26
241	75	-
242	43	RCL
243	39	39
244	54	)
245	85	+
246	43	RCL
247	36	36
248	55	÷
249	43	RCL
250	49	49
251	33	X²
252	55	÷
253	43	RCL
254	29	29
255	65	×
256	53	(
257	43	RCL
258	30	30
259	75	-
260	43	RCL
261	16	16
262	55	÷
263	43	RCL
264	39	39
265	65	×
266	53	(
267	43	RCL
268	44	44
269	85	+

270	43	RCL
271	31	31
272	54	)
273	54	)
274	95	=
275	65	×
276	43	RCL
277	51	51
278	55	÷
279	43	RCL
280	32	32
281	95	=
282	85	+
283	43	RCL
284	39	39
285	95	=
286	42	STO
287	40	40
288	65	×
289	43	RCL
290	16	16
291	65	×
292	53	(
293	43	RCL
294	49	49
295	85	+
296	43	RCL
297	31	31
298	54	)
299	75	-
300	43	RCL
301	30	30
302	95	=
303	55	÷
304	43	RCL
305	40	40
306	33	X²
307	95	=
308	52	EE
309	22	INV
310	52	EE
311	42	STO
312	47	47
313	43	RCL
314	43	43

315	59	INT
316	42	STO
317	43	43
318	67	EQ
319	19	D'
320	43	RCL
321	47	47
322	75	-
323	43	RCL
324	46	46
325	95	=
326	59	INT
327	42	STO
328	33	33
329	67	EQ
330	19	D'
331	43	RCL
332	43	43
333	77	GE
334	10	E'
335	43	RCL
336	33	33
337	77	GE
338	14	D
339	61	GTO
340	19	D'
341	76	LBL
342	10	E'
343	43	RCL
344	33	33
345	77	GE
346	19	D'
347	76	LBL
348	14	D
349	76	LBL
350	00	00
351	61	GTO
352	14	D
353	76	LBL
354	19	D'
355	43	RCL
356	27	27
357	44	SUM
358	38	38
359	65	×

```
360  43 RCL
361  36  36
362  94 +/-
363  95  =
364  44 SUM
365  42  42
366  43 RCL
367  49  49
368  42 STO
369  40  40
370  43 RCL
371  48  48
372  42 STO
373  39  39
374  43 RCL
375  47  47
376  42 STO
377  34  34
378  43 RCL
379  27  27
380  42 STO
381  51  51
382  22 INV
383  86 STF
384  00  00
385  43 RCL
386  38  38
387  99 PRT
388  43 RCL
389  34  34
390  59 INT
391  99 PRT
392  61 GTO
393  11  A
```